UNIVERSITÀ DEGLI STUDI DI MILANO

FACOLTÀ DI SCIENZE E TECNOLOGIE

XXIX Ph.D. CYCLE IN CHEMISTRY

STUDY AND DEVELOPMENT OF FLEXIBLE POLYMERIC SUBSTRATES FOR ELECTRONIC DEVICES AND SMART MATERIALS

Dr. Valentina Sabatini

R10678

Tutor: Professor Silvia Ardizzone

Co-Tutor: Professor Giuseppe Di Silvestro

A.A. 2016-2017

Analytical Index

Summary

In the field of smart materials for photovoltaic (PV) industry and Organic Electronic (OE), polymeric films that exhibit modular wetting properties and conductive features are considered very promising for several applications. Self-cleaning films for the covering of photovoltaic cells and conductive polymer films are two important examples.

The present work is related to the use of Sulfonated Polyarylethersulfone (SPES) for two different applications:

i) for PV industry, as flexible and transparent polymeric film having both hydrophilic and hydrophobic features;

ii) in the research area of OE, as doping agent for both electrical conductive and polymeric films, and screen printer inks.

Polymers based on Polyarylethersulfones (PESs) are favorable materials for preparing membranes for several applications due to their excellent thermal and chemical stability, ion exchange properties, oxidation resistance as well as good mechanical behavior. PES-based membranes have been widely used in advanced separation technologies, including low-cost alternatives to expensive fluorinated polymers in fuel cells, in biomedical fields (as medical devices for blood purification and dialysis) and in food industry as membranes for wine, water and fruit-juices purification.

In order to diversify membrane properties and therefore widen possible application fields, chemical modifications of PES matrices can be studied; such modifications can be achieved by supplying different functional groups on the polymer matrix, i.e. sulfonic ($-SO_3^-$), hydroxyl (-OH), carboxyl (-COOH) and amino ($-NH_2$) moieties.

SPES has received great attention in the last decade due to the possibility to improve the wetting properties of PES membranes thanks to the incorporation of sulfonic groups. This allowed the development of SPES membranes as advanced materials for a variety of separation processes, such

as ion exchange, reverse osmosis and electro dialysis process; in all these fields, materials with highly hydrophilic behavior are requested.

SPESs can be prepared via two polymerization routes, either via post-sulfonation reaction with different sulfonating agents and solvents of the pre-formed PES polymer -heterogeneous synthesis-, or starting from pre-sulfonated monomers -homogeneous synthesis-. Although homogeneous synthesis allows an easy control of the degree of sulfonation (DS) of the resulting polymer and to avoid side and degradations reactions, heterogeneous synthesis is widely used, both in the industrial and academic area, due to its simplicity and low cost.

i) SPES films characterized by both hydrophobic and hydrophilic behavior.

In this work, a series of SPESs with different DS were synthesized via homogeneous synthesis starting from 4,4'-difluorodiphenylsulfone, 4,4'–dihydroxydiphenyl and a sulfonated comonomer, 2,5-dihydroxybenzene-3-sulfonate potassium salt (sulfonated hydroquinone in potassium salt). The macromolecular structure was determined via ^{1}H NMR and ^{1}H-^{1}H COSY spectroscopy and the presence of sulfonic groups was confirmed by Fourier Transform Infrared (FT-IR) spectra; the real DS values of SPESs were determined by ^{1}H NMR calculations and confirmed by potentiometric tritation data. Intrinsic viscosities were measured using dimethylacetamide (DMAc) as solvent with and without lithium bromide (LiBr) solution in order to investigate polyelectrolyte effect on SPES samples. The effects of DS increasing on the thermal properties of SPES membranes obtained via solvent casting deposition in DMAc were studied by Thermogravimetric (TGA) analyses and Differential Scanning Calorimetry (DSC); wetting features were investigated by static water contact angle (SWCA).

Wettability measurements are commonly used to characterize the relative hydrophilicity or hydrophobicity of a polymer surface; here, in order to investigate the wetting properties of SPES membranes, SWCA measures for all the samples, obtained from solution casting in DMAc, were performed.

The samples were solution casted onto a PTFE mold; the wetting features of the membranes were measured both at the air-side and at the PTFE-side surface. Table I shows the results obtained.

Sample	*DS* (*meq* SO_3^-*g^{-1}) (^{1}*H NMR*)	θ_w (*air-side*)	θ_w (*PTFE-side*)
SPES_0.5	*0.48*	$\overline{65}$*±2*	$\overline{89}$*±1*
SPES_0.75	*0.70*	*50±2*	$\overline{85}$*±1*
SPES_1	*0.98*	$\overline{43}$*±1*	$\overline{81}$*±2*

Table I. Static water contact angles of samples synthesized.

The results reported indicate that the hydrophilicity of SPES membranes improves as -$SO_3^-K^+$ amount in the SPES membranes increases, due to the high polarity of the -SO_3^- groups. It is important to underline that, thanks to a direct sulfonation reaction of, the hydrophilic properties of SPES samples are greatly enhanced using low amounts of sulfonic groups.

The increase of θ_w observed on the PTFE-side for SPES membranes with respect to the air-side is due to the different organization of the $SO_3^-K^+$ groups of the polymeric chains occurring during the evaporation of the solvent, as confirmed by FT-IR spectra performed on both air-side and PTFE one of the polymeric films.

Standard materials used as photovoltaic cells cover are characterized by an internal hydrophilic side, optimal for the deposition on solar cells and by an external hydrophobic or hyper-hydrophobic side, designed ad hoc as protective self-cleaning layer from pollution.

To improve the hydrophobic properties, the use of SPESs can be very advantageous in fields where hydrophilic/hydrophobic properties can be modulated; moreover, the use of Ionic Liquids (I.Ls.) combined with SPES can be a way to create tailor-made hydrophobic materials for solar cells covering.

I.Ls., a class of molten salts, have excellent thermal stability and their physical-chemical properties can be modulated changing the nature of the cation or anion. Modulating cationic apolar groups can dramatically influence the tendency of I.L. towards efficient ion packing and, in turn, its hydrophobic features, e.g. the longer the alkyl chains, the more hydrophobic the salt.

The wetting properties of SPES could therefore be modulated by introducing different cationic apolar groups through a novel ionic exchange reaction between the K^+ cation of the sulfonic moiety of SPES and the cation of an I.Ls.. The structure of I.Ls. used are reported in Figure I.

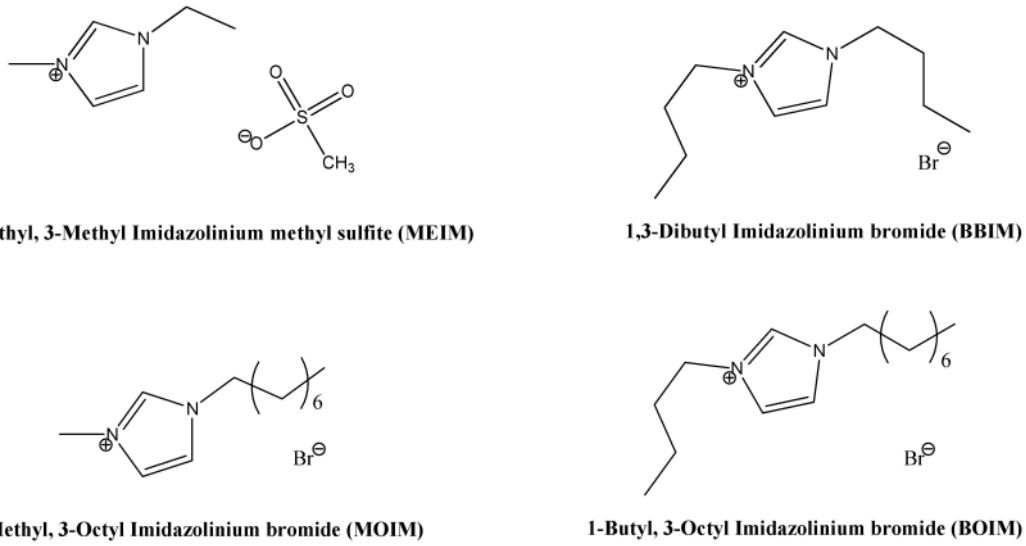

Figure I. Ionic Liquids used for the cation exchange reactions with SPES.

The hydrophobic properties of SPES treated with I.Ls. were found to improve with the DS of sulfonation of SPES, i.e. with the number of K^+ ions available for substitution by I.Ls. cations, obtaining contact angles up to $\overline{131}°$ (Table II) leading to self-cleaning surfaces (Figure II).

Scanning Electron Microscopy (SEM) and Atomic Force Microscopy (AFM) analyses for SPESs and SPES_I.Ls. samples were performed in order to clarify the influence of I.Ls. on the surface properties of the polymeric membranes prepared. Figure III presents SEM morphologies of representative membranes from both air-side and PTFE-side of SPESs and SPES_I.Ls. samples.

In the case of SPES_1, no surface differences are detectable between the air-side (IIIa) and the mold-side of the polymeric membrane (IIIb). When I.Ls. are added, it is possible to observe that the surface at the air-side remains smooth (IIIc), while the surface at the mold-side of the membrane changes from smooth to rough (IIId). The roughness of PTFE-side of SPES_I.Ls. membranes increases as the DS of SPESs increases, i.e. with the number of hydrophobic I.Ls. cations exchanged, as it is possible to observe comparing SPES_MEIM_0.5 (IIId) with SPES_MEIM_0.75 (IIIe) and SPES_MEIM_1 (IIIf), and it enhances as the length of the imidazolinium alkyl chains enhances, as shown in Figure IIIf for SPES_MEIM_1, in Figure IIIg for SPES_BBIM_1, in Figure IIIh for SPES_MOIM_1 and in Figure IIIi for SPES_BOIM_1.

Samples	θ_w *(air-side)*	θ_w *(PTFE-side)*
SPES_MEIM_0.5	$\overline{86}$±*2*	$\overline{108}$±*1*
SPES_MEIM_0.75	$\overline{85}$±*1*	$\overline{116}$±*1*
SPES_MEIM_1	$\overline{89}$±*1*	$\overline{121}$±*1*
SPES_BBIM_0.5	$\overline{88}$±*1*	$\overline{123}$±*1*
SPES_BBIM_0.75	$\overline{84}$±*2*	$\overline{124}$±*2*
SPES_BBIM_1	$\overline{81}$±*2*	$\overline{126}$±*1*
SPES_MOIM_0.5	$\overline{77}$±*1*	$\overline{124}$±*1*
SPES_MOIM_0.75	$\overline{80}$±*1*	$\overline{125}$±*2*
SPES_MOIM_1	$\overline{81}$±*1*	$\overline{128}$±*1*
SPES_BOIM_0.5	$\overline{85}$±*1*	$\overline{130}$±*1*
SPES_BOIM_0.75	$\overline{80}$±*1*	$\overline{131}$±*1*
SPES_BOIM_1	$\overline{81}$±*1*	$\overline{131}$±*1*

Table II. Static water contact angles of samples synthesized.

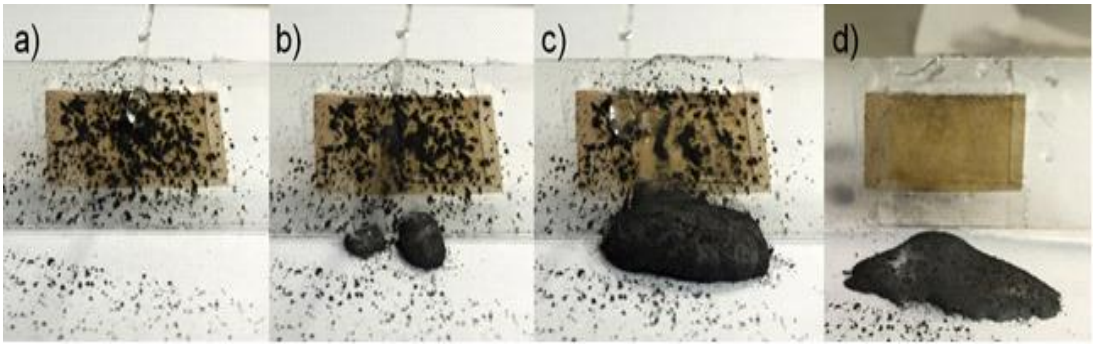

Figure II. Self-cleaning SPES films.

Comparing AFM topographies of the mold-side of pristine SPES (Figure IVa) and SPES_I.Ls. samples (Figure IVb, c, d, f, g and h), it is clear that the surfaces of SPES_I.Ls. are much rougher than the surface of SPES sample without I.Ls. When I.Ls. are present, it is possible to observe that the surface at the air-side of the membrane remains smooth (IVe). Conversely, the surface at PTFE-side changes from smooth to rough (IVd); Root-mean-square (RMS) roughness data range from 66.65 nm for the air-side to 185.15 nm for its PTFE- mold side.

The roughness of PTFE-side of SPES_I.Ls. membranes increases as the DS of SPESs increases, as it is possible to observe comparing SPES_MEIM_0.5 (IVb) with SPES_MEIM_0.75 (IVc) and SPES_MEIM_1 (IVd). This behavior was confirmed by RMS roughness values that for SPES_MEIM_0.5, SPES_MEIM_0.75 and SPES_MEIM_1 are 101.01 nm, 163.87 nm and 185.15 nm, respectively.

The influence of I.Ls. characterized by difference length of the imidazolinium alkyl chains was also investigated and the results obtained suggest that the roughness of the mold-side of SPES_I.Ls. membranes increases as the length of the imidazolinium alkyl chains increases, as shown in Figure IVe for SPES_MEIM_1 -RMS of 185.15 nm-, in Figure IVf for SPES_BBIM_1 -RMS of 192.78 nm-, in Figure IVg for SPES_MOIM_1 -RMS of 206.34 nm- and in Figure IVh for SPES_BOIM_1 -RMS of 236.85 nm-.

All AFM images and RMS roughness values obtained agree well with both SWCA data -i.e. the higher the contact angles, the rougher the surface- and SEM analyses, as previously shown in Figure III, confirming that the hydrophobic imidazolinium alkyl chains, orienting themselves during the evaporation of the solvent towards the mold surface, change the membrane surface in correspondence of PTFE-side from smooth to rough.

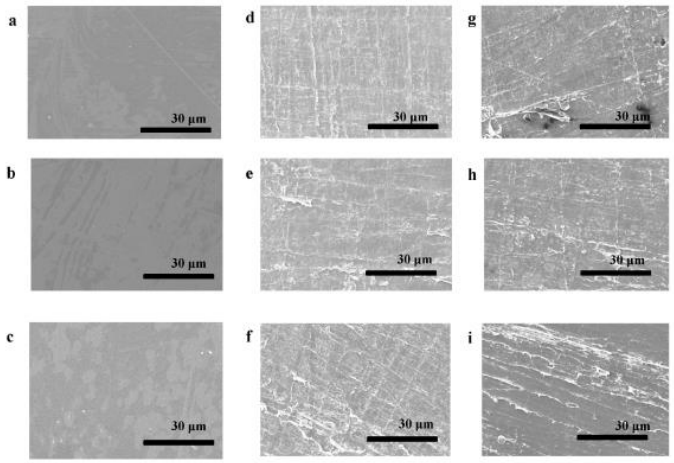

Figure III. (a) SPES_1 air-side; (b) SPES_1 PTFE-side; (c) SPES_MEIM_0.5 air-side; (d) SPES_MEIM_0.5 PTFE-side; (e) SPES_MEIM_0.75 PTFE-side; (f) SPES_MEIM_1 PTFE-side; (g) SPES_BBIM_1 PTFE-side; (h) SPES_MOIM_1 PTFE-side and (i) SPES_BOIM_1 PTFE-side.

Figure IV. (a) SPES_1 PTFE-side; (b) SPES_MEIM_0.5 PTFE-side; (c) SPES_MEIM_0.75 PTFE-side; (d) SPES_MEIM_1 PTFE-side; (e) SPES_MEIM_1 air-side; (f) SPES_BBIM_1 PTFE-side; (g) SPES_MOIM_1 PTFE-side and (h) SPES_BOIM_1 PTFE-side.

ii) SPES as dopant agent for both electrical conductive and polymeric films and screen printer inks.

OE based on polymers is a research field that is gaining more and more interest, both from an academic and an industrial point of view. Organic conductive materials could open several possibilities in the production of new advanced electronic devices: in fact, these materials can conjugate useful features such as flexibility, transparency, durability and lightness typical of polymers, with conductive properties, conferred by highly conjugated organic systems.

Polycarbonate (PC) is a polymer characterized by high durability and mechanical resistance, coupled with good thermal properties. One of the most valuable features of PC relies on its extremely good optical behavior: PC is often used as a substitute of glass because the refractive index of the two materials is very similar (1.5237 for glass and 1.5856 for PC at λ = 580 nm) but PC has higher mechanical properties, is lighter and is not fragile. Within this context also Polymethyl Methacrylate (PMMA) is an optimal material for transparent layers (PMMA = 1.4910 at λ = 580 nm) and its monomers can be easily functionalized.

The goal of this project was to develop an innovative material bearing at the same time carbonate moieties, useful for optical features, and acrylate groups, functionalized with conductive molecules, in order to obtain transparent conductive films. At first Polyallyl carbonate homopolymers were successfully synthesized through free radical polymerization (NMR, Gel Permeation Chromatography (GPC) and thermal studies were performed). As result of homopolymerization kinetics, it seems that the radical of the propagating species is a stable "pseudo-living" radical, able to initiate the growth of another polymeric chain characterized by conductive functionalities, in order to obtain block copolymers with high molecular weights and conductive continuity along the chain.

Acrylate monomers based on conductive molecules were synthesized; the organic molecules used are based on highly aromatic structure, Fluorene Bisphenol, known as "cardo structure". The high level of electronic delocalization given by the aromatic groups guarantees not only the conductivity, but also high thermal resistance. Polyallyl carbonate and functionalized PMMA block copolymers

were indeed successfully synthesized (Figure V) and fully characterized by NMR, GPC and thermal characterizations.

Starting from this new material, a transparent polymer film was obtained through solvent casting deposition. In order to improve the conductive features of this material, functional end-capped conducting 3,4-ethylene dioxy thiophene (EDOT) oligomers were synthesized. In particular, EDOT is the monomer adopted for the polymerization of Poly(3,4-ethylene dioxy thiophene) (PEDOT) oligomers, a famous commercial conductive polymer -known as Baytron®- usually doped with Sulphonated Polystyrene (PSS), that it is insoluble in the common organic solvent and therefore difficult to process.

In the present work a synthetic route able to enhance PEDOT solubility and conductivity was developed. Methacrylate-terminated PEDOTs were successfully synthesized via oxidative polymerization of EDOT and cross-linkable methacrylate end-capped EDOT, with ferric sulfate as oxidant (Figure VI). EDOT end-capping monomer was prepared through Friedel Crafts acylation starting from EDOT and methacryloyl chloride. The chemical structure and the degree of polymerization of the end-capped PEDOTs were determined by ^{1}H NMR spectroscopy.

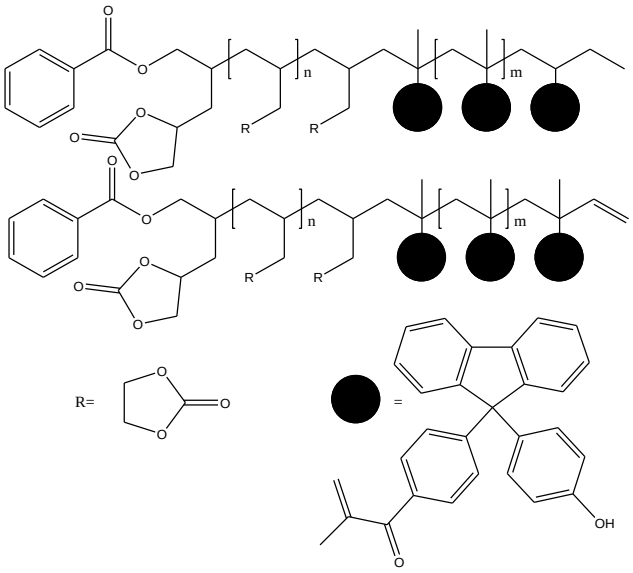

Figure V. Block copolymers of Polyallyl carbonate and functionalized methacrylic polymers.

End-capped PEDOTs have excellent solubility in several organic and chlorinated solvents. Furthermore, the use of cross-linkable end-caps makes EDOT-based oligomers soluble in organic and chlorinated solvents; the cross-linking of PEDOT film is then possible after UV exposure.

In order to improve PEDOT conductive properties, the dopant agents based on sulfonic groups commonly used with PEDOT are 2-Naphthalenesulfonic acid, paratoluene sulfonic acid or others. Besides these molecules, also SPES, obtained as reported previously, can be used as dopant agent thanks to both the charge separation deriving from the use of the pre-sulfonated comonomer and the possibility to modulate the moieties of sulfonic groups in the polymeric chains.

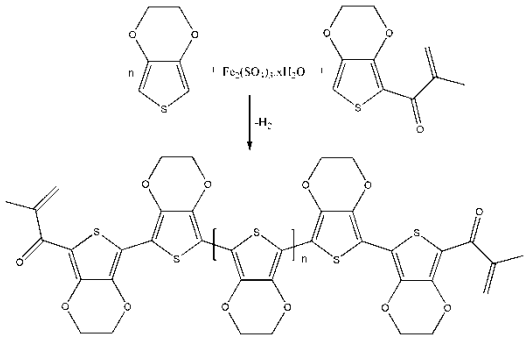

Figure VI. Synthetic route for methacrylate end-capped PEDOT.

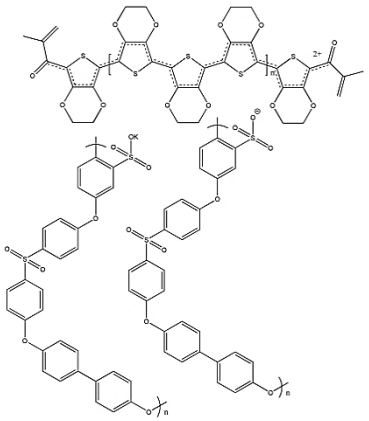

Figure VII. SPES as dopant agent for methacrylate end-capped PEDOT.

In this work, the oxidative polymerization of EDOT and functional end-capped EDOT monomers with ferric sulfate as oxidant and SPES as dopant was performed (Figure VII); it was found that PEDOT conductive features increase as SPES DS increases reaching 210 S/cm, a value 50 S/cm far higher than the one of commercial PEDOT (160 S/cm). The cross-linking of end-capped PEDOT with the block copolymers of Polyallyl carbonate and functionalized methacrylic polymers, through the vinyl functionalities, in then possible after UV exposure.

1. Polyarylether sulfones and Sulfonated Polyarylether sulfones

Background on Polymerization Route

Mechanism

Polyarylether sulfones (PES) form from polymerization of aryl halides with aryl hydroxy compounds. Polymerization involving these two functionalities may be carried out either as an AB-type homopolymerization or as an A2+B2-type copolymerization. The main chain is thus a sequence of aromatic rings connected via ether linkages formed by nucleophilic attack of the aryloxy anion on the electron-deficient carbon atom of the haloarene.

Reaction mechanism and kinetics have been widely studied and are known to agree with a bimolecular nucleophilic aromatic substitution, SN2Ar. Kinetic investigation by Attwood et al. (1) reports a general second-order rate with deviations according to reactants and catalyst. The general mechanism is one of addition/substitution as shown in Figure 1.

The activated site for the nucleophilic attack is the carbon atom bearing the halide. The attack by the phenolate ion yields a resonance-stabilized intermediate known as "Meisenheimer complex", whose formation is the rate-determining step of the reaction. The second step is faster and involves the leaving of the halide anion while aromaticity is re-activated in the phenyl ring.

Johnson et al. (2) excluded a monomolecular nucleophilic aromatic -SN1- mechanism (i.e. no free aryl cation or halide anion are formed) as no reaction between a dihalide and dimethyl sulfoxide (DMSO) was observed even at high temperature.

A benzyne-intermediate mechanism was ruled out too, as no 1, 2 neither 1, 3 linkages were observed; they concluded PES could only be obtained as an all 1, 4 product.

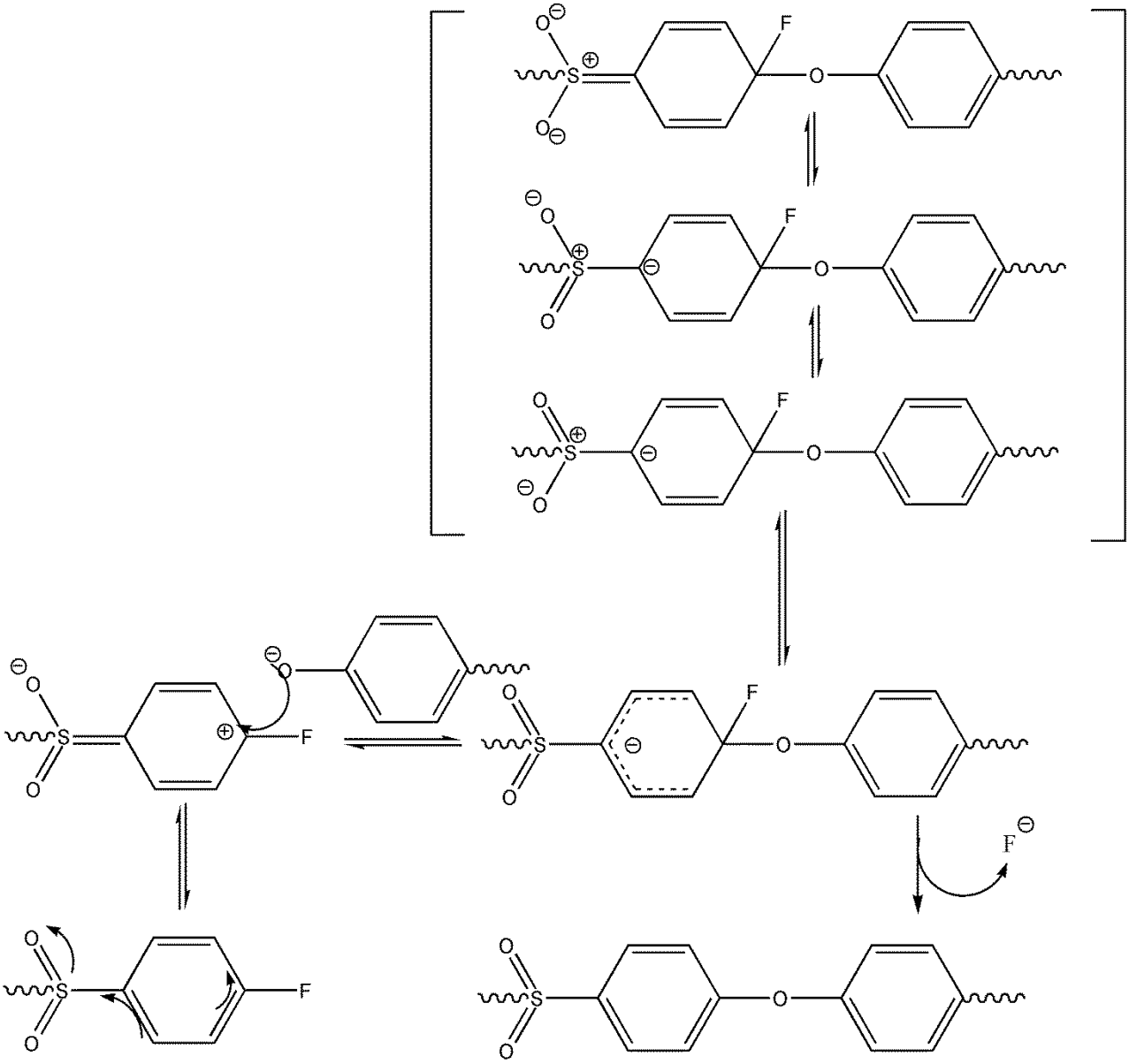

Figure 1. Mechanism of aromatic nucleophilic substitution with formation of the activated Meisenheimer complex.

Monomers reactivity

As the works by Attwood and Johnson demonstrated, grade of polymerization, reaction kinetics and, to some extent, mechanism show a dependence upon halide acidity and phenolate nucleophilicity (1), (2). An A2+B2 approach allows for a wider choice on monomer structure, thus highly reactive monomers can be employed both as A2 and B2 monomers, so that equilibrium can

be shifted more towards the products than by a homopolymerization. Moreover, since monomers can be varied independently, a tailored polymer microstructure can be achieved, e.g., selectively varying concentration of a bridging group or sulfonic acid group.

With respect to a homopolymerization, the drawback is sensitivity to unbalance in functional groups ratio, maximum degree of polymerization (DPn) being limited according to Carothers' equation (3).

Correlation between monomer structure, degree of polymerization, and reaction kinetics was reported in the study by Johnson et all. (2). They carried out several A2+B2-type polymerizations and explored a wide range of both dihalides and bis-phenolates.

Experimental results from that study proved diarylhalides with an electron-withdrawing group within the 4-4'-linkage more reactive due to stabilization of the intermediate complex by electron delocalization. To explain this, Attwood proposed a "bridge" mechanism, consistent with experimental reaction rates, according to which the electronic effect of a substituent in a phenyl ring is transmitted to other ring via the bridging group, so that a halogen in 1 position enhances reactivity of the halogen in 1'-position; conversely, an electron-donor phenoxide in the same position would slow down the halogen displacement and therefore the nucleophilic attack (1).

Results from the work by Johnson also emphasize the effect of the leaving halogen on the reaction kinetic rate: higher polymers are obtained when fluorides are used rather than chlorides, bromides and iodides. The accepted general trend of leaving group ability for a SN2Ar is therefore $F \gg Cl > Br \approx I$, though the carbon-halogen bond is increasingly weaker down the group.

This means favorable factors for diaryl halides to be reactive are reduced steric hindrance and electronegativity of the halogen atom, while halogen detachment appears not to be involved in the complex formation.

As to phenolate ion, experimental results proposed enhanced nucleophilicity arises when two phenyl rings are directly coupled or are connected by electron-releasing groups, such as ether, sulfide, and alkyl. On the contrary, electronegative substituents (e.g. in the AB monomer a halogen

in para position) and bridging ketone or sulfone groups between phenyl rings slow down the reaction by stabilization of the negative charge (2).

Since the actual reactant in the mechanism is an alkali bis-phenolate salt, influence of the metal cation on the reactivity of the nucleophile is of interest. A much higher reactivity was observed for potassium salts of the bis-phenolate compared to sodium salts. Magnesium, lithium and calcium salts were not considered in that study due to insolubility in DMSO (2). A different kind of ionic couple was reported by Kricheldorf (4), in which the bisphenol is silylated and reacted in situ with a catalytic amount of cesium fluoride in order to generate the nucleophilic bis-phenolate.

Solvents choice

Effectiveness of dipolar aprotic solvents in SN2Ar-type reactions was reported in an early paper by Miller and Parker (5). They observed higher rate constants for reactions in dipolar aprotic solvents with respect to reactions in protic solvents, due to a decreased hydrogen-bonding capacity and increased shielding of the dipole charges in the solvent molecule, e.g., an ion is less solvated in nitrobenzene than in water despite the latter having a lower dipole moment.

Obvious requirement for a solvent is inertness with respect to the reactants: as the SN2Ar like polymerization of PES involves bis-phenolates, an aprotic solvent is required. A high-boiling solvent is needed when reacting a monomer that is a poor nucleophile and possesses reduced solubility (e.g., bisphenol S), or when polymer is semi-crystalline, e.g. Polyether ether ketone (PEEK), and its precipitation is only prevented by employing high reaction temperatures.

Reaction in melted diphenylsulfone (DPS) allows for temperatures as high as 330°C, so that melting range of the polymer is approached. Solvation of alkali salts of bis-phenolate and sulfonic acid-bearing monomers requires not just a high temperature, but a highly dipolar solvent as well. Though no apparent correlation between polarity and reaction kinetics was reported (5): a highly polar

solvent provides a looser bis-phenate-cation ionic couple, thus enhancing bis-phenate nucleophilicity.

Common solvents for SN2Ar reactions are thus dimethylacetamide (DMAc), DMSO, N-methyl-2-pyrrolidone (NMP), sulfolane, molten diphenylsulfone and diphenylketone, since they all possess a dipole moment as high as 4 Debye and a boiling temperature above 150°C.

Catalyst choice

In the synthesis of PESs, a base catalyst is needed in order to deprotonate the aromatic diol to the more reactive bis-phenate. The obvious choice would be a strong base like sodium hydroxide (NaOH) or potassium hydroxide (KOH), whose reaction with bisphenol readily yields the di-anion. As it was reported in the pioneering study by Johnson, however, strict stoichiometric control of the amount of the hydroxide is needed: on the one hand, excess base starts hydrolytic side reactions; on the other hand, an insufficient amount of base offsets stoichiometry, preventing formation of high polymers (2).

A weak-base approach, such as potassium carbonate (K_2CO_3), was then followed starting from the work of Clendinning and Farnham (6).

Two feasible deprotonation mechanisms are proposed:

a) a dimethyl bis-phenate is formed by double deprotonation and reacts with two halide equivalents;

b) a mono-phenate (i.e., a hydroxy-diaryl halide) forms by reaction with one equivalent of K_2CO_3 and reacts with one halide; the AB dimer is then deprotonated to phenolate.

Actually, no di-substituted product is reported to form within the first 100 minutes of reaction. Exact stoichiometric amount of weak base is not required, in fact a 20% molar excess of K_2CO_3 is commonly employed. However, need for a water azeotropic agent arises, as reaction of diol with potassium carbonate yields potassium hydrocarbonate and carbonic acid, which in turn

disproportionate to water and CO_2. Like strong bases, water is detrimental to the degree of polymerization, therefore, toluene or xylene are usually employed as co-solvents.

Side reactions

Side reactions with water involve hydrolysis of phenolate anion (stoichiometric unbalance) and cleavage of aryl-ether bond (chain breaking). As was reported by Parker, no direct hydrolysis of the aryl halide is involved.

Presence of a strong base, like excess sodium or potassium hydroxide with respect to catalytic amount, affects final DPn in that it is a stronger nucleophile than the phenolate, thus preferentially attacking aryl halides. Other than unbalancing functional groups, this side reaction yields an unreactive para-hydroxy diaryl halide, which can also self-react.

Furthermore, a strong base cleaves aryl-ether bond, both hampering DPn and water content in polymerization vessel (5) leaving unreactive by-products.

A high reaction temperature, which is an advantage when considering solubility issues and reaction rate, can also activate side reactions by the halide anion liberated by the nucleophilic attack. Normally, F– or Cl– are salted out of solution when reacting with the alkali cation from the phenolate.

In dipolar aprotic solvent, fluoride ion is a powerful nucleophile and, at above 200°C, KF is soluble in the reaction mixture, allowing F– to disrupt ether linkages. Attwood found a linear increase in chain fission rate with the concentration of excess KF in solution (1); Colquhoun observed trans-etherification owing to the same process (7).

Sulfonated Polyarylether sulfones (SPESs)

As described so far, PES must carry anionic moieties along the chain in order to be effective as ionomers. Given its very high acidity, sulfonic acid is the preferred anionic group; values of pKa as low as -6 and -12 are known for, respectively, aryl sulfonic acid and perfluorosulfonic acid.

Introduction of the sulfonic acid moiety had initially been performed by post-sulfonation of an aromatic polymer. Especially with aryl sulfonic acid, solubility issues render the extent of sulfonation hardly controllable and inhomogeneously distributed between chains.

In addition, when electron-donor and electron-withdrawing linkages are both present, e.g., alternated ether and sulfone linkages in PES, sulfonation selectively occurs on the more activated phenyl ring.

Compared to post-sulfonation reaction of a polymer, copolymerization of sulfonated with unsulfonated monomers allows for a selective adjustment of the concentration of sulfonic acid and for regioselection of the acidic moiety. Sulfonation via co-polymerization must take into account the change in reactivity of sulfonated monomers, e.g., sulfonated dihydroxy compounds are less reactive than the unsulfonated compound. Nonetheless, quantitative introduction of sulfonated repeating units is established.

A different, non-random approach gained interest in recent years following the first accurate characterization of nano-phase separation in ionomer membranes. It consists in densely locating anionic groups along the main chain or in pendants by copolymerization of quantitatively sulfonated and unsulfonated oligomers, so that more effectual aggregation of highly ionic segments can take place to form large hydrophilic channels with hydrophobic regions aside.

2. Homogeneous synthesis and characterization of Sulfonated Polyarylether sulfones having low degree of sulfonation and highly hydrophilic behavior[1,2,3]

Overview

In the present work, the wettability of PESs was promoted through the controlled introduction of sulfonic groups in PES polymeric chain. Homogeneous synthesis using a sulfonated comonomer introduced sulfonic groups while exerting a tight control over the DS and avoiding the undesired side reactions brought about by heterogeneous sulfonation reactions.

A series of SPESs with very low amounts of sulfonic groups -0.5, 0.75 and 1 meq $SO_3^-*g^{-1}$ of polymer- was synthesized via polycondensation using 4,4'-difluorodiphenylsulfone, 4,4'-dihydroxydiphenyl and a sulfonated comonomer, 2,5-dihydroxybenzene-1-sulfonate potassium salt.

The presence of sulfonic groups was confirmed by FT-IR spectra; the macromolecular structure and the real DS of SPESs were determined by ^{1}H-NMR; the molecular weights were investigated by GPC measurements; Ion Exchange Capacity (IEC) values, measured by potentiometric titration, are in good agreement with the experimental DS.

The polyelectrolyte effect was studied via intrinsic viscosity measurements (IV). The effect of DS on the thermal properties of SPES membranes was studied by TGA and DSC analyses; wetting

[1] *Sabatini, V.; Checchia, S.; Farina, H.; Ortenzi, M.A. "Homogeneous synthesis and characterization of Sulfonated Polyarylethersulfones having low degree of sulfonation and highly hydrophilic behavior", 2016, Macromolecular Research. DOI: 10.1007/s13233-016-4105-6.*

[2] *Falciola, L.; Checchia, S.; Pifferi, V.; Farina, H.; Ortenzi, M. A.; Sabatini, V. "Electrodes modified with sulphonated poly(aryl ether sulphone): effect of casting conditions on their enhanced electroanalytical performance", 2016, Electrochimica Acta. DOI.org/10.1016/j.electacta.2016.02.110.*

[3] *Checchia, S.; Sabatini, V.; Farina, H.; Ortenzi, M.A. "Combining control of branching and sulfonation in one-pot synthesis of random sulfonated polyarylethersulfones: effect on thermal stability and water retention", 2017, Polymer Bullettin. DOI: 10.1007/s00289-017-1933-2.*

properties were characterized by SWCA measurements on membranes obtained via solution casting. The results showed that an increased DS results in higher T_g and lower water contact angles, the latter dropping from $\overline{91}°$ to $\overline{43}°$ as DS was raised from 0 to 1.0 meq $SO_3^-*g^{-1}$.

This work demonstrates that homogeneous synthesis of SPES is an efficient way to prepare SPES membranes with tightly controlled DS and enhanced hydrophilic properties, leading to an excellent hydrophilic SWCA even at very low amounts of sulfonic moieties.

Introduction

PES based membranes are widely used in advanced separation technology. Thanks to their excellent thermal tolerance, chemical stability, oxidation resistance as well as good mechanical behaviour, they make low-cost alternatives to expensive fluorinated polymers in fuel cells and in biomedical fields such as medical devices used for blood purification (8). Despite the many interesting features, the application of the PES membranes can be limited by their hydrophobic nature, which may lead to membranes fouling due to the absorption of non-polar solutes, hydrophobic particles or different kinds of bacteria (9).

Chemical modification of the PES macromolecular structure by introduction of a single functional groups (or their combination) on the polymeric matrix, such as sulfonic ($-SO_3H$), hydroxyl (-OH), carboxyl (-COOH), amino ($-NH_2$), or fluoro benzene groups, can largely affect the properties of PES membranes (10). Amon the "chemically modified" PESs, one of them, SPES, has received great attention in the last decade thanks to the improved wetting properties of PES membranes brought by the incorporation of sulfonic groups along the macromolecular chain. This allowed developing SPES membranes for a variety of separation processes, such as ion exchange, reverse osmosis, electro dialysis process and others (11), in which highly hydrophilic materials are required. Random SPES can be prepared via two different synthetic routes; one is the synthesis of PES followed by post-sulfonation reaction with sulfonating agents, commonly defined "heterogeneous synthesis"; the other one uses pre-sulfonated monomers in the feed of the polymerization reaction and is known as "homogeneous synthesis" (12). Since in the heterogeneous synthesis electrophilic sulfonating agents such as concentrated chlorosulfonic acid, sulphur trioxide-triethylphosphate complex, or trimethylsilyl chlorosulfonate (13) quantitatively attack the electron-rich aromatic rings along the polymeric chains, homogeneous synthesis is preferable because it allows a good control of the macromolecular architecture and of the DS of the polymer (14). In absence of a good control of the DS due to undesired reactions, in fact, it is difficult to correlate the DS variation of SPES with the change of the wetting properties of the

resulting membranes: this implies that SPESs with high DS are necessary in order to obtain SPES membranes with satisfactory hydrophilic features (15). Besides, sulfonation reaction of the pre-formed PES necessary for the heterogeneous synthesis involves side and degradation reactions (16), but despite all these drawbacks, heterogeneous synthesis is widely used due to its simplicity and low cost (17).

In order to improve hydrophilicity of SPES obtained via heterogeneous synthesis, Zhu et al. synthesized a PES bearing amino-substituted groups: several hydrophilic monomers such as N-isopropyl acrylamino and N, N-dimethylamino-2-ethyl methacrylate were successfully introduced into PES polymeric matrix using the amino substituted groups (18). Therefore, the combination of the amino substituted groups and post-sulfonation reactions resulted in a facile method for preparing SPES membranes with hydrophilic properties. However, the disadvantage of this method lies in the impossibility to control the substitution degree of the polymer, and to avoid side and degradation reactions during the post sulfonation of PES. This implies that there is no correspondence between DS of SPES and the wettability of SPES membranes thereof.

Furthermore, Wang et al. indicated that the hydrophilicity of PES membranes was significantly improved thanks to introduction of heparin-like PES (HLPES), synthesized by a combination of polycondensation and post-carboxylation method (19). However, since HLPES shows poor mechanical properties, it was necessary to blend HLPES with PES to achieve good mechanical properties.

The overall aim of this work was to establish a correlation between the DS of SPES copolymers obtained via one-pot synthesis, i.e. through homogeneous synthesis, and wetting features of SPES membranes, in order to develop new SPES membranes as advanced materials for several separation processes, such as ion exchange. As result, a tight control of the DS allowed to obtain SPES membranes characterized by highly hydrophilic behavior thanks to a concentration of sulfonic groups along the macromolecular chains far lower than the one used in previous scientific literature (20).

In this work, a series of SPESs with different DS were synthesized via direct condensation copolymerization starting from 4,4'-difluorodiphenylsulfone, 4,4'-dihydroxydiphenyl and a sulfonated comonomer, 2,5-dihydroxybenzene-1-sulfonate potassium salt.

The macromolecular structure of the polymers was determined via ^{1}H NMR spectra. The progressive increase of sulfonic groups as the DS increases was qualitatively determined by FT-IR analyses; real DS values of SPESs were quantitatively determined by ^{1}H NMR spectra and real IEC values were measured by potentiometric titration. Molecular weight data were investigated by SEC and intrinsic viscosities were measured using DMAc as solvent both with and without LiBr in solution in order to investigate polyelectrolyte effect on SPES samples.

On the basis of these analyses, the effects of DS on the thermal properties of SPES membranes obtained via solvent casting deposition were studied via TGA and DSC analyses; wetting features were investigated by SWCA measurements.

Experimental

Materials

4,4'-difluorodiphenylsulfone (BFPS, ≥99%), 4,4'-dihydroxydiphenyl (BHP, ≥97%), sodium chloride (NaCl, ≥99%), benzoic acid (≥99.5%) and lithium bromide (LiBr, ≥99%) were supplied by Sigma Aldrich; 2,5-dihydroxybenzene-1-sulfonate potassium salt (sulfonated hydroquinone, SHQ, ≥98%) was obtained from Alfa Aesar and potassium carbonate (K_2CO_3, ≥98% anhydrous) was purchased from Fluka; all the reagents were dried at 30°C in vacuum oven (about 4 mbar) for at least 24 h before use and employed without further purification. N-methyl-2-pyrrolidone (NMP, ≥99.5% anhydrous), dimethylacetamide (DMAc, ≥99.5%), N, N-dimethylformamide (DMF, 99.8% anhydrous), toluene (99.8% anhydrous), distilled water Chromasolv® (≥99.9%), hydrochloric acid (1.00 M HCl), standard sodium hydroxide solution (0.01 M NaOH) and dimethyl sulfoxide-d_6 (DMSO-d_6, 99.96 atom % D) were supplied by Sigma Aldrich and used without purification. Commercial Polyarylethersulfone -Radel® A-A-300A- was purchased from Solvay SA S.p.A.

Synthesis of PES and SPESs

One PES and three SPESs with increasing nominal DS, expressed as meq $SO_3^-*g^{-1}$ of polymer, -SPES_0.5, SPES_0.75, SPES_1- were synthesized. The exact amounts of the monomers used for the syntheses are reported in Table 1.

In a representative polymerization procedure, respectively BFPS, BHP and K_2CO_3 -the latter used as proton scavenger- for PES and BPS, BHP, SQH and K_2CO_3 for SPESs are introduced into a 100 cm^3 one neck round-bottom flask equipped with magnetic stirring.

Toluene and NMP are loaded in order to have a 10% mass/volume concentration of the reactants in the solution. The flask, equipped with a modified Dean-Stark device and under nitrogen atmosphere, is put in an oil bath and the polymerization reaction is carried out under reflux for 6 hr; the water formed during the reaction is continuously removed as an azeotrope with toluene

through the modified Dean-Stark device. After complete water removal, the temperature is gradually increased to 198°C and then the reaction mixture is kept 18 hr at 198°C. The hot, viscous, and dark-purple solution thus formed is precipitated into a large excess of cold water under stirring and a brown solid precipitated is obtained. The solid is recovered via filtration and then residual monomers, solvents and K_2CO_3 are removed carefully by washing with water. The difficult removal of solvents like NMP and toluene from PES and SPESs required repeating the purification procedure several times. After drying in a vacuum oven (about 4 mbar) at 50°C for 24 hr, the presence of residual solvents was checked via isothermal TGA analyses (2 hr at 150°C under nitrogen flow). Real DS is determined by ^{1}H NMR and confirmed by potentiometric titration.

Samples	nominal DS (meq SO_3^-*g^{-1} of polymer)	BFPS (g)	BHP (g)	SHQ (g)	K_2CO_3 (g)
PES	-	3.29	2.37	-	3.80
SPES_0.5	0.5	3.17	1.85	0.58	3.72
SPES_0.75	0.75	3.15	1.69	0.76	3.70
SPES_1	1	3.10	1.32	1.16	3.64

Table 1. Feed of the reagents for SPESs with different DS.

Characterization of polymers

Fourier transform- infrared (FT-IR)

The introduction of SO_3^- groups in SPES through the homogeneous synthesis was first checked by FT-IR spectroscopy, performed on a Spectrum 100 spectrophotometer (Perkin Elmer) in attenuated total reflection (ATR) mode using a resolution of 4.0 and 256 scans, in a range of

wavenumber between 4000 and 400 cm^{-1}. A single-bounce diamond crystal was used with an incidence angle of 45°.

Nuclear magnetic resonance: ^{1}H NMR

^{1}H NMR spectra were collected at 25°C with a BRUKER 400 MHz spectrometer. Samples for the analyses were prepared dissolving 10-15 mg of polymer in 1 cm^3 of DMSO-d_6.

Potentiometric Titration (PT)

A solution of benzoic acid (60 mg in 50 cm^3 of water) was prepared. A 0.01 M NaOH solution was used for titration. The titration of pure water (75 cm^3 of water) was performed first, giving the NaOH solution volume used for the titration, VH_2O (cm^3) (21); then, 10 cm^3 of benzoic acid solution were titrated, giving the NaOH solution volume used for the neutralization, Vbenz (cm^3). Solvent factor (f) was calculated using the following equation (Equation 1):

$$f = \frac{m}{Vtitr * Mbenz * [NaOH]} \qquad (1)$$

Where m is the weight of benzoic acid in solution (g); Vtitr is given by the difference between Vbenz and VH_2O (cm^3); [NaOH] is the concentration of 0.01 M NaOH solution ($mol*cm^{-3}$) and Mbenz is the molecular weight of benzoic acid (122.12 $g*mol^{-1}$).

SPES samples were converted to the acid form by immersion of 200-300 mg of each sample in 40 cm^3 of 1 M HCl solution for 24 hr at 80°C, followed by washing with water for 24 hr at room temperature. IEC of SPESs was measured after soaking the protonated sample in 20 cm^3 of 2M NaCl solution for at least 24 hr. The solution was then titrated with a 0.01 M NaOH solution using a Titrino751 GPD automatic potentiometric titrator (Metrohm).

IEC data can be calculated using the following equation (Equation 2):

$$IEC = \frac{[NaOH]*V*f}{x} \qquad (2)$$

where [NaOH] is the concentration of 0.01 M NaOH solution (mol*cm^{-3}); V is the NaOH solution volume used during the neutralization of each sample (cm^3); f is the solvent factor obtained as described in Equation 1 and x is the weight of sample (g).

Intrinsic viscosity (IV)

The intrinsic viscosity of the polymers was measured using an Ubbelohde viscometer in a thermostatic water bath at 25°C. Samples were dissolved in DMAc with and without 0.05 M LiBr solution and analysed in the concentration range 1-0.3 g*dl^{-1}.

Size Exclusion Chromatography (SEC)

The molecular weight of the polymers was evaluated using a SEC system consisting of a Waters 1515 Isocratic HPLC pump, four Waters Styragel columns set (HR3-HR4-HR5-HR2), and a Refractive Index (RI) detector Waters 2487 Detector. Analyses were performed at room temperature, using a flow rate of 1 cm^3/min and 40 µl as injection volume. Samples were prepared by dissolving 40 mg of polymer in 1 cm^3 of anhydrous DMF; before the analysis, the solution was filtered with 0.45 µm filters. Molecular weight data were expressed in polystyrene (PS) equivalents. The calibration was built using monodispersed PS standards having the following nominal peak molecular weight (Mp) and molecular weight distribution (D): Mp = 1600000 Da (D≤1.13), Mp = 1150000 Da (D≤1.09), Mp = 900000 Da (D≤1.06), Mp = 400000 Da (D≤1.06), Mp = 200000 Da (D≤1.05), Mp =90000 Da (D≤1.04), Mp =50400 Da (D=1.03), Mp= 30000 Da (D=1.06), Mp = 17800 Da (D=1.03), Mp = 9730 Da (D=1.03), Mp = 5460 Da (D=1.03), Mp = 2032 Da (D=1.06), Mp = 1241 Da (D=1.07), Mp = 906 Da (D=1.12), Mp = 478 Da (D=1.22); Ethyl benzene (molecular weight = 106 g/mol). For all analyses, 1,2-dichlorobenzene was used as internal reference.

Preparation of PES and SPESs membranes

Membranes of PES and SPES were obtained from solution casting. The polymers were dissolved in DMAc using 21% mass/volume concentration and the corresponding solutions were cast onto a PTFE substrate. The solvent was evaporated for 24 hr in vacuum oven (about 4 mbar) at 40°C. Membrane thickness was in the range 120-125 μm, as evaluated using a Nikon eclipse ME600 optical microscope with Nikon digital camera light DS_Fi1, software Nis-Elementi BR, magnification 50X.

Characterization of the membranes

Thermogravimetric Analyses (TGA)

TGA measurements were performed using a TGA4000 Perkin Elmer instrument; analyses were conducted under nitrogen atmosphere on samples weighting from 5 to 10 mg each, in a single heating ramp from 30°C to 800°C at a 10°C/min rate.

Differential Scanning Calorimetry (DSC)

DSC analyses were conducted using a Mettler Toledo DSC 1, on samples weighting from 5 to 10 mg each. T_g of the samples were measured using the following temperature program:

i) heating from 25°C to 340°C at 10°/min;

ii) 5 min isotherm at 340°C;

iii) cooling from 340°C to 25°C at 10°C/min;

iv) 5 min isotherm at 25°C;

v) heating from 25°C to 340°C at 10°C/min (T_g data were measured here).

Static Water Contact Angle (SWCA)

Surface wetting properties of membranes were characterized by static contact angle measurement using a Krüss Easydrop Instrument. A 5*5 cm membrane was attached on a glass slide. For the measure, a total of 1 μl of double distilled water was dropped on the air-side

surface of the membranes. At least five measurements were taken on each sample to get reliable values. The measurements error was ±3°. The same procedure was performed on the PTFE-side surface of the membranes.

Results and Discussion

Synthesis and characterization of PES and SPESs: FT-IR, ^{1}H NMR, PT, IV and SEC analyses

A series of SPES copolymers with three nominal DS -0.5-0.75-1.0- were successfully synthesized by the aromatic nucleophilic substitution reaction of 4,4'-difluorodiphenylsulfone (BFPS), 4,4'-dihydroxydiphenyl (BHP) and a sulfonated comonomer, 2,5-dihydroxybenzene-1-sulfonate potassium salt (SHQ), in toluene and NMP (see Scheme 1).

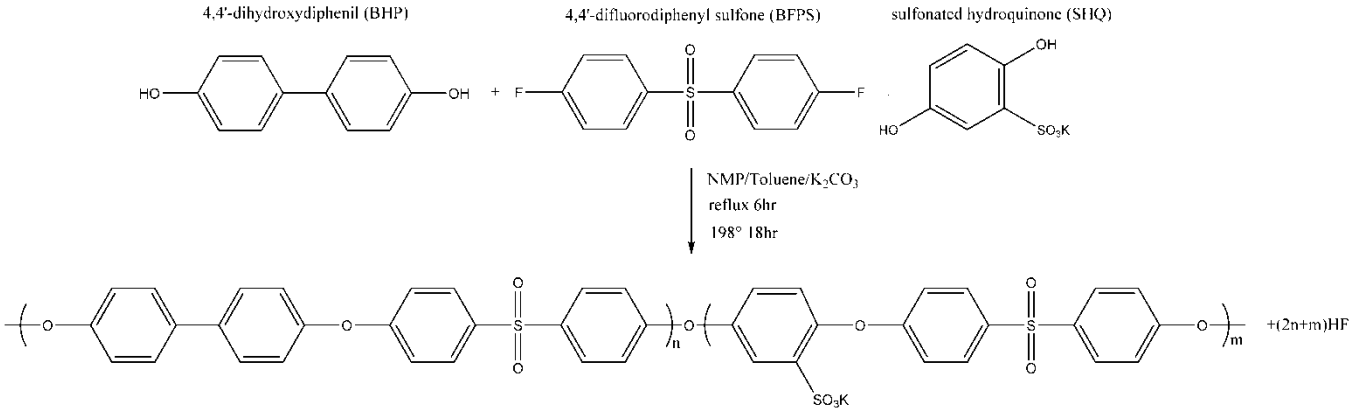

Scheme 1. Synthesis route for sulfonated PES.

Toluene was used to form the NMP/toluene/water ternary azeotrope, required for dehydrating the system in the first stage of the reaction since water is produced by the protonation/disproportionation of K_2CO_3. For comparison, by the same procedure, a PES copolymer was synthesized using BHP and BFPS 1:1 stoichiometry; its chemical structure is illustrated in Figure 2.

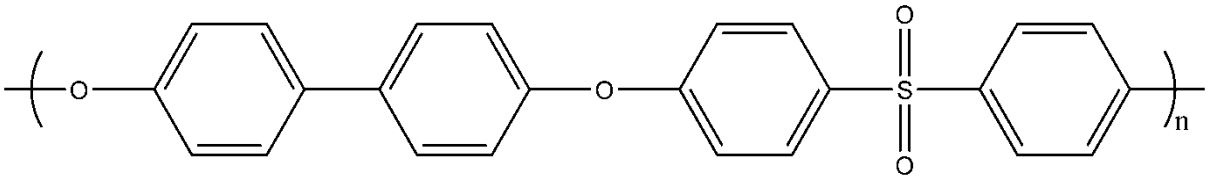

Figure 2. PES chemical structure.

The introduction of SO_3^- groups in SPES by direct copolymerization reaction was qualitatively confirmed by FT-IR spectra, as shown in Figure 3. The peaks at ~1580 cm^{-1} (**a**) and 1490 cm^{-1} (**b**) are related to vibration of the aromatic ring; the peak for aryl oxide is at ~1245 cm^{-1} (**c**) and the characteristic absorption band for the aromatic sulfone group appears at ~1152 cm^{-1} (**d**) (22). The absorption peak at ~1028 cm^{-1} (**e**) is characteristic of the aromatic SO_3^- symmetric stretching vibration, indicating the presence of SO_3^- groups in SPES samples: the intensity of this absorption peak gets higher as the DS increases (23). This behaviour indicates that the homogeneous synthesis of SPESs with different DS was successfully conducted.

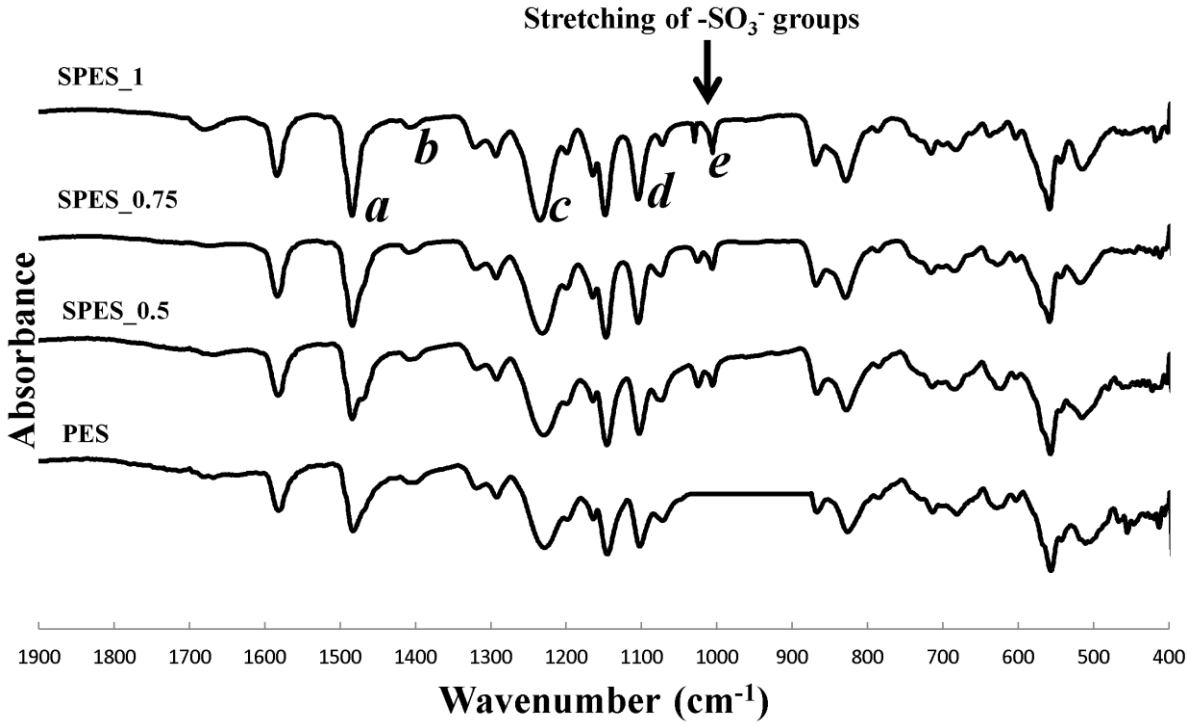

Figure 3. FT-IR spectra of PES and SPES with different DS.

^{1}H NMR was used to determine the macromolecular structure of PES and SPES copolymers and the real DS of SPES samples. The ^{1}H NMR spectrum of SPES_0.5 (Figure 4) shows that signals relative to the presence of SHQ monomer and those relative to its interaction with BFPS give rise to five peaks: **(e)**: doublet at 7.00 ppm**; (h)**: wide doublet at 7.05 ppm; **(i)**: overlapping with peak **(c)** at 7.15 ppm; **(g)**: doublet at 7.45 ppm; **(f)**: doublet at 7.85 ppm**.**

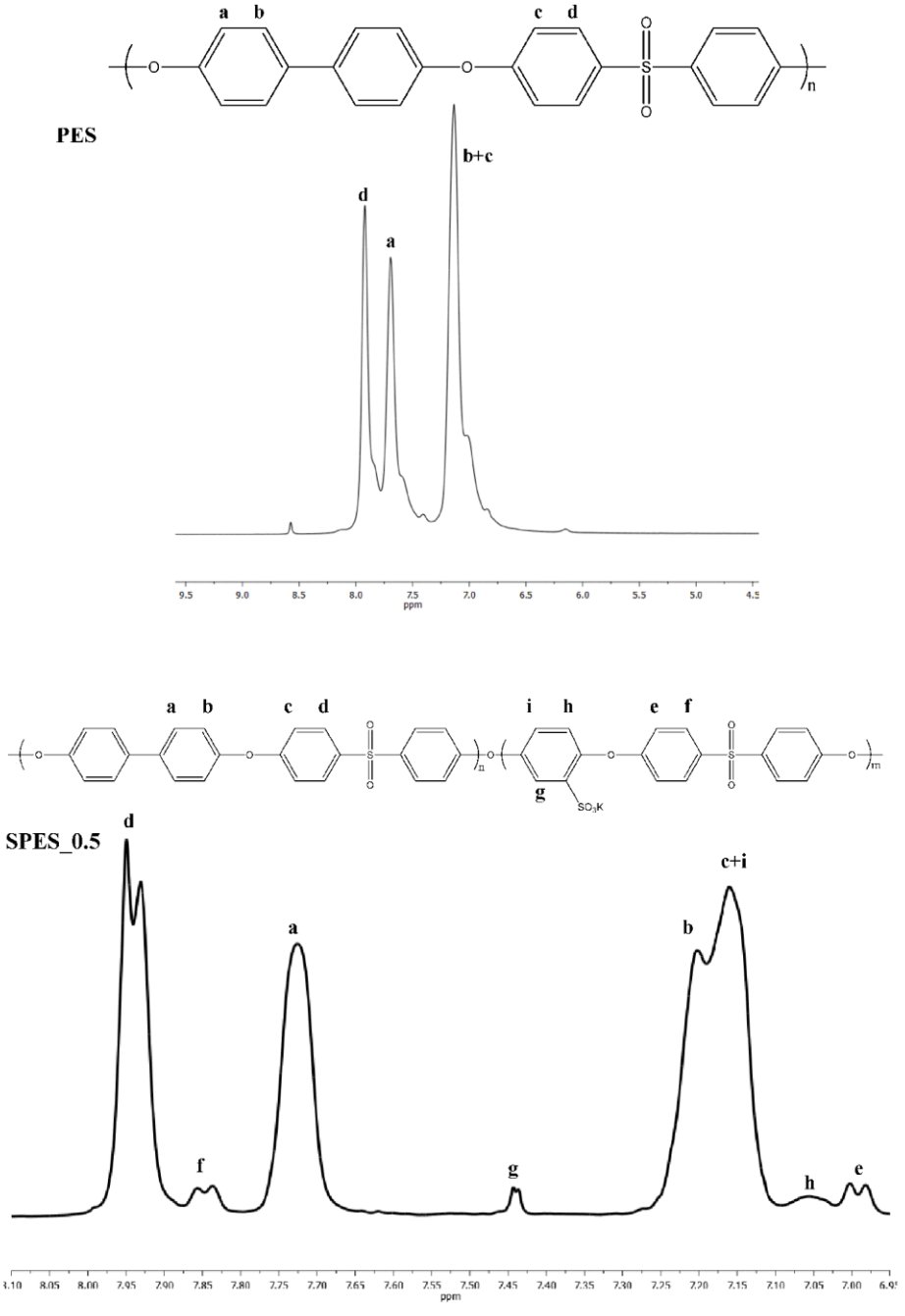

Figure 4. ^{1}H NMR spectra of PES (top) and SPES_0.5 (bottom).

The comparison of ^{1}H NMR spectra of SPES samples with different concentration of SO_3^- groups (Figure 5) shows the increase of the integral areas of the peaks relative to SHQ (**i**, **g** and **h**), and of those related to its interaction with BFPS (**e** and **f**), as a function of the DS.

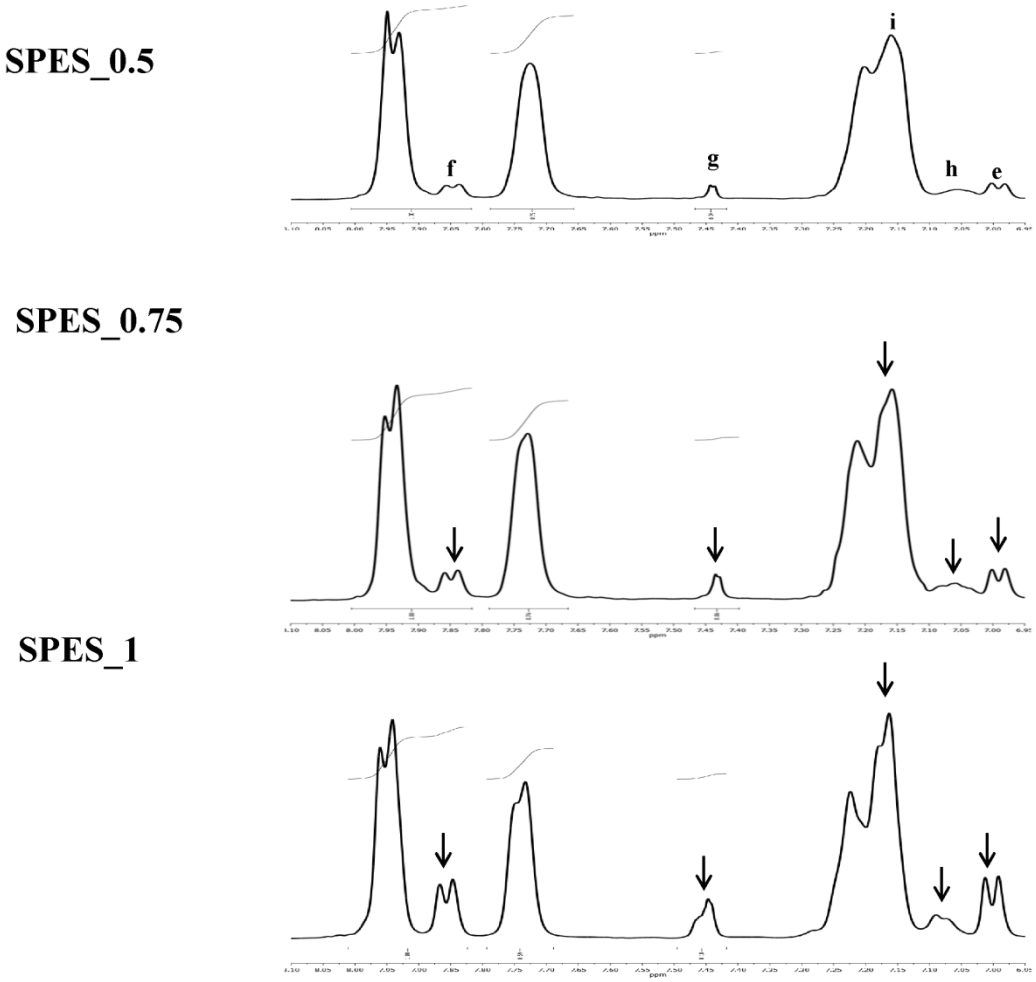

Figure 5. ^{1}H NMR spectra of SPES_0.5 (top), SPES_0.75 (middle), and SPES_1 (bottom).

The presence of SO_3^- groups in SPES samples was quantitatively measured via ^{1}H NMR calculating the integral ratios between the proton in ortho to the sulfonic group **[g]** of SHQ and the ones of BFPS **[d], [f]** and of BHP **[a]**, using Equation 3:

$$DS = \frac{(Ig*1000)}{\left(\frac{Id,f*UrBFPS}{4}\right)+\left(\frac{Ia*UrBP}{4}\right)+(Ig*UrSHQ)} \qquad (3)$$

where Ig is the integral area of peak **[g]**; Id,f is the total integral area of the peaks **[d]** and **[f]**; Ia is the integral area of the peak **[a]**; UrBFPS corresponds to the molecular weight of BFPS repeat unit (216.25 g*mol^{-1}); UrBP corresponds to the molecular weight of BP repeat unit (184.21 g*mol^{-1}) and UrSHQ corresponds to the molecular weight of SHQ repeat unit (226.26 g*mol^{-1}).

In Table 2 the real DS values of SPES samples, determined using Equation 3, are listed; all the values are in good agreement with the nominal DS expected for SPESs, which suggests that the homogeneous synthesis was successfully performed for all SPES samples and that undesired degradation and side reactions typical of heterogeneous sulfonation method are negligible.

Samples	nominal DS (meq $SO_3^{-*}g^{-1}$ of polymer)	^{1}H NMR DS (meq $SO_3^{-*}g^{-1}$ of polymer)	PT IEC (meq $SO_3^{-*}g^{-1}$ of polymer)	[η] (dl*g^{-1})	$\overline{Mn}$ (Da)	$\overline{Mw}$ (Da)	D
Radel® A-A-300A	-	-	-	0.17	22199	39871	1.79
PES	-	-	-	0.16	21522	37918	1.76
SPES_0.5	0.50	0.48	0.49	0.34	23727	43460	1.83
SPES_0.75	0.75	0.70	0.74	0.49	25431	48573	1.91
SPES_1	1.00	0.98	0.95	0.72	26679	52870	1.98

Table 2. DS, IEC, Intrinsic Viscosity (η) and GPC values of PES and SPES samples.

To verify the accuracy of the DS data obtained, the IEC values of SPESs were measured by PT. As seen in Table 2, the IEC values measured by PT are close to DS data determined by ^{1}H NMR, confirming the accuracy of measurements performed from ^{1}H NMR spectra. Solution viscosity, and especially intrinsic viscosity, is one of the most important parameters used to characterize PES and SPES molecular weights; dilute solution viscosity measurements are widely used in

polymer science, but have not been well developed for ion-containing proton exchange membranes (24). One possible reason is that by comparing neutral and ion-charged macromolecules, neutral systems retain their random coil conformation down to very low concentrations. By contrast, it is well known that the polyelectrolyte effect appears when ion-charged macromolecules are diluted in solution; this effect causes higher "dilute-solution" reduced viscosities as the concentration gets lower, largely due to charge repulsion (25). Therefore dilute solution viscosities of polyelectrolytes should be measured in the presence of a low-molar mass salt, which is able to neutralize the charges (26).

Li et al provided IV data for SPES copolymers and they found that the values obtained were not comparable to those of non-sulfonated PES, since the polymer electrolyte chains interact via sulfonic groups; they found out that 0.05 M LiBr is enough to get the correct IV values when analysing SPES (27).

In the present work, the IV of PES and SPES samples was measured in DMAc both with and without LiBr using a polymer concentration in the range of 1-0.3 $g*dl^{-1}$, in order to investigate the interaction of the electrolyte chains having sulfonic groups.

For the SPES_1 sample, correlations of viscosities and concentration are plotted in Figure 6 (i) without LiBr and (ii) with 0.05 M LiBr.

When the polymer concentration is decreased and no LiBr is used, the reduced viscosity decreases while the inherent viscosity increases; this behaviour is not consistent with the polyelectrolyte effect (28). However, the use of LiBr has little or no effect, leaving the viscosities (reduced and inherent) - concentration relationships very similar to what attained in pure DMAc; by comparing the IV data measured no significant difference emerges between the values obtained with and without LiBr. One possible explanation is that the small amount of $SO_3^-K^+$ groups present, i.e. the small amount of polymer electrolyte chains, is not able to interact via sulfonate groups, suggesting that the polyelectrolyte effect might depend on the amount of $SO_3^-K^+$ groups present in the polymer chains (29).

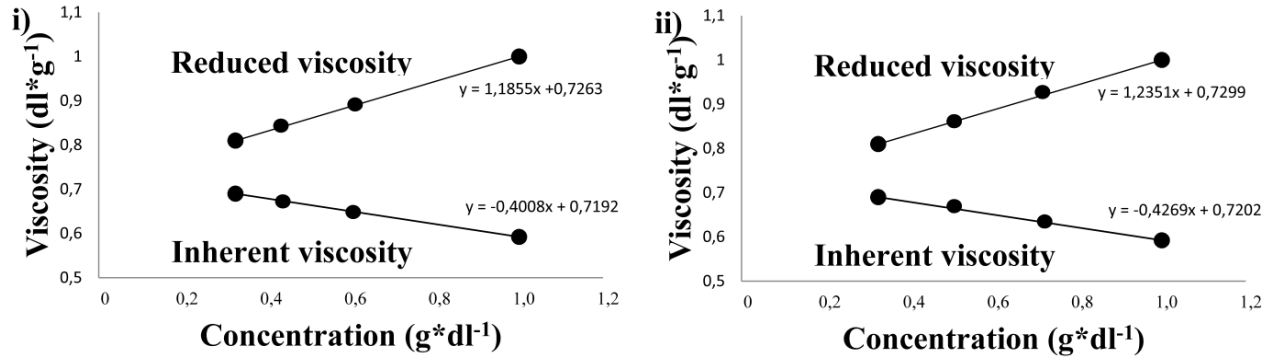

Figure 6. Correlation of reduced and inherent viscosities for SPES_1 in pure DMAc (i) and DMAc containing 0.05 M LiBr (ii).

IV of the samples was calculated considering the values obtained when no LiBr is used and the resulting values (Table 2) range from 0.34 to 0.72 dl*g^{-1}. Furthermore, a comparison of number average molecular weights ($\overline{Mn}$), weight average molecular weights ($\overline{Mw}$) and molecular weight distribution (D) between commercial PES, Radel® A-A-300A, and PES/SPESs samples prepared, determined via SEC and expressed as polystyrene equivalents, is provided in Table 2; the data reported confirm that high molecular weights were obtained.

Membranes characterization: TGA, DSC and SWCA analyses

Thermogravimetric analyses (TGA)

Given the difficulty in completely removing solvents like NMP and toluene from PES and SPESs, the polymers were washed with water for a week, dried in a vacuum oven (about 4 mbar) at 50°C for 24 hr and then the absence of residual solvents was checked via isothermal TGA analyses (2 hr at 150°C under nitrogen flow). The thermal stability of PES and SPES samples was estimated evaluating temperatures corresponding to 1%, 5%, 10%, 30% and 60% of weight loss ($T_{1\%}$, $T_{5\%}$, $T_{10\%}$, $T_{30\%}$ and $T_{60\%}$); results obtained are reported in Table 3.

PES is a very thermostable polymer which completely decomposes only at high temperatures, up to 560°C. In the case of SPES, two characteristic steps of weight loss are visible: the thermal decomposition of SO_3^- groups at around 300-330°C and the thermal degradation of the polymer starting from around 450-500°C, related respectively to the breaking of -SO_2 bonds and the degradation of the polymeric chains respectively (30).

Associating $T_{1\%}$ with the thermal decomposition of SO_3^- groups and $T_{60\%}$ with the breaking of -SO_2 bonds, it can be clearly seen from Table 3 that $T_{1\%}$ of SPES samples tends to decrease with respect to unsulfonated PES as the more SO_3^- groups were introduced into the polymer chains during the homogeneous synthesis, namely, on increasing DS.

$T_{1\%}$ of SPES_0.5 is 91.7°C lower than the one of PES and $T_{1\%}$ of SPES_1 was even lower, 107.9°C below $T_{1\%}$ of PES. The trend of $T_{60\%}$, 565.6°C, 457.0°C, 450.6°C and 444.1°C, respectively, for PES, SPES_0.5, SPES_0.75 and SPES_1, indicates that also the thermal degradation temperature of SPES main chain tends to decrease with an increased amount of SO_3^- groups in the polymer chains.

As a general statement, the high temperatures of thermal decomposition of SO_3^- groups measured - higher than 300°C in each case- evidence the good thermal stability of all the SPESs.

Samples	$T_{1\%}$ (°C)	$T_{5\%}$ (°C)	$T_{10\%}$ (°C)	$T_{30\%}$ (°C)	$T_{60\%}$ (°C)
PES	420.1	431.2	473.2	547.4	565.6
SPES_0.5	328.4	338.4	378.5	398.5	457.0
SPES_0.75	315.2	325.2	376.7	396.1	450.6
SPES_1	312.2	322.2	372.1	390.8	444.1

Table 3. Degradation data of the samples synthesized.

Differential Scanning Calorimetry analyses (DSC)

In addition, DSC was used to assess the thermal properties of PES and SPES samples. As reported in Figure 7, SPESs synthesized have very high T_g compared to PES: PES T_g is 209.7°C, a value that increases up to 259.7°C for SPES_0.5, to 290.9°C for SPES_0.75 and to 303.6°C for SPES_1. Generally T_g tends to rise with the increased amount of SO_3^- groups introduced into the polymer chains, owing to the increasing quantity of the rigid and bulky SHQ present in the polymer chains (31). Besides, as the quantity of SO_3^- increases, T_g gets closer and closer to $T_{1\%}$, i.e. to the beginning of SPES thermal degradation, indicating that the latter occurs as soon as polymer chains are able to move.

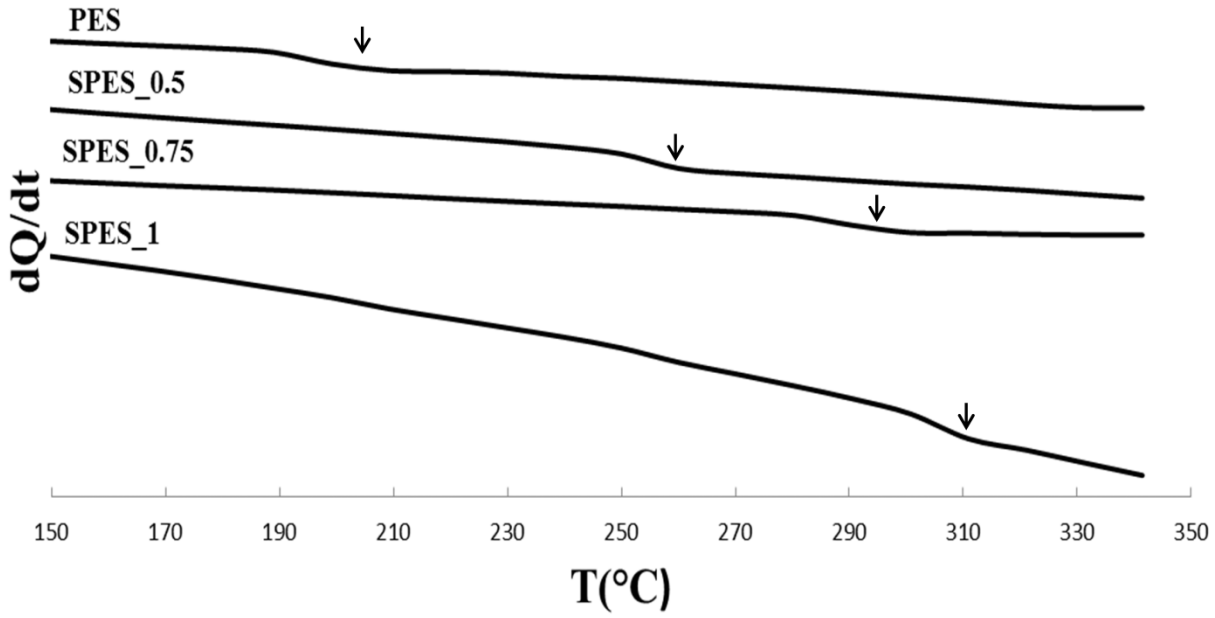

Figure 7. Second heating DSC curves of PES and SPES samples.

Static Water Contact Angle analyses (SWCA)

Water contact angle measurements are commonly used to characterize the hydrophilicity or hydrophobicity of an inorganic/organic surface; in the present work, SWCA measurements were

conducted in order to investigate the wettability of SPES membranes obtained from solution casting.

The samples were solution cast onto a PTFE mould, obtaining membranes having a thickness of 120-125 μm; the wetting properties of the membranes were measured both at the air-side and at the PTFE-side surface and Table 4 shows the results obtained.

Water contact angle of the PES membrane is as high as $\overline{91}$°, which is consistent with the results reported by other authors in previous works (31). The water contact angles measured for SPES_0.5, SPES_0.75 and SPES_1, $\overline{65}$°, $\overline{50}$° and $\overline{43}$°, respectively, indicate that the hydrophilicity of SPES membranes is enhanced by a higher concentration of $-SO_3^-K^+$ in the SPES membranes, as expected from the high polarity of the $-SO_3^-$ groups.

Samples	θ_w side air (°)	θ_w side PTFE (°)
PES	$\overline{91}$±1	$\overline{93}$±1
SPES_0.5	$\overline{65}$±2	$\overline{83}$±1
SPES_0.75	$\overline{50}$±2	$\overline{74}$±1
SPES_1	$\overline{43}$±1	$\overline{59}$±2

Table 4. Static water contact angle of samples synthesized.

It is important to underline that, thanks to the homogenous synthesis of SPES, the hydrophilic properties are greatly improved by low amounts of sulfonic groups. Zhao et al., studying a heterogeneous sulfonation reaction of PES, reported that the hydrophilicity of PES membranes was improved by blending PES sample with SPES having DS up to 1.5 meq $SO_3^-*g^{-1}$, i.e. 24.5% m/m of sulfonic groups. Their PES/SPES blends were characterized by different percentages of SPES, from 1 to 4% wt., and the water contact angles ranged from $\overline{83}$° to $\overline{62}$° (32).

SPES obtained by homogeneous synthesis in our case result in contact angle values far below those reported for SPES obtained from heterogeneous synthesis: water contact angle measured for SPES_1, containing 20.9% m/m of sulfonic moieties, is 25° lower than the one measured by Zhao in the case of SPES with 1.5 meq $SO_3^-*g^{-1}$. Also, Klaysom et al., who described the synthesis of SPESs through the introduction of sulfonate groups to PES by means of sulfonation reaction using chlorosulfonic acid as the sulfonating agent, reported that the best SWCA data, $\overline{67.82}°$ and $\overline{58.69}°$, were obtained with SPES having 0.53 and 0.73 meq $SO_3^-*g^{-1}$, respectively (33).

In this work, better values of SWCA were attained using lower concentrations of sulfonic groups, respectively, 0.50 and 0.70 meq $SO_3^-*g^{-1}$.

Results reported suggest that homogeneous synthesis of SPESs, as illustrated in Figure 8, allowing a tight control over DS, is an efficient way to prepare SPES membranes having enhanced hydrophilic features, i.e. excellent hydrophilic SWCA data, and low concentration of sulfonic groups. By contrast, PES sulfonation reactions require high concentrations of sulfonic groups in order to obtain comparable wetting properties in SPES membranes. Furthermore, the heterogeneous sulfonation routes are often troubled by side reactions leading to polymer degradation or crosslinking, as well as loss of sulfonic groups from the unstable position during ion-exchange operations.

The increase of θ_w observed on the PTFE-side for SPES membranes with respect to the air-side is probably due to the organization of the $SO_3^-K^+$ groups of the polymeric chains occurring during the evaporation of the solvent and to the interaction with the high hydrophobic PTFE surface. Therefore, as reported for θ_w observed on the air-side of SPES membranes, the water contact angles significantly decrease with the increase of DS.

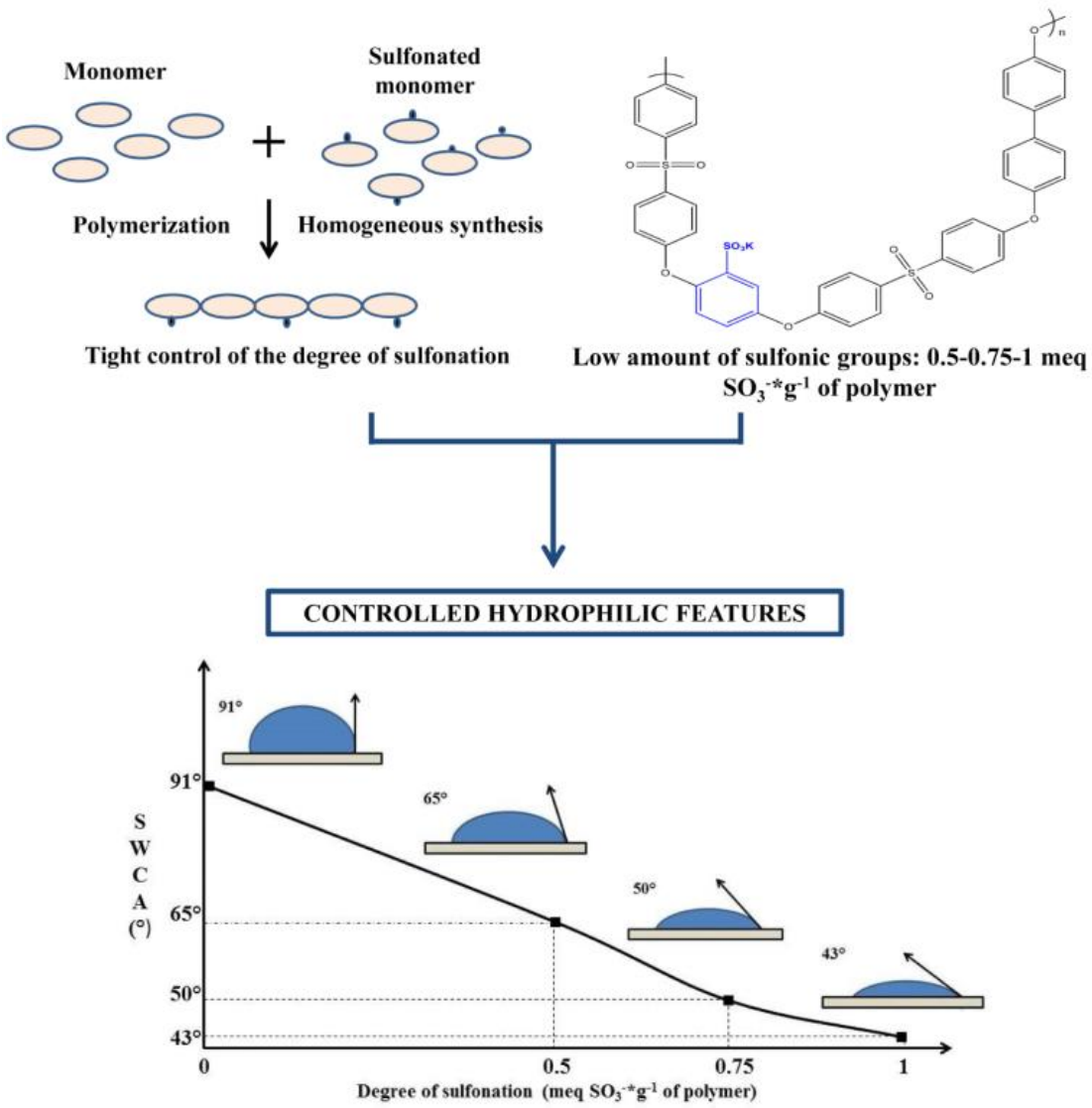

Figure 8. Correlation between the DS of PES/SPES samples prepared and SWCA data.

Conclusion

In this work a series of SPESs copolymers with different DS was successfully synthesized via homogeneous synthesis starting from a sulfonated comonomer, 2,5-dihydroxybenzene-1-sulfonate potassium salt; this procedure permits easy control of DS and allows good molecular weight, thermal and hydrophilic properties of the resulting polymers.

Combining ^{1}H NMR, Potentiometric Titration, Intrinsic Viscosity and FT-IR, it is possible to conclude that homogeneous synthesis of SPESs described in this work permits to easily modulate the DS of the polymers, to avoid both the side reactions and degradation that are likely to occur in indirect sulfonation reactions, and to obtain high molecular weight copolymers, whose intrinsic viscosities range from 0.34 to 0.72 $dl*g^{-1}$. Study of the polyelectrolyte effect on intrinsic viscosity data showed that the effect is absent in SPES with low amounts of sulfonic groups. The thermal properties of SPESs are significantly affected by increasing the DS: T_g data increase, rising from 259.7°C (SPES_0.5) to 303.6°C (SPES_1) and approaching the onset of thermal degradation; the weight loss of SPESs at 330°C tends to increase with the increased amount of SO_3^- groups introduced into the polymer chains. The contact angle characterization of SPES samples provided very useful guidelines in designing SPES membranes with close correlation between DS and hydrophilic properties; the water contact angles decrease from $\overline{91}°$ to $\overline{43}°$ as the DS is raised, showing that a tight control of the DS promotes a highly hydrophilic behavior of SPES membranes already in presence of a very low amount of sulfonic groups.

The results obtained suggest that homogeneous synthesis of SPES allows a direct control over DS during the polymerization; it is an efficient way to prepare SPES membranes having arbitrary hydrophilic features, i.e. excellent hydrophilic SWCA data, involves lower concentrations of sulfonic groups and proves to be more effective than the more traditional heterogeneous synthesis.

3. A novel synthetic approach to tune the surface properties of polymeric films: Ionic Exchange Reaction between Sulfonated Polyarylether sulfones and Ionic Liquids[1,2]

Overview

Currently, no studies dealing with the role played by Ionic Liquids (I.Ls.) on tailoring surface features of polymer films are available. In this work, the wetting properties of SPESs were modulated through a novel ionic exchange reaction between the K^+ cation of SPESs sulfonic moiety and different I.Ls., synthesized changing the length of the cation apolar groups. I.Ls. rate of substitution was determined by ^{1}H-NMR and SPES_I.Ls. thermal properties were evaluated by DSC analyses. The photo-chemical stability of SPES_I.Ls. samples was also successfully tested via a preliminary aging study. SPES_I.Ls. films were characterized by SWCA measurements to study the resultant wetting properties and by Scanning Electron Microscopy (SEM), Atomic Force Microscopy (AFM) and FT-IR analyses to determine morphology and surface roughness; their self-cleaning capability was also successfully tested.

The hydrophobic properties of SPES_I.Ls. films were found to improve with both the increase of SPESs DS and with the length of I.Ls. alkyl chains, allowing obtaining SPES_I.Ls. films having contact angles as high as $\overline{130}°$.

[1,] Sabatini, V.; Farina, H.; Montarsolo, A.; Ardizzone, S.; Ortenzi, M.A. "A novel synthetic approach to tune the surface properties of polymeric films: Ionic Exchange Reaction between Sulfonated Polyarylethersulfones and Ionic Liquids", 2016, Polymer Plastics Technology & Engineering. DOI: 10.1080/03602559.2016.1227845.

[2.] Soliveri, G.; Sabatini, V.; Farina, H.; Ortenzi, M. A.; Meroni, D.; Colombo, A. "Double side self-cleaning polymeric materials: the hydrophobic and photoactive approach". 2015, Colloids and surfaces A: Physochemical and engineering aspects. DOI: 10.1016/j.colsurfa.2015.06.059.

Introduction

Surface properties, such as wettability, morphology and surface chemistry, play a crucial role in designing possible application fields of a polymeric material. Surface wettability is among the most important features useful to determine potential application of a polymeric material.

In fact, material wettability and the modulation of its wetting properties play a key role in the development of new polymeric materials for a very large number of industrial applications, i.e. the fields related to coating (34), printing (35), filtration membranes (36) and biomedical devices (37).

The wetting properties of solid surfaces are affected by both their intrinsic chemical composition and by their morphology (38); for example hydrophobic surfaces roughened on purpose can become super hydrophobic, showing an efficient mechanism of self-cleaning (39).

Self-cleaning surfaces are arising a lot of interest in different technological fields because they have the potential to bring great convenience in daily life as well in many industrial processes, especially in the photovoltaic field: many deleterious phenomena causing a progressive loss of efficiency on manufacture performance, such as contamination, snow sticking or current conduction, are expected to be inhibited on such surfaces.

Both efficiency and service life of a solar cell could be enhanced by preventing accumulation of dust and filth on cell covers (e.g. using a self-cleaning surface), thus reducing the loss of incident light due to absorption or scattering (38).

In this technological field, many inorganic and organic materials or coatings with self-cleaning properties are currently available on the market, e.g. self-cleaning glasses for windows (40) and Polytetrafluoroethylene (PTFE)-based coatings (41), but the issue related to surface cleaning of solar cells covers causes still considerable troubles, such as high consumption of energy and chemical detergents and, consequently, high costs (38).

The self-cleaning capability of a surface can be ascribed to two different mechanisms. The first involves the wettability of the surface itself (42), the second involves its photocatalytic features (43).The wettability of a surface is very important and is governed by both the chemical

composition and the geometrical microstructure (44): a hydrophobic surface prevents polar molecules from adsorbing at the material interface, and polar water droplets roll away bringing dirt with them (45).

Conventionally, self-cleaning surfaces are obtained mainly in two ways. Starting from the fundamental studies of Wenzel (46), one is the creation of a rough surface characterized by hydrophobic features (47), and the other is the modification of a rough surface using materials with low surface free energy, in order to improve the surface hydrophobic properties (48).

Up to now, many methods have been developed to produce rough surfaces, including solidification of melted alkyl ketene dimer (49), plasma polymerization/etching of polypropylene (PP) in the presence of PTFE (50), microwave plasma-enhanced chemical vapor deposition (51), anodic oxidization of aluminium (52), immersion of porous alumina gel films in boiling water (52), phase separation (53) and molding. Furthermore, to obtain self-cleaning surfaces, coating with low surface energy materials, such as fluoroalkylsilane, is often necessary (54).

The growing demand for self-cleaning materials in the prospect of photovoltaic manifold applications has now become a pressing issue for academic laboratories as well as hi-tech companies and is closely related to the development of polymers and materials that could satisfy this requirement.

This work addresses the need of keeping different kinds of surfaces, such as the surface of solar cells covers, clean and free of dust and dirt, being suitable for both indoor and outdoor applications. The development of an innovative self-cleaning material is described; a flexible polymeric material with hydrophobic properties was obtained by combining the useful UV, thermal and mechanical properties of SPES with hydrophobic features of different I.Ls. in a novel synthetic approach.

As described previously, SPES has received great attention in the last decade due to the possibility to use it for a variety of separation processes, e.g. ion exchange membranes (55), reverse osmosis (56) and electro dialysis process (57). It is a completely amorphous polymer, characterized by excellent UV and thermal resistance, as previously reported on page 40, optical properties

(refractive index: n=1.63 at λ=589.3 nm) chemical stability (58), oxidation resistance (59), as well as by good mechanical properties (60) and easy processability, e.g. for the production of films and layers- useful features for photovoltaic applications-.

In order to investigate new solutions for the development of hydrophobic materials, I.Ls. are interesting candidates for this purpose. I.Ls. are a class of molten salts usually composed by linear or cyclic ammonium cations, imidazolinium and pyridinium being the ones most commonly reported in literature, thanks to their easy preparation (61). It is known that I.Ls. have excellent thermal stability (up to 400°C) (62) and that their physical-chemical properties can be modulated changing the nature of the cation or anion (63). In fact, the modulation of non-polar groups on the cation, characterized by strong hydrophobic properties, can produce major changes in the tendency of I.Ls. to modify the efficiency of ion packing and therefore in their hydrophobic features; increasing the length of alkyl chains, the hydrophobic properties of the salt increase.

In this study, SPESs with different DS were successfully synthesized using a sulfonated monomer, 2,5-dihydroxybenzene-1-sulfonate potassium salt, via homogeneous synthesis in order to have a tight control over the DS of the polymers. SPESs were characterized by ^{1}H-NMR and DSC measurements; despite their hydrophilic properties, due to the presence of sulfonic moieties, wetting properties were modulated thanks to an innovative synthesis with I.Ls., through an ionic exchange reaction between the potassium cation of sulfonated hydroquinone comonomer of SPES and the cation of I.Ls., which can be substituted with different apolar groups. After the addition of I.Ls., the hydrophobic properties increase both as the quantity of sulfonated groups increases, due to the higher number of potassium ions available for substitution with I.Ls. cations, and as I.Ls. apolar alkyl chains length increases.

1-Ethyl,3-Methyl Imidazolinium methyl sulfite (MEIM), 1,3-Dibutyl Imidazolinium bromide (BBIM), 1-Methyl, 3-Octyl Imidazolinium bromide (MOIM) and 1-Butyl, 3-Octyl Imidazolinium bromide (BOIM) were synthesized and used as I.Ls.; their content in SPESs was determined by ^{1}H NMR spectroscopy and the thermal properties of the resultant polymers were evaluated by DSC.

The effect of the four I.Ls. on wetting, morphology and surface roughness of SPES_I.Ls. membranes, obtained via solvent casting deposition, were studied by SWCA, SEM and AFM analyses, and FT-IR spectroscopy. The photo-chemical stability of SPES_I.Ls. samples was also successfully tested via a preliminary aging study.

The polymeric films based on SPES and I.Ls. prepared in this work could be, in a future, used as innovative self-cleaning materials for very large number applications, including covers for solar cells.

What's an Ionic Liquid?

**This chapter is based on the review of Ghandi, K. (64)*

Room-temperature I.Ls., organic salts that are liquid below 100˚C, have received considerable attention in the last decade as suitable substitutes for volatile organic solvents. Since they are non-flammable, non-volatile and recyclable, they are classified as green solvents. Due to their remarkable properties, such as outstanding solvating potential, thermal stability and their tunable properties by suitable choices of cations and anions, they are considered favorable medium candidates for chemical syntheses.

I.Ls. are usually categorized into four types based on their cation segment (Figure 9):

1) alkyl ammonium;

2) dialkylimidazolium;

3) phosphonium;

4) *N*-alkylpyridinium.

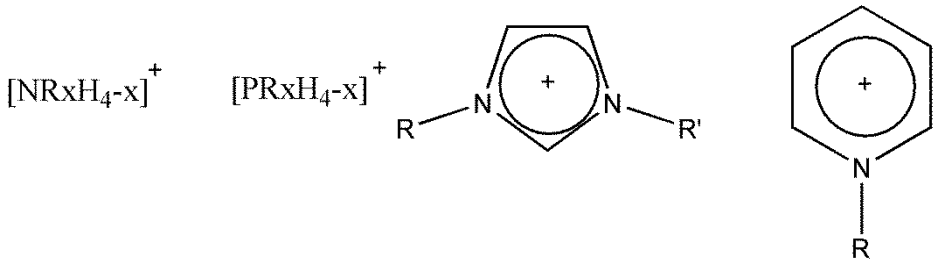

Figure 9. Alkyl ammonium, phosphonium, dialkylimidazolium and N-alkylpyridinium cations.

Although these I.Ls. are used successfully as solvents and catalysts in many reactions, there are some limitations in their use.

Ammonium-based I.Ls. have been used widely as electrolytes in high-energy electrochemical devices owing to their good electrochemical cathodic stabilities, low melting points and low viscosities.

Popular imidazolium-based I.Ls. are among the most studied I.Ls; selection of the imidazolium ring as a cation (Figure 10) is often due to its stability within oxidative and reductive conditions, low viscosity of imidazolium I.Ls. and their ease of synthesis. There are also several reports regarding the application of imidazolium- based I.Ls. as catalysts for the improvement of reaction time, yield and chemo-selectivity of many organic reactions.

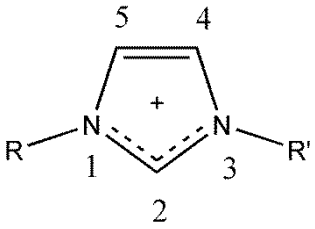

Figure 10. Imidazolinium cation structure.

However, Olofson et al., in 1964, reported on a kinetics study demonstrating that the proton sandwiched between the two nitrogen atoms (N1-N3) in the imidazolium cation undergoes deuterium exchange in deuterated solvent because of its acidic nature. Two later studies reported that deprotonation of the imidazolium cation to the highly reactive carbine and hence showed the reactive nature of imidazolium-based I.Ls. under basic conditions.

In another investigation, the low yield of a base catalyzed Baylis-Hillman reaction in the presence of imidazolium-based I.Ls. was attributed to a side reaction involving the imidazolium-based I.L. (Scheme 2).

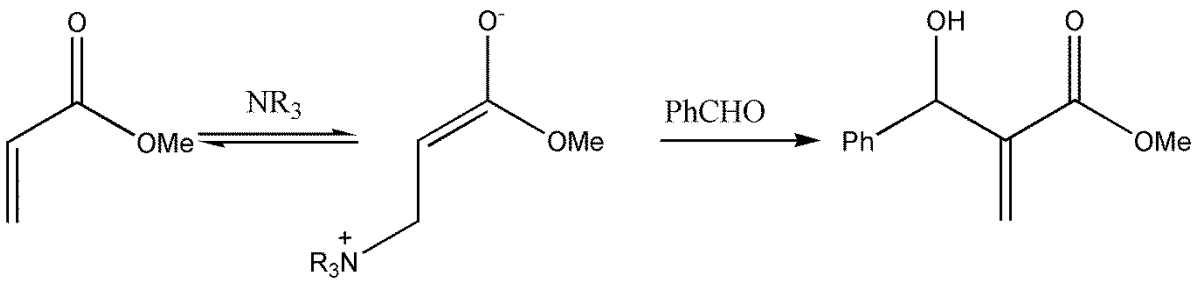

Scheme 2. Base-catalyzed Baylis-Hillman reaction.

This observation also confirmed that using this type of I.L. under basic conditions needs to be considered with more precaution to avoid unexpected side reactions (Scheme 3).

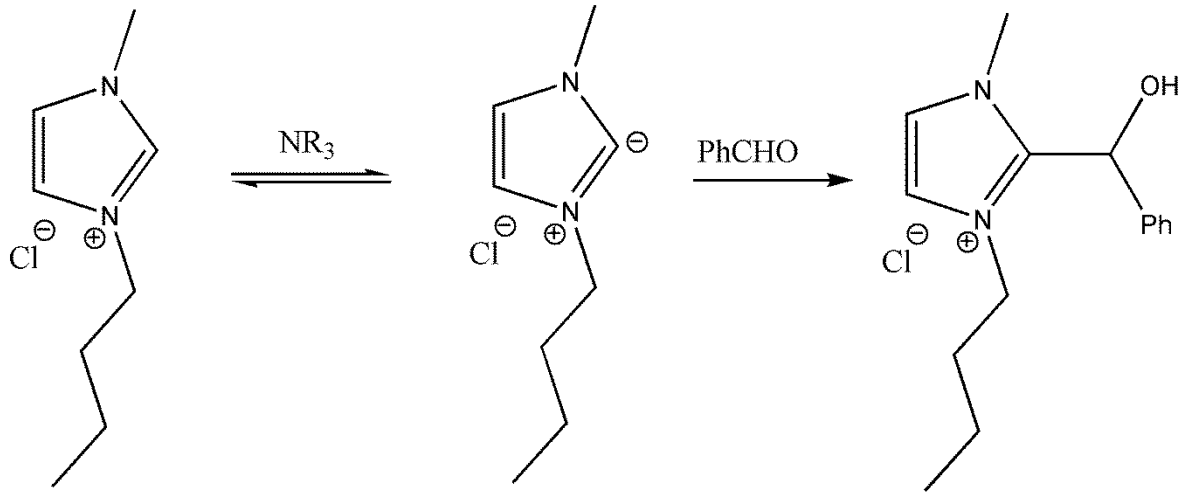

Scheme 3. The side reaction of an imidazolium-based I.L. with benzaldehyde in the Baylis-Hillman reaction.

Pyridinium-based I.Ls. are more recent in comparison with their imidazolium-based counterparts, and research on their stability, reactivity and catalytic role in organic synthesis is still in progress. Although they show poor region-selectivity in palladium-catalyzed telomerization of butadiene with methanol, and they have a negative effect on the rate of some Diels-Alder reactions, applications of this type of I.Ls. are quite successful in reactions such as Friedel-Crafts and Grignard.

The catalytic role of pyridinium-based I.Ls. has been shown to be remarkable in the synthesis of some pharmaceutical agents such as 1,4-dihydropyridine, dihydropyrimidinones and 3,5-bis(dodecyloxycarbonyl)- 1,4-dihydropyridine derivatives.

Phosphonium-based I.Ls. are more novel than the imidazolium- and pyridinium-based I.Ls. They are more thermally stable (in some cases up to nearly 400˚C) in comparison with ammonium and imidazolium salts, and this remarkable property makes them suitable for reactions that are carried out at more than 100˚C. Phosphonium- based I.Ls. are used as the catalyst and solvent for hydro

formylation, palladium-catalyzed Heck reactions and palladium-mediated Suzuki cross-coupling reactions. In addition, they are also powerful phase-transfer catalysts for the Halex reaction.

Recently, phosphonium-based I.Ls. have been used for CO_2 capture. Along with their application in the synthesis of a novel polystyrene-based material, the styrene derivatives of phosphonium-based I.Ls. are used as monomers in the synthesis of phosphonium-containing random copolymers. The cyclohexadienyl radical in trihexyl (tetradecyl) phosphonium chloride has been studied. These studies showed that reactive free radicals do not react with phosphonium I.Ls.

Although phosphonium-based I.Ls. showed good stability in the presence of bases (even in reactions involving strong bases such as Grignard reagents), they are still susceptible to reaction with weak bases (Scheme 4).

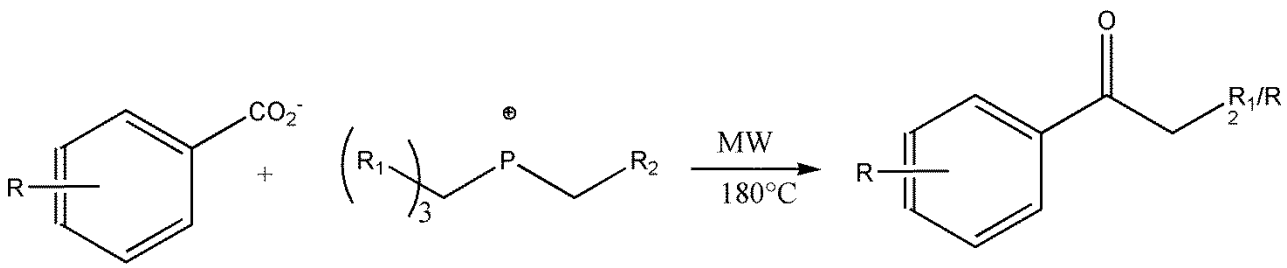

Scheme 4. Reactions of benzoate salts with trihexyl (tetradecyl) phosphonium chloride under microwave irradiation.

Experimental

Materials

4,4'-difluorodiphenylsulfone (BFPS, ≥99%) and 4,4'–dihydroxydiphenyl (BHP, ≥97%) were supplied by Sigma Aldrich; 2,5-dihydroxybenzene-1-sulfonate potassium salt (sulfonated hydroquinone, SHQ, ≥98%) was obtained from Alfa Aesar and potassium carbonate (K_2CO_3, ≥98% anhydrous) was purchased from Fluka; all the reagents were dried at 30°C in vacuum oven (about 4 mbar) for at least 24 hr before use and employed without further purification. 1-methylimidazole (≥99%), 1-butylimidazole (≥98%), butyl bromide (≥99%) and octyl bromide (≥99%) were obtained from Sigma Aldrich and used as received. N-methyl-2-pyrrolidone (NMP, ≥99.5% anhydrous), dimethylacetamide (DMAc, ≥99.5%), N, N-dimethylformamide (DMF, 99.8% anhydrous), toluene (99.8% anhydrous), acetonitrile (99.8% anhydrous), ethyl acetate (99.8% anhydrous), distilled water Chromasolv® (≥99.9%), dimethyl sulfoxide-d_6 (DMSO-d_6, 99.96 atom % D) and deuterium oxide (D_2O, 99.9 atom % D) were supplied by Sigma Aldrich and used without purification.

Synthesis of SPESs

SPESs syntheses were performed as reported on pages 27-28.

Synthesis of I.Ls.

Four Imidazolinium based I.Ls. were synthesized: 1-Ethyl,3-Methyl Imidazolinium methyl sulphite (MEIM), 1,3-Dibutyl Imidazolinium bromide (BBIM), 1-Methyl,3-Octyl Imidazolinium bromide (MOIM) and 1-Butyl, 3-Octyl Imidazolinium bromide (BOIM).

For the syntheses of MEIM and BBIM, respectively methyl ethyl sulphite (2.03 g) and 1-methylimidazole (1.25 g) for MEIM and 1-bromobutane (2.55 g) and 1-butylimidazole (1.89 g) for BBIM, are introduced in a 100 cm^3 one-neck round bottom flask equipped with magnetic stirring; the flask, under nitrogen atmosphere, is put in an oil bath and the synthesis is kept for 1 hr at 110°C

and then cooled to room temperature. The product is purified from the unreacted monomers thanks to several washings with water.

The syntheses of MOIM and BOIM were conducted as follows: a 100 cm^3 three-necked round bottom flask is equipped with a nitrogen inlet adapter, an internal thermometer adapter, an overhead mechanical stirrer and a reflux condenser. The flask is flushed with nitrogen, charged with 20 cm^3 of acetonitrile and respectively with octylbromide (3.59 g) and 1-methylimidazole (1.25 g) for MOIM and with octyl bromide (3.59 g) and 1-butylimidazole (1.89 g) for BOIM, and brought to reflux in an oil bath. The solution is heated under reflux for 48 hr and then cooled to room temperature. Volatiles are removed from the resulting yellow solution under reduced pressure (about 4 mbar). The remaining light-yellow oil is re-dissolved in acetonitrile (20 cm^3) and added drop wise via cannula in a 250 cm^3 one-necked round bottom flask of a well-stirred solution of 100 cm^3 of ethyl acetate. The imidazolinium salt begins to crystallize almost immediately and, after the addition of the acetonitrile solution is completed, the flask is cooled at -30°C for 12 hr. The supernatant solution is removed via filtration through a filter cannula and the resulting white solid is dried under pressure (about 4 mbar) at 30°C for 6 hr. The structure of the products obtained is determined via ^1H NMR: Figure 11 shows the structures and abbreviations of all the ions used in this work.

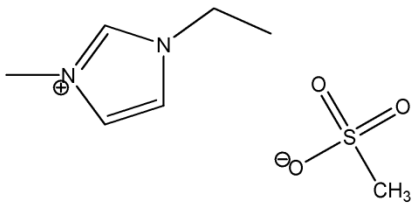

1-Ethyl, 3-Methyl Imidazolinium methyl sulfite (MEIM)

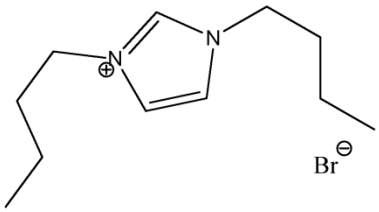

1,3-Dibutyl Imidazolinium bromide (BBIM)

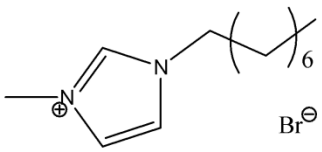

1-Methyl, 3-Octyl Imidazolinium bromide (MOIM)

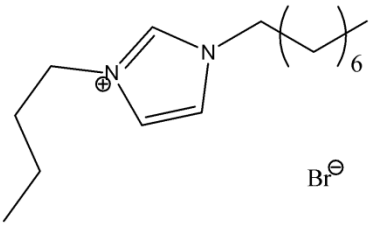

1-Butyl, 3-Octyl Imidazolinium bromide (BOIM)

Figure 11. Structures of the I.Ls. synthesized.

Synthesis of SPESs with I.Ls.

An ionic exchange reaction between the K^+ cation of SPESs and the cations of the four I.Ls. synthesized was conducted. The exact amount of the reagents used for the syntheses is reported in Table 5. In a representative synthesis procedure, the cation exchange reaction was performed as follows: SPES and I.L. are introduced in a one-neck round bottom flask containing DMAc (15 cm^3) equipped with magnetic stirring; the flask is transferred to the oil bath and the synthesis is kept under nitrogen atmosphere for 24 hr at 110°C.The reaction mixture is then precipitated into a large excess of water and recovered via filtration; the product is purified from the residual reagents thanks to several washings with water. The resultant polymer is finally collected by filtration and fully dried in a vacuum oven (about 4 mbar) at 50°C for 24 hr. The rate of substitution (RS) is measured via ^1H NMR.

Samples	^{1}H NMR DS (meq SO_3*g^{-1} of polymer)	SPES (g)	I.L. (g)
SPES_MEIM_0.5	0.48	0.90	0.20
SPES_MEIM_0.75	0.70	0.90	0.29
SPES_MEIM_1	0.98	0.90	0.41
SPES_BBIM_0.5	0.48	0.90	0.25
SPES_BBIM_0.75	0.70	0.90	0.37
SPES_BBIM_1	0.98	0.90	0.52
SPES_MOIM_0.5	0.48	0.90	0.27
SPES_MOIM_0.75	0.70	0.90	0.39
SPES_MOIM_1	0.98	0.90	0.55
SPES_BOIM_0.5	0.48	0.90	0.36
SPES_BOIM_0.75	0.70	0.90	0.53
SPES_BOIM_1	0.98	0.90	0.74

Table 5. Amounts of the reagents adopted for the syntheses of SPES_I.Ls.

Characterization of polymers

Nuclear magnetic resonance: ^{1}H NMR

^{1}H NMR spectra were collected at 25°C with a BRUKER 400 MHz spectrometer. Samples for the analyses were prepared dissolving 10-15 mg of SPESs or SPES_I.Ls. samples in 1 cm^3 of DMSO-d_6 and 8-10 mg of I.Ls. in 1 cm^3 of D_2O.

Size Exclusion Chromatography (SEC)

SEC data were obtained as reported on page 30.

Differential Scanning Calorimetry (DSC)

DSC analyses were conducted using a Mettler Toledo DSC 1, on samples of SPESs and SPES_I.Ls. weighting from 5 to 10 mg each. Temperature program was divided in five parts:

i) heating from 25°C to 330°C at 10°C/min;

ii) 5 min of isotherm at 330°C;

iii) cooling from 330°C to 25°C at 10°C/min;

iv) 5 min isotherm at 25°C;

v) heating from 25°C to 330°C at 10°C/min (T_g was measured here).

Aging study

Aging study was conducted by exposing SPESs and SPES_I.Ls. samples an irradiating ultraviolet light "Ultra Vitalux Osram 300W 230Ve27", characterized by an UVA emission between 400 and 315 nm, and by an UVB emission between 315 and 280 nm; aging test was performed for 100 hr.

Preparation of SPESs and SPES_I.L. membranes

Given the difficulties in completely removing solvents like NMP, toluene and DMAc from SPESs and SPES_I.Ls., the polymers were repeatedly washed with water for several days under stirring, dried in a vacuum oven (about 4 mbar) at 50°C for 24 hr and then the absence of residual solvent was checked via isothermal TGA (2 hr at 250°C under nitrogen flow). Polymers weights obtained after TGA analyses are reported in Table 6.

Samples	Residual weight (%) at 250°C	Weight loss (%) at 250°C
SPES_0.5	99.1	0.9
SPES_0.75	98.9	1.1
SPES_1	99.5	0.5
SPES_MEIM_0.5	99.0	1.0
SPES_MEIM_0.75	99.2	0.8
SPES_MEIM_1	99.0	1.0
SPES_BBIM_0.5	98.7	1.3
SPES_BBIM_0.75	99.1	0.9
SPES_BBIM_1	99.0	1.0
SPES_MOIM_0.5	99.3	0.7
SPES_MOIM_0.75	98.6	1.4
SPES_MOIM_1	99.5	0.5
SPES_BOIM_0.5	98.9	1.1
SPES_BOIM_0.75	98.9	1.1
SPES_BOIM_1	98.7	1.3

Table 6. Residual weights obtained by TGA curves of SPESs and SPES_I.Ls. polymers.

Membranes of both SPESs and SPES_I.Ls. were obtained via solution casting: polymers were dissolved in DMAc using 21% mass/volume concentration and the corresponding solutions were cast onto a PTFE substrate. The solvent was evaporated for 24 hr in vacuum oven (about 4 mbar) at 40°C; the absence of residual solvent was checked via isothermal TGA (2 hr at 250°C under nitrogen flow) and membranes weights obtained after TGA analyses are reported in Table 7.

Membranes	Residual weight (%) at 250°C	Weight loss (%) at 250°C
SPES_0.5	99.6	0.4
SPES_0.75	99.4	0.6
SPES_1	99.4	0.6
SPES_MEIM_0.5	99.0	1.0
SPES_MEIM_0.75	99.3	0.7
SPES_MEIM_1	99.5	0.5
SPES_BBIM_0.5	99.6	0.4
SPES_BBIM_0.75	99.6	0.4
SPES_BBIM_1	99.5	0.5
SPES_MOIM_0.5	99.6	0.4
SPES_MOIM_0.75	99.1	0.9
SPES_MOIM_1	99.0	1.0
SPES_BOIM_0.5	99.6	0.4
SPES_BOIM_0.75	99.4	0.6
SPES_BOIM_1	99.3	0.7

Table 7. Residual weights obtained by TGA curves of SPESs and SPES_I.Ls. membranes.

In all cases, residual weight is very close to 100% and can be considered within the experimental error, confirming that solvents were removed both from the polymers and from membranes.

Membranes thickness was in the range 120-125 μm; it was evaluated by Nikon eclipse ME600 optical microscope with Nikon digital camera light DS_Fi1, software Nis-Elementi BR, magnification 50X.

Characterization of the membranes

Static Water Contact Angle (SWCA)

Surface wetting properties of the membranes surface were assessed by contact angle measurement using a Krüss Easydrop Instrument, attaching a 4*4 cm membrane on a glass slide. For the measure, a total of 1 μl of double distilled water was dropped on the air-side surface of the membranes. At least five measurements were taken on each sample to get reliable values. The measurements error was ±3°. The same procedure was performed on the PTFE-side surface of the membranes.

Scanning Electron Microscopy (SEM)

SEM studies were carried out by a Leica Electron Optics 435 VP microscope. The investigations were performed with an acceleration voltage of 15 kV, 50 pA of current probe, and 20 mm of working distance. The samples were mounted on aluminium specimen stubs with double-sided adhesive tape and sputter-coated with a 20 nm thick gold layer in rarefied argon, using an Emitech K550 Sputter Coater, with a current of 20 mA for 180 s.

Atomic Force Microscopy (AFM)

AFM characterizations were carried out with a Nano-R2 AFM produced by Pacific Nanotechnology (USA) and were evaluated from 10 μm^2 images. The AFM imaging technique used was Close Contact mode and APPNANO (USA) highly doped single crystal silicon probes of 125 μm nominal length were used. Data were acquired by means of SPM Cockpit Software, processed and analysed

by Nanorule+ software, both equipped with the Nano-R_2 system. Surface roughness was measured by image analysis of 10 μm*10 μm areas and expressed as root-mean-square (RMS).

Fourier Transform-Infrared (FT-IR)

The presence of different hydrophobic I.Ls. on the surface of both sides (mold-side and air-side) of the polymeric membranes prepared was checked by FT-IR spectroscopy, performed on a Spectrum 100 spectrophotometer (Perkin Elmer) in attenuated total reflection (ATR) mode using a resolution of 4.0 and 256 scans, in a range of wavenumber between 4000 and 400 cm^{-1}. A single-bounce diamond crystal was used with an incident angle of 45°.

Results and Discussion

Synthesis and characterization of SPESs

SPESs samples were synthesized and characterized as described in section named "Homogeneous synthesis and characterization of Sulfonated Polyarylethersulfones having low degree of sulfonation and highly hydrophilic behavior" on pages 27-43.

Cation exchange reaction and characterization of SPES_I.Ls.

^{1}H NMR spectra obtained of I.Ls. synthesized are shown respectively in Figure 12 (MEIM), Figure 13 (BBIM), Figure 14 (MOIM) and Figure 15 (BOIM).

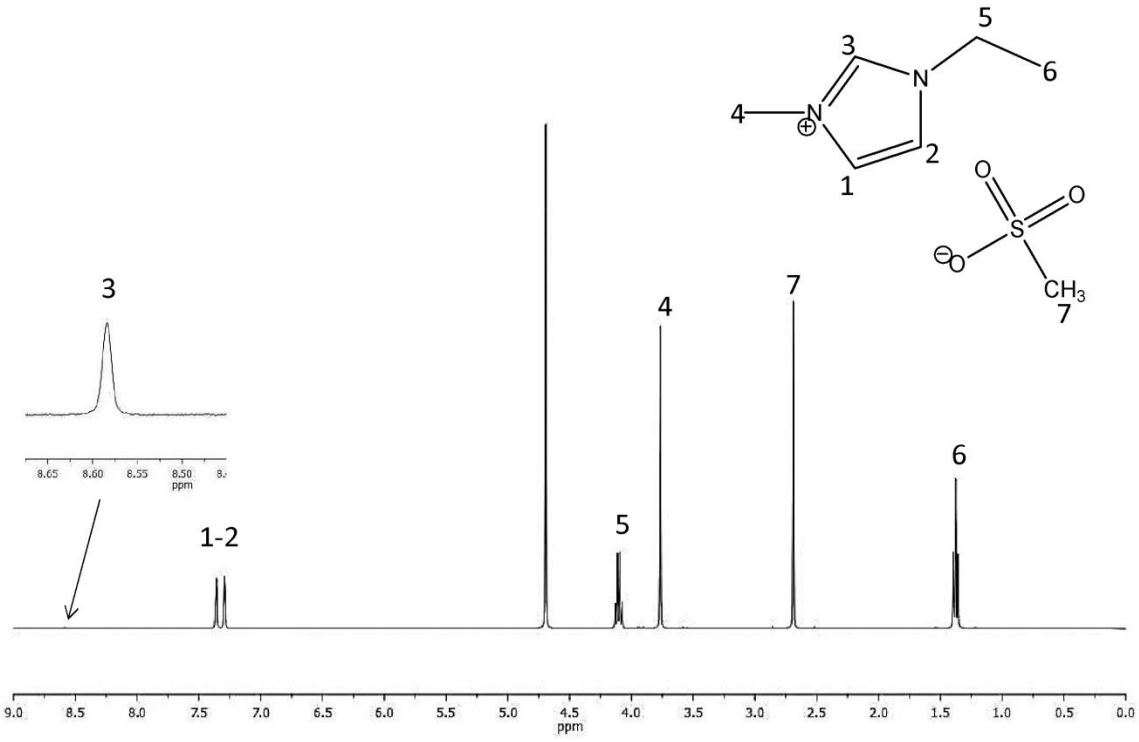

Figure 12. ^{1}H NMR of MEIM.

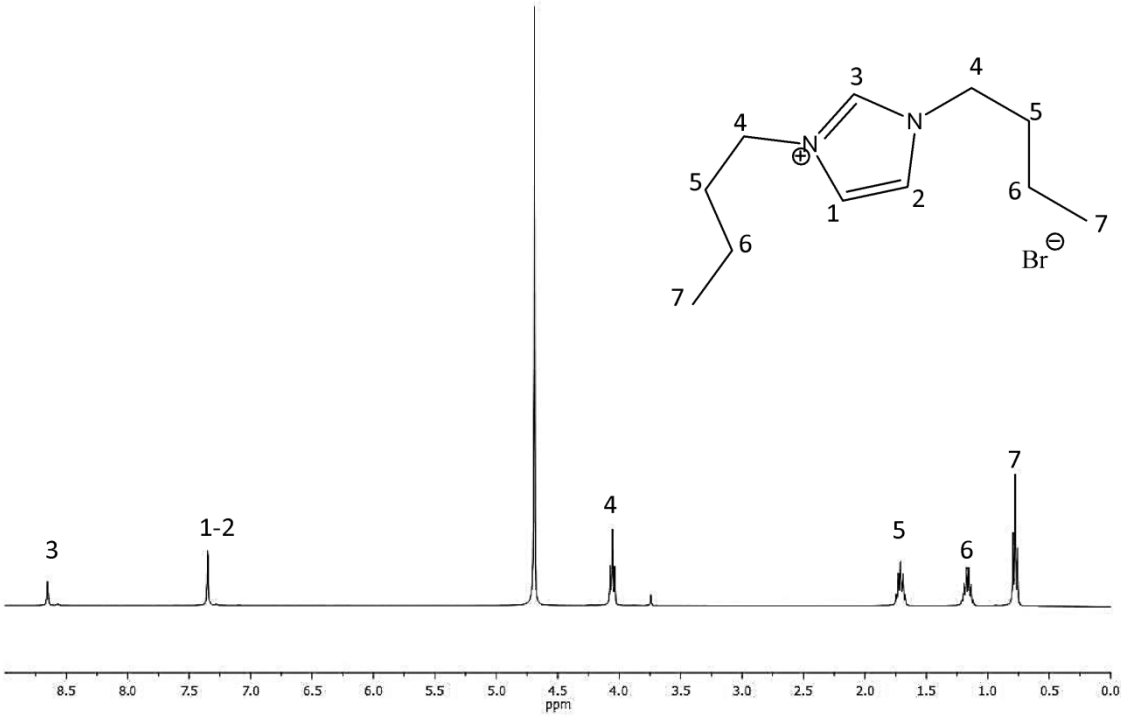

Figure 13. ^{1}H NMR of BBIM.

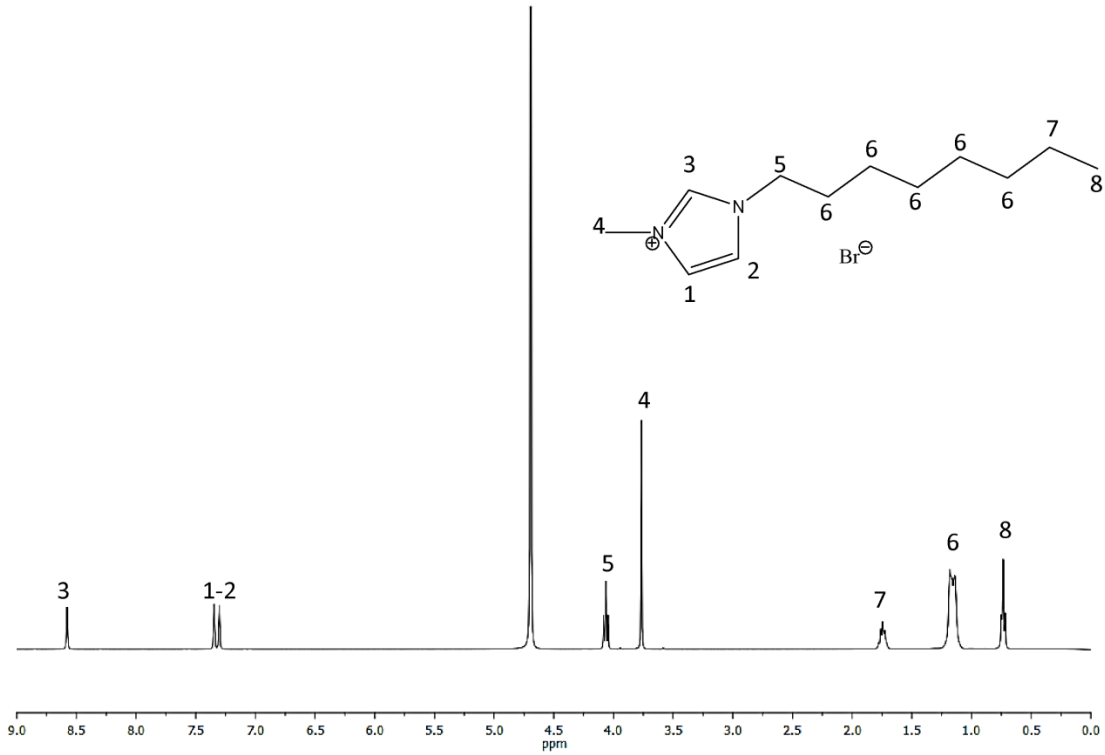

Figure 14. ^{1}H NMR of MOIM.

Figure 15. ^{1}H NMR of BOIM.

Ionic exchange reactions between the potassium cation of SPESs and the imidazolinium cations of MEIM, BBIM, MOIM and BOIM were conducted. Scheme 5 shows the representative procedure for the cation exchange reaction of SPESs with I.Ls.

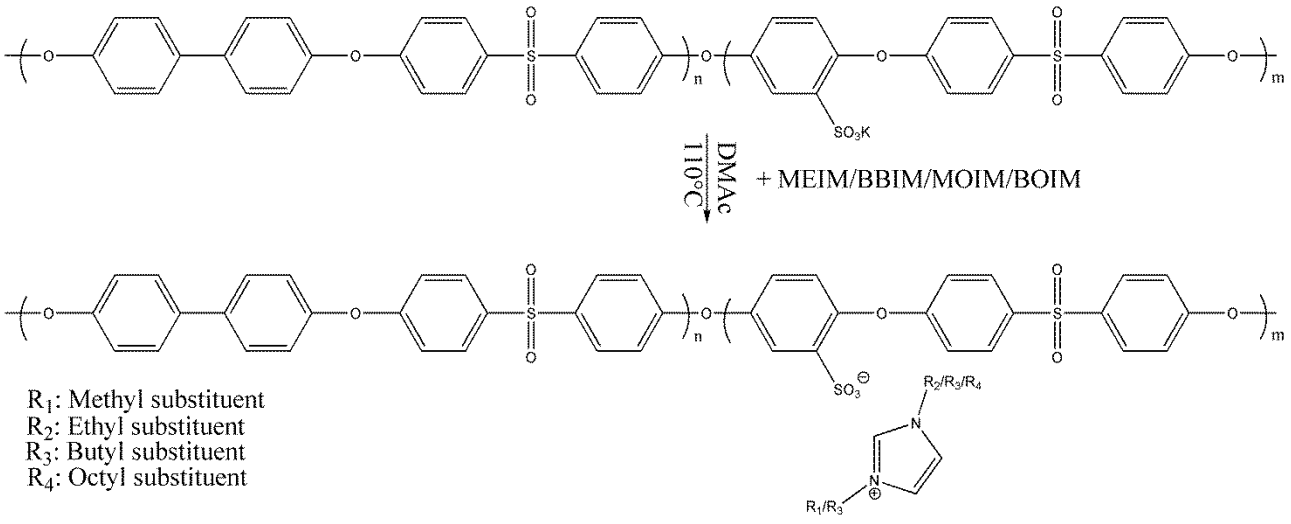

Scheme 5. Synthesis route for the cation exchange reaction of SPES_I.L.

^{1}H NMR spectrum collected on the material after the ionic exchange reaction between SPES_0.5 and MEIM is reported in Figure 16; furthermore, in Figure 17, 18 and 19 ^{1}HNMR spectra of SPES_ BBIM_0.5, SPES_ MOIM_0.5 and SPES_ BOIM_0.5 are reported.

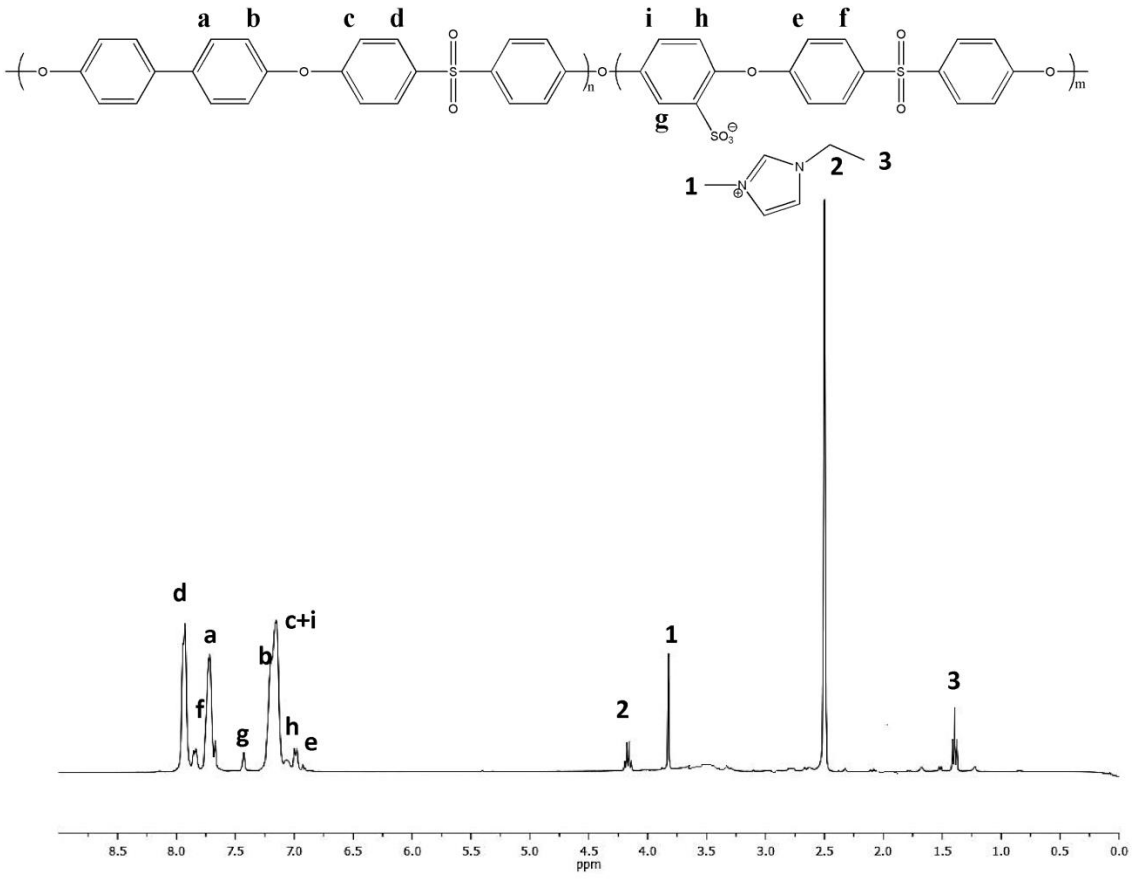

Figure 16. ^{1}H NMR of SPES_MEIM_0.5.

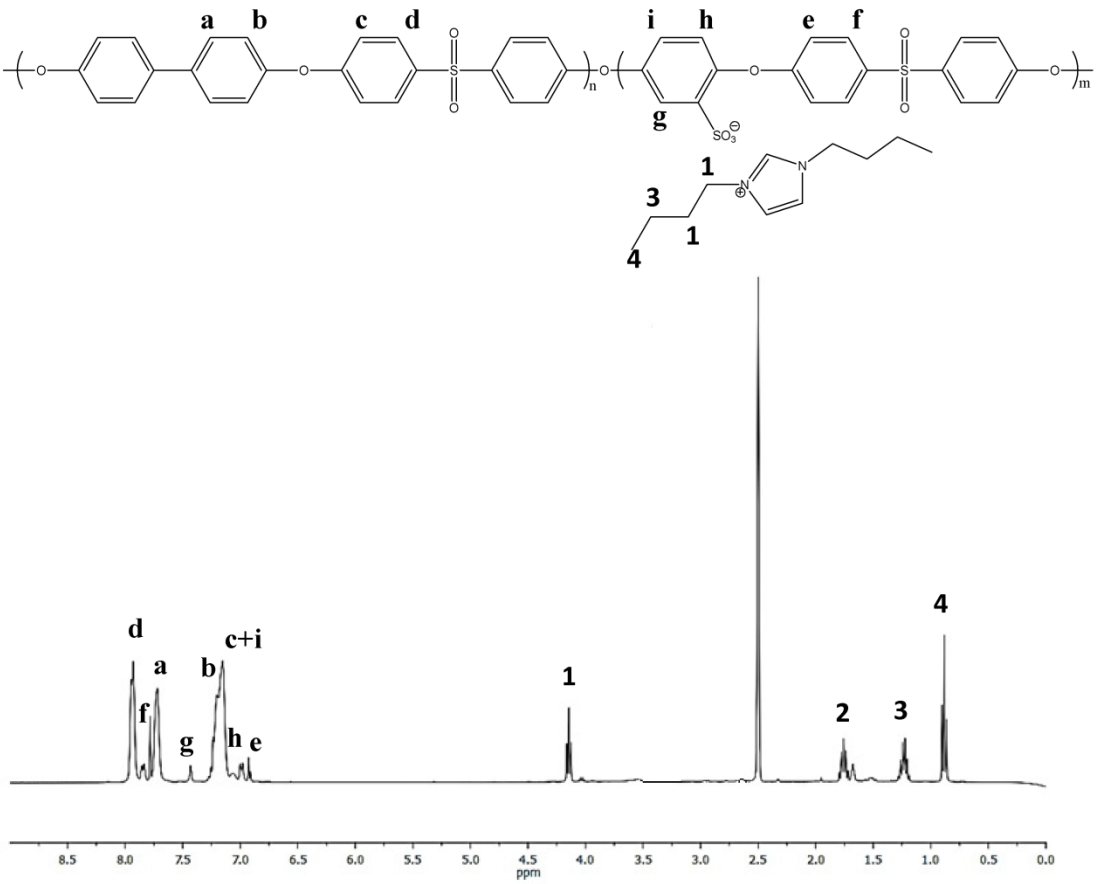

Figure 17. ^{1}H NMR of SPES_BBIM_0.5.

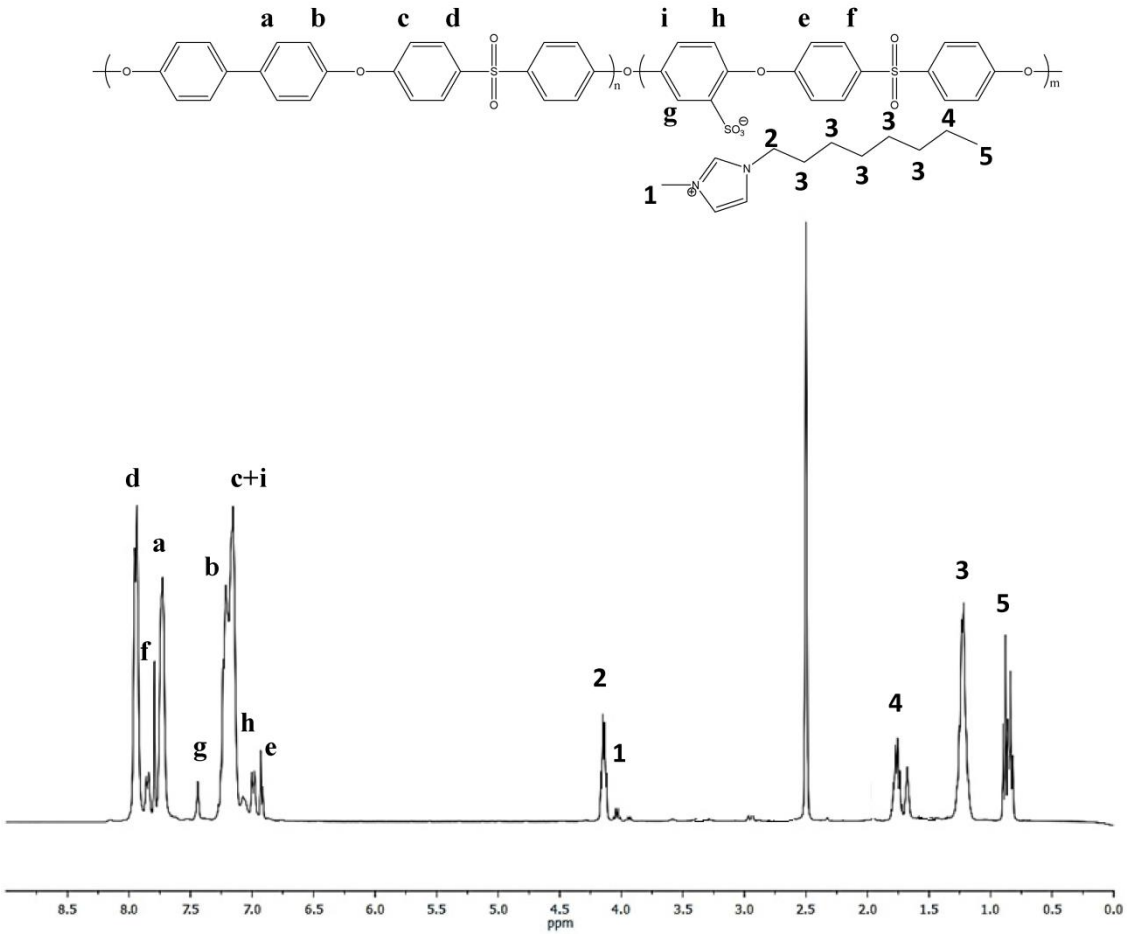

Figure 18. ^{1}H NMR of SPES_MOIM_0.5.

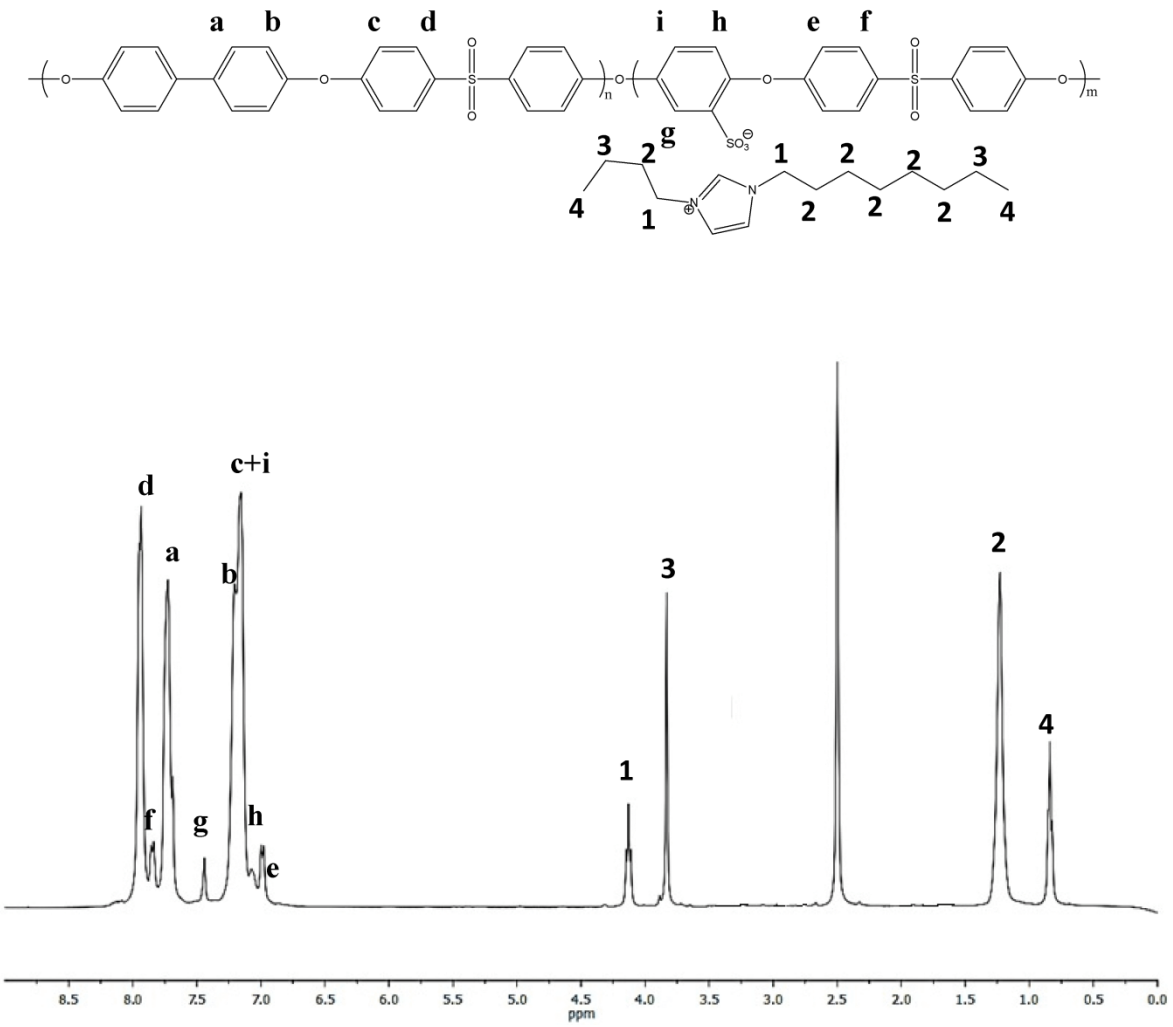

Figure 19. ^{1}H NMR of SPES_BOIM_0.5.

A list of the samples synthesized with the rate of substitution (RS) obtained is shown in Table 8.

To assess the possible application temperature range of SPES_I.Ls., DSC analyses were performed. As shown in Table 8, SPESs with I.Ls. have a T_g similar to the ones of SPESs samples previously reported in Figure 7, suggesting that the ionic exchange reaction does not significantly affects the excellent thermal properties of these materials.

Samples	^{1}H NMR RS (%)	T_g (°C)
SPES_MEIM_0.5	81	247.9
SPES_MEIM_0.75	68	286.1
SPES_MEIM_1	78	299.5
SPES_BBIM_0.5	96	252.3
SPES_BBIM_0.75	87	263.2
SPES_BBIM_1	94	272.4
SPES_MOIM_0.5	97	249.5
SPES_MOIM_0.75	98	299.4
SPES_MOIM_1	98	292.3
SPES_BOIM_0.5	98	246.1
SPES_BOIM_0.75	90	298.4
SPES_BOIM_1	97	280.6

Table 8. List of SPES_I.Ls. synthesized with their RS and T_g data.

The photo-chemical stability of SPESs and SPES_I.Ls. samples was tested via a preliminary aging study (100 hr of exposition), evaluating the photo-chemical stability through the exposure of polymeric samples to an irradiating ultraviolet UVA light between 400 and 315 nm, and by an UVB one between 315 and 280 nm. The photo-chemical stability of SPESs and SPES_I.Ls. was checked via ^{1}H NMR spectroscopy comparing, in the case of SPESs samples, the DS measured before and after the aging study, and in the case of SPES_I.Ls. samples, the RS determined before and after the aging test. The results reported in Table 9, showing no differences between both the DS and the RS measured before and after the aging study, confirm the excellent photo-chemical stability features of SPESs and SPES_I.Ls. samples.

Samples	^{1}H NMR DS (meq SO_3^-*g^{-1} of polymer) before aging study	^{1}H NMR DS (meq SO_3^-*g^{-1} of polymer) after aging study	^{1}H NMR RS (%) before aging study	^{1}H NMR RS (%) after aging study
SPES_0.5	0.48	0.48	-	-
SPES_0.75	0.70	0.70	-	-
SPES_1	0.98	0.98	-	-
SPES_MEIM_0.5	-	-	81	81
SPES_MEIM_0.75	-	-	68	68
SPES_MEIM_1	-	-	78	78
SPES_BBIM_0.5	-	-	96	96
SPES_BBIM_0.75	-	-	87	87
SPES_BBIM_1	-	-	94	94
SPES_MOIM_0.5	-	-	97	97
SPES_MOIM_0.75	-	-	98	98
SPES_MOIM_1	-	-	98	98
SPES_BOIM_0.5	-	-	98	98
SPES_BOIM_0.75	-	-	90	90
SPES_BOIM_1	-	-	97	97

Table 9. List of SPEs and SPES_I.Ls. synthesized with their DS and RS measured before and after the aging study.

Membranes characterization: SWCA, SEM and AFM analyses

Static water contact angle analyses (SWCA)

Static water contact angles of membranes of SPESs and SPES_I.Ls., obtained from solution casting in DMAc, were evaluated. The samples were cast onto a PTFE substrate: wetting properties were measured both at the air-side surface and at the PTFE-side surface of the membranes. Table 10 shows the results obtained.

Samples	θ_w (air-side)	θ_w (PTFE-side)
SPES_0.5	$\overline{65}$±2	$\overline{83}$±1
SPES_0.75	$\overline{50}$±2	$\overline{74}$±1
SPES_1	$\overline{43}$±1	$\overline{59}$±2
SPES_MEIM_0.5	$\overline{86}$±2	$\overline{108}$±1
SPES_MEIM_0.75	$\overline{85}$±1	$\overline{116}$±1
SPES_MEIM_1	$\overline{89}$±1	$\overline{121}$±1
SPES_BBIM_0.5	$\overline{88}$±1	$\overline{123}$±1
SPES_BBIM_0.75	$\overline{84}$±2	$\overline{124}$±2
SPES_BBIM_1	$\overline{81}$±2	$\overline{126}$±1
SPES_MOIM_0.5	$\overline{77}$±1	$\overline{124}$±1
SPES_MOIM_0.75	$\overline{80}$±1	$\overline{125}$±2
SPES_MOIM_1	$\overline{81}$±1	$\overline{128}$±1
SPES_BOIM_0.5	$\overline{85}$±1	$\overline{130}$±1
SPES_BOIM_0.75	$\overline{80}$±1	$\overline{131}$±1
SPES_BOIM_1	$\overline{81}$±1	$\overline{131}$±1

Table 10. SWCA of SPESs and SPES_I.Ls.

Contact angles of SPESs decrease as the quantity of $-SO_3^-K^+$ groups increases, due to the high polarity of the $-SO_3^-$ groups. The increase of θ_w observed on the PTFE-side for SPES membranes with respect to the air-side is probably due to the organization of the $SO_3^-K^+$ groups of the polymeric chains occurring during the evaporation of the solvent and to the interaction with the high hydrophobic PTFE mold surface. Therefore, as reported for θ_w observed on the air-side of SPES membranes, the water contact angles significantly decrease with the increase of SPES DS.

After cation exchange reaction between SPESs and I.Ls., the values of static water contact angles dramatically change: thanks to the addition of I.Ls., the hydrophobic properties measured on the PTFE-side surface increase as the quantity of sulfonated groups increases, due to the higher number of I.L. exchanged. Increasing the length of the apolar alkyl chains of the imidazolinium cations, the static water contact angles increase: θ_w of SPES_MEIM_0.5 is $\overline{108}°$, a value that increases up to $\overline{123}°$ for SPES_BBIM_0.5, to $\overline{124}°$ for SPES_MOIM_0.5 and up to $\overline{130}°$ for SPES_BOIM_0.5.

The measurements of the static water contact angles on the air-side have not revealed significant differences between different DS and length of the imidazolinium alkyl chains.

In order to explain the difference between air-side and PTFE-mold side SWCA data, a hypothesis that can be done is that, during the evaporation of the solvent, the apolar $SO_3^-I.Ls^+$. groups in contact with a hydrophobic surface -the PTFE mold- are orientated towards the hydrophobic surface, since they are less affine to the solvent. Thanks to the selective orientation of the imidazolinium alkyl chains on the PTFE-side surface of SPES_I.L. membranes, the mold-side is characterized by higher SWCAs, ranging from $\overline{108}°$ to $\overline{131}°$, than the ones measured at the air-side of the membranes themselves.

Scanning Electron Microscopy analyses (SEM)

SEM analyses for SPESs and SPES_I.Ls. samples were performed in order to clarify the influence of different hydrophobic I.Ls. on the surface properties of the polymeric membranes prepared.

Figure 20 presents the morphologies of representative membranes from both air-side and PTFE-side of SPESs and SPES_I.Ls. samples.

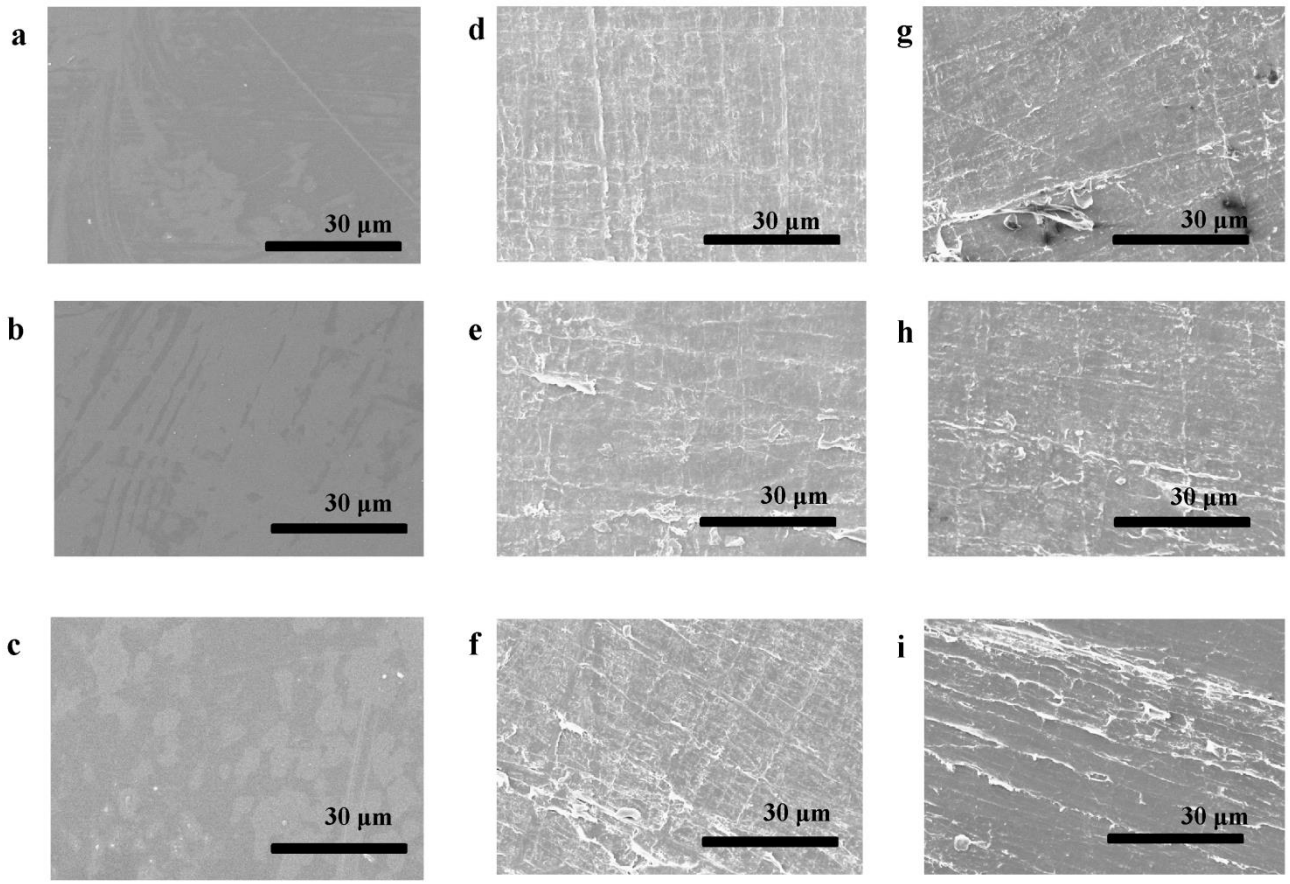

Figure 20. (a) SPES_1 air-side; (b) SPES_1 PTFE-side; (c) SPES_MEIM_0.5 air-side; (d) SPES_MEIM_0.5 PTFE-side; (e) SPES_MEIM_0.75 PTFE-side; (f) SPES_MEIM_1 PTFE-side; (g) SPES_BBIM_1 PTFE-side; (h) SPES_MOIM_1 PTFE-side and (i) SPES_BOIM_1 PTFE-side.

In the case of SPES_1, no surface differences are detectable between the air-side (20a) and the mold-side of the polymeric membrane (20b). When I.Ls. are added, it is possible to observe that the surface at the air-side remains smooth (20c), while the surface at the mold-side of the membrane changes from smooth to rough (20d).

The roughness of the PTFE-side of SPES_I.Ls. membranes increases as the DS of SPESs increases, i.e. with the number of hydrophobic I.Ls. cations exchanged, as it is possible to observe comparing

SPES_MEIM_0.5 (20d) with SPES_MEIM_0.75 (20e) and SPES_MEIM_1 (20f), and it enhances as the length of the imidazolinium alkyl chains enhances, as shown in Figure 20f for SPES_MEIM_1, in Figure 20g for SPES_BBIM_1, in Figure 20h for SPES_MOIM_1 and in Figure 20i for SPES_BOIM_1.

SEM analyses of SPES_I.Ls. air-side samples are reported in Figure 21.

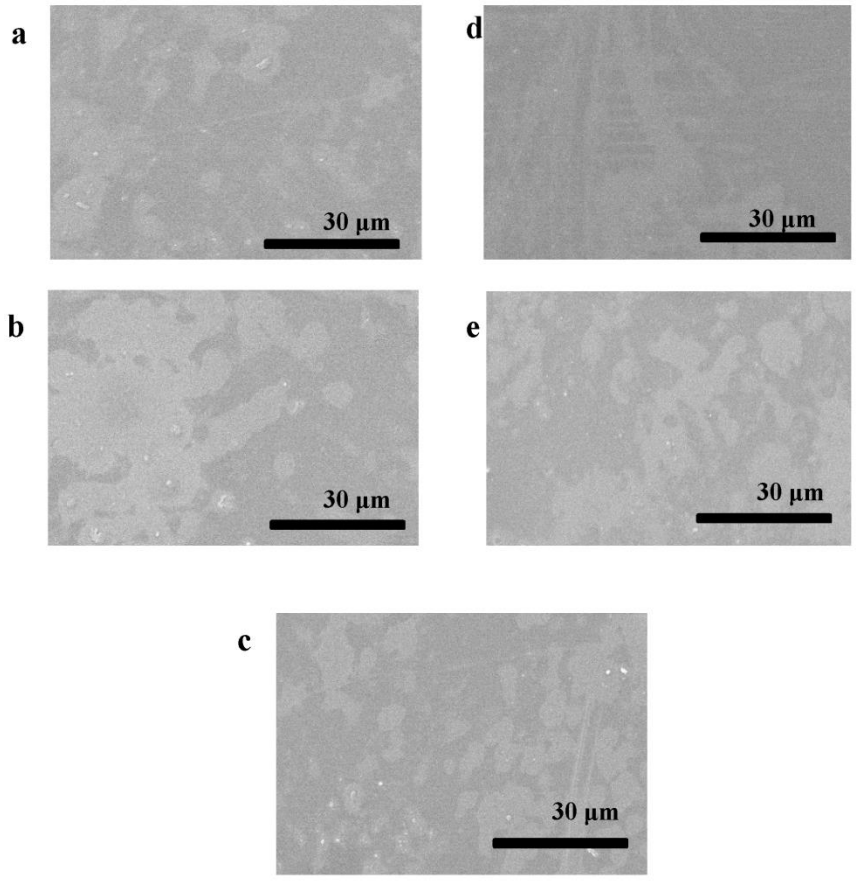

Figure 21. (a) SPES_MEIM_0.75 air-side; (b) SPES_MEIM_1 air-side; (c) SPES_BBIM_1 air-side; (d) SPES_MOIM_1 air-side and (e) SPES_BOIM_1 air-side.

SEM images are in good agreement with SWCA data reported in Table 9. These results are due to the selective orientation of the imidazolinium alkyl chains on the hydrophobic PTFE mold during the evaporation of the solvent, thus changing the membranes surface in correspondence of the PTFE-side from smooth to rough and promoting the formation of highly hydrophobic surfaces.

Atomic Force Microscopy analyses (AFM)

It is well known that wetting of a surface by a solvent is affected by the roughness of the surface itself; the effect of roughness on the wetting properties of some representative membranes of both unmodified SPESs and SPES_I.Ls. samples, presented in Figure 22, have been examined by AFM analyses; the corresponding RMS roughness values are reported in Table 11.

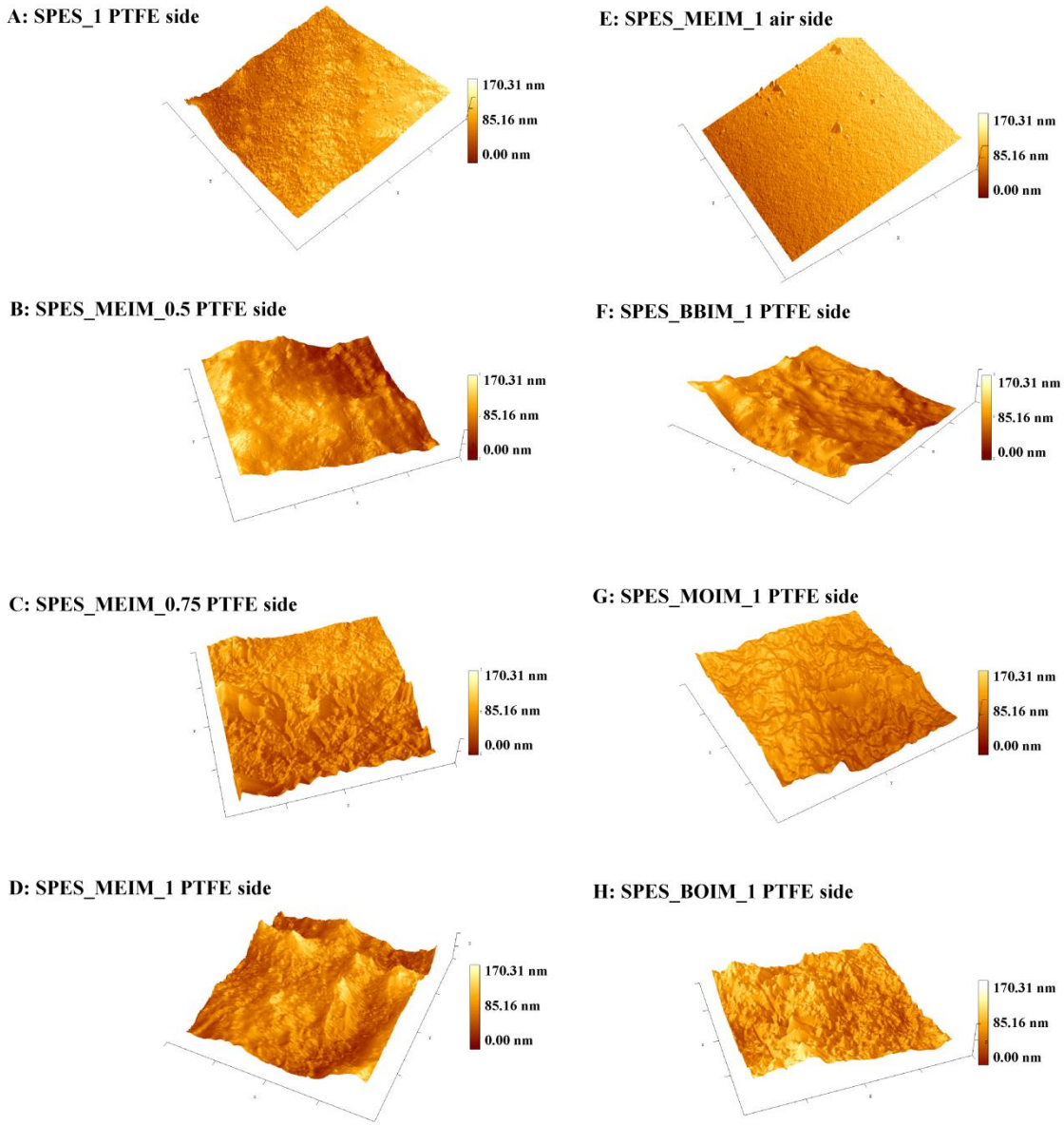

Figure 22. (a) SPES_1 PTFE-side; (b) SPES_MEIM_0.5 PTFE-side; (c) SPES_MEIM_0.75 PTFE-side; (d) SPES_MEIM_1 PTFE-side; (e) SPES_MEIM_1 air-side; (f) SPES_BBIM_1 PTFE-side; (g) SPES_MOIM_1 PTFE-side and (h) SPES_BOIM_1 PTFE-side.

Samples	air-side RMS (nm)	PTFE-side RMS (nm)
SPES_1	45.55	67.27
SPES_MEIM_0.5	46.41	101.01
SPES_MEIM_0.75	60.38	163.87
SPES_MEIM_1	66.65	185.15
SPES_BBIM_1	87.89	192.78
SPES_MOIM_1	88.53	206.34
SPES_BOIM_1	93.22	236.85

Table 11. RMS roughness values of SPESs and SPES.I.Ls. samples.

Comparing AFM topographies of the mold-side of pristine SPES (Figure 22a) and SPES_I.Ls. samples (Figure 22b, c, d, f, g and h), it is clear that the surfaces of SPES_I.Ls. are much rougher than the surface of SPES sample without I.Ls., as indicated by the RMS roughness values measured (Table 10). When I.Ls. are present, it is possible to observe that the surface at the air-side of the membrane remains smooth (22e). Conversely, the surface at the PTFE-side changes from smooth to rough (22d); RMS roughness data range from 66.65 nm for the air-side of the membrane to 185.15 nm for its PTFE- mold side.

The roughness of the PTFE-side of SPES_I.Ls. membranes increases as the DS of SPESs increases, i.e. with the number of the hydrophobic I.Ls. cations exchanged, as it is possible to observe comparing SPES_MEIM_0.5 (22b) with SPES_MEIM_0.75 (22c) and SPES_MEIM_1 (22d). This behavior was confirmed by RMS roughness values that for SPES_MEIM_0.5, SPES_MEIM_0.75 and SPES_MEIM_1 are 101.01 nm, 163.87 nm and 185.15 nm, respectively.

The influence of I.Ls. characterized by different length of the imidazolinium alkyl chains was also investigated and the results obtained suggest that the roughness of the mold-side of SPES_I.Ls. membranes increases as the length of the imidazolinium alkyl chains increases, as shown in Figure

22e for SPES_MEIM_1 -RMS of 185.15 nm-, in Figure 22f for SPES_BBIM_1 -RMS of 192.78 nm-, in Figure 22g for SPES_MOIM_1 -RMS of 206.34 nm- and in Figure 22h for SPES_BOIM_1 -RMS of 236.85 nm-. As reported in the introduction, the control of surface morphology can enhance the hydrophobicity of the material and, consequently, promote its self-cleaning performances.

Fourier transform- infrared (FT-IR)

In order to explain the differences observed between the air-side and the PTFE-mold side of SPES_I.Ls. films, FT-IR spectra were collected on both sides of the films in order to investigate a possible conformational rearrangement of I.Ls. on the surfaces of the polymeric membranes prepared. Figure 23 shows FT-IR spectra of representative membranes from both air-side and PTFE-side of SPES_I.Ls. samples.

Comparing FT-IR spectra of SPES_MEIM membranes between the mold-side (Figure 23a) and the air-one (Figure 23b), it is possible to observe the presence of MEIM alkyl substituents peaks only on the mold-side surfaces: in fact, the absorption peaks between ~2800 cm^{-1} and 2950 cm^{-1} (1) are characteristic of the alkyl groups C-H stretching. The intensity of these absorption peaks gets higher as the length of I.Ls. alkyl chains increases (Figure 23c, d and e).

FT-IR spectra of SPES_BBIM, SPES_MOIM and SPES_BOIM air-side samples show the same behavior of SPES_MEIM samples: they are reported in Figure 24.

This behaviour indicates that a concentrated solution of SPES_I.L. behaves as a colloidal dispersion of molecules having apolar tails, i.e. imidazolinium alkyl chains, and polar heads, i.e. polymeric chains; in contact with a hydrophobic surface -the PTFE mold- the apolar tails, less affine to the solvent, are orientated to the hydrophobic surface. Thanks to the selective orientation of the imidazolinium alkyl chains on the PTFE-side surface of all SPES_I.L. membranes the mold side is

characterized by higher SWCAs and RMS data than the ones measured at the air-side of the membranes themselves.

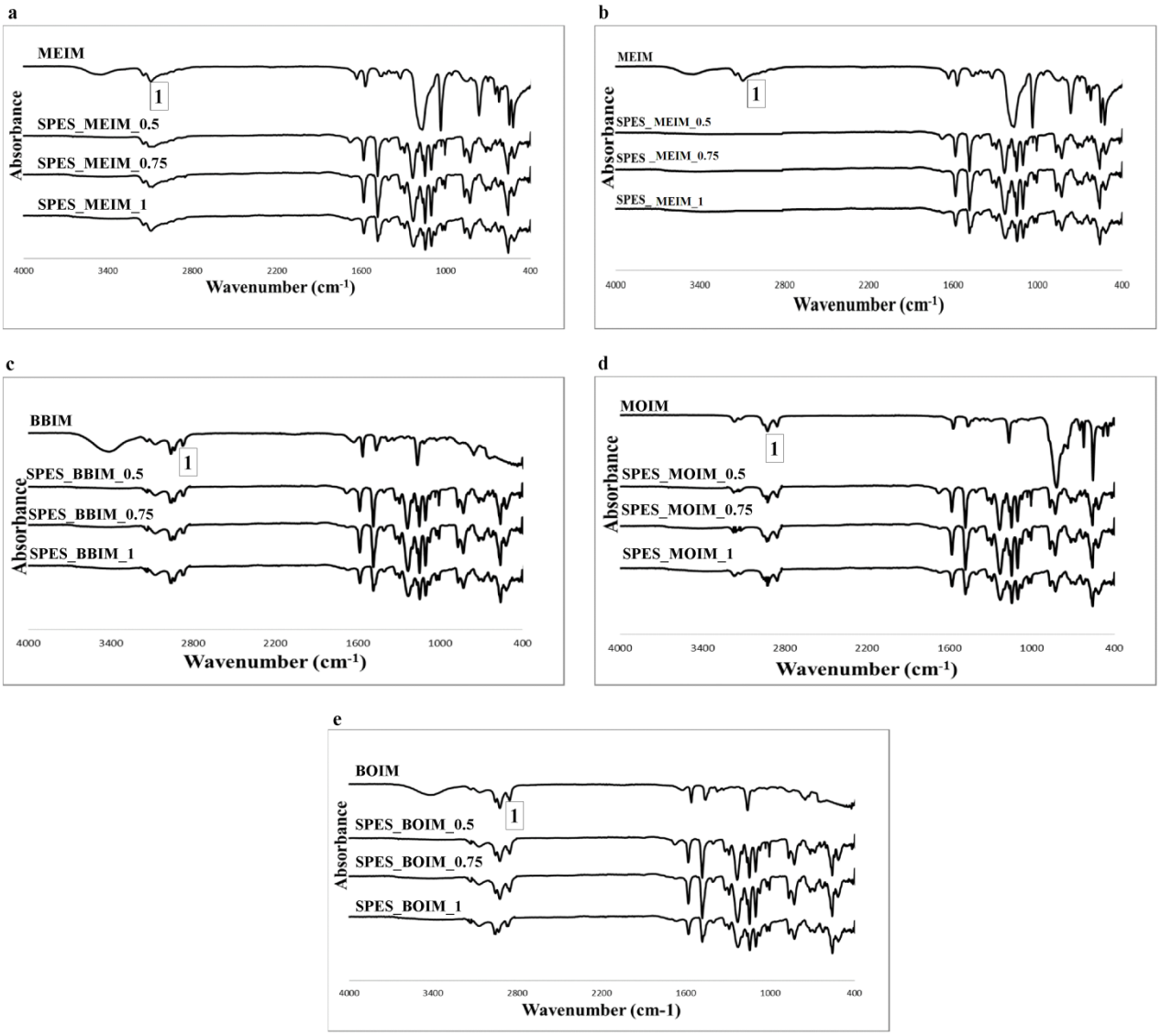

Figure 23. (a) FT-IR spectra of MEIM and SPES_MEIM films on the PTFE-side; (b) FT-IR spectra of MEIM and SPES_MEIM films on the air-side; (c) FT-IR spectra of BBIM and SPES_BBIM films on the PTFE-side; (d) FT-IR spectra of MOIM and SPES_MOIM films on the PTFE-side; (e) FT-IR spectra of BOIM and SPES_BOIM films on the PTFE-side.

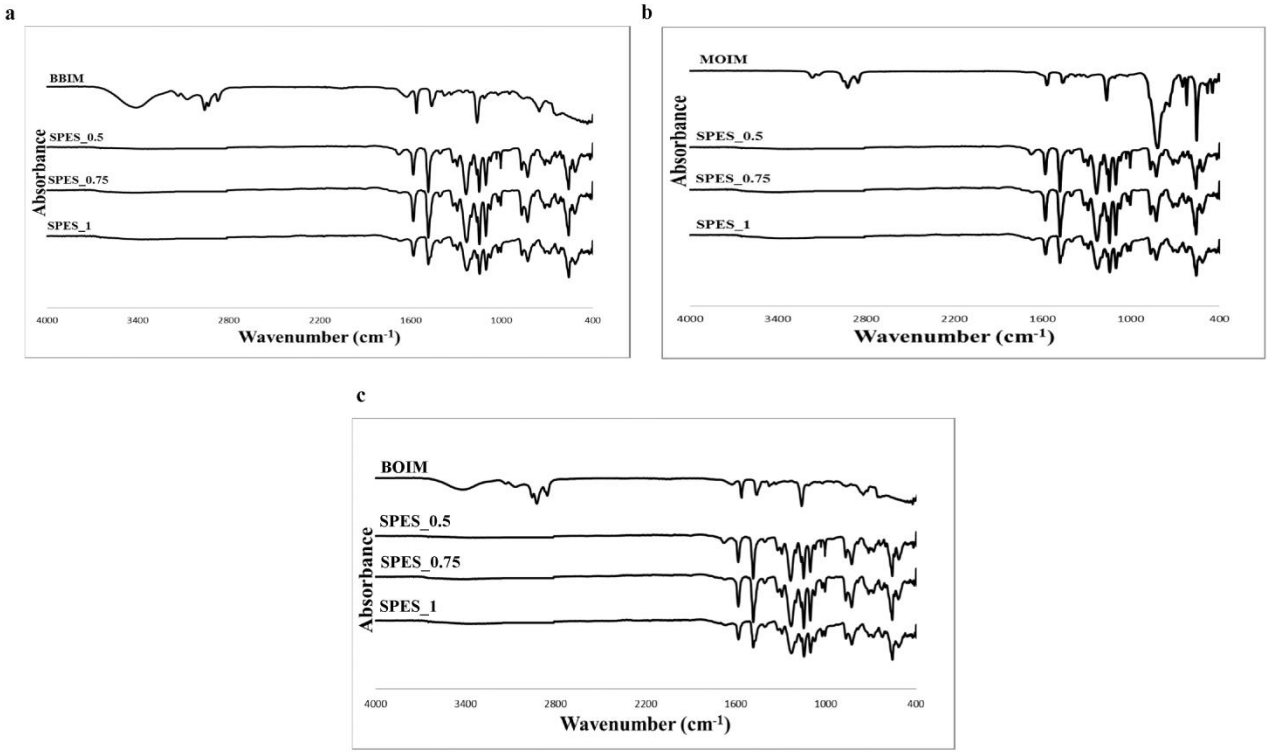

Figure 24. (a) FT-IR spectra of BBIM and SPES_BBIM films on the air-side; (b) FT-IR spectra of MOIM and SPES_MOIM films on the air-side; (c) FT-IR spectra of BOIM and SPES_BOIM films on the air-side.

Self-cleaning test

The self-cleaning capability of SPES_I.Ls. films prepared in this work were tested. Carbon-based filth was simulated by homogenous deposition of a carbon based dust on a film obtained from a representative sample, SPES_BOIM_1, characterized by θ_w (PTFE-side) of$\overline{131°}$. Figure 25 shows the polymeric surface of SPES_I.L. film, before (25a) and after the deposition of carbon stains (25b) through spray drying. Water droplets, were dripped from above the sample surface, simulating rain (Figure 25c and Figure 26) and carried carbon dust with them: the surface of the film appears clean after few water drops (25d).

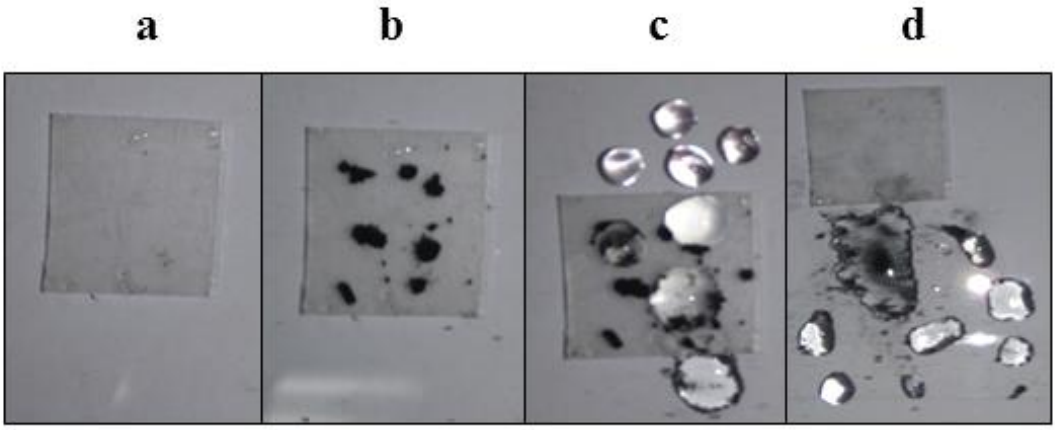

Figure 25. Self-cleaning test on SPES_BOIM_1 film.

Figure 26. Dripping water on SPES_I.Ls. during self-cleaning test.

Conclusion

The use of SPESs, bearing sulfonic acid groups covalently bonded along the polymeric chain, is very advantageous in fields when the modulation of wetting properties is requested. Within this context, the use of I.Ls. combined with SPESs can be a way to create tailor-made hydrophobic materials.

In this work, a series of SPESs with different DS were successfully prepared via homogeneous synthesis. An ionic exchange reaction between the K^+ cation of the sulfonic comonomer of SPESs and different cationic apolar groups based I.Ls. was performed in order to modulate the wetting properties of SPESs; four different I.Ls. were synthesized with apolar alkyl chains characterized by increasing length: 1-Ethyl,3-Methyl Imidazolinium methyl sulfite (MEIM), 1,3-Dibutyl Imidazolinium bromide (BBIM), 1-Methyl,3-Octyl Imidazolinium bromide (MOIM) and 1-Butyl,3-Octyl Imidazolinium bromide (BOIM).

SPES_I.Ls. samples were cast onto a PTFE mold to obtain membranes; wetting properties were measured both on the air-side surface and on the PTFE-side surface of the membranes themselves. Thanks to the addition of I.Ls., the hydrophobic properties measured on the PTFE-side surface increase as the quantity of sulfonated groups increases, due to the higher number of I.Ls. cations exchanged. Increasing the length of the apolar alkyl chains of the I.Ls. cations, the static water contact angles increase: θ_w of SPES_MEIM_0.5 is $\overline{108}°$, a value that increases up to $\overline{123}°$ for SPES_BBIM_0.5, to $\overline{124}°$ for SPES_MOIM_0.5 and up to $\overline{130}°$ for SPES_BOIM_0.5. Furthermore, SWCA measurements on the air-side do not reveal significant differences changing DS and the length of the alkyl chains.

Combining SWCA data with both SEM and AFM analyses, it was possible to conclude that the increase of hydrophobic features on the mold-side for SPES_I.Ls. membranes with respect to the air-side is probably due to the organization of the apolar imidazolinium alkyl chains occurring

during the evaporation of the solvent and to the interaction with high hydrophobic PTFE mold surface.

To the authors' best knowledge the present observation, i.e. of an induced roughness of the surface of films promoted by an ionic exchange reaction between cationic moieties of SPESs polymers and hydrophobic cationic I.L.s groups, has never been reported in previous scientific literature.

Furthermore, the photo-chemical stability of SPESs and SPES_I.Ls. samples and the self-cleaning properties of SPES_I.Ls. films prepared were successfully tested.

4. Conductive inks based on methacrylate end-capped poly (3,4-ethylenedioxythiophene) for printed and flexible electronics[1,2,3,4,5]

Overview

The synthesis of a new methacrylate end-capped Poly(3,4-ethylenedioxythiophene) (PEDOT) was performed: the end-capped PEDOT obtained is soluble in common organic solvents, thus overcoming the well-known technical problems related to the use of commercial PEDOT, Baytron®, in different printing technologies, such as screen printing, due to its poor processability and compatibility in formulations with other resins and polymers.

The synthetic method developed is based on the direct oxidative polycondensation of 3,4-ethylenedioxythiophene (EDOT) in the presence of an oxidant species and a cross-linkable end-capper, i.e. methacrylate end-capped EDOT (mEDOT), prepared via Friedel Crafts acylation with methacryloyl chloride. The oxidative polycondensation between EDOT and mEDOT monomers in the presence of a new kind of doping agent, SPES -characterized by different DS- was conducted,

---

1. Sabatini, V.; Farina, H.; Ortenzi, M.A. "Conductive inks based on methacrylate end-capped poly (3,4-Ethylenedioxythiophene) for printed and flexible electronics", 2016, Polymer Engineering&Science. DOI: 10.1002/pen.24502.

2. Sabatini, V.; Farina, H.; Ortenzi, M.A. "Functional End-Capped Conducting Poly (3,4-Ethylenedioxythiophene), 2016, American Institute of Physics. DOI: 1063/1.4949657.

3. Sabatini, V.; Bisutti, G.; Di Silvestro, G.; Farina, H.; Ortenzi, M. A. "Sistema di trasferimento per stampa", 2016, P62129IT00.

4. Sabatini, V.; Bisutti, G.; Di Silvestro, G.; Farina, H.; Ortenzi, M. A. "Sistema migliorato di trasferimento per stampa", 2016, P62528IT00.

5. Sabatini, V.; Bisutti "Sistema di trasferimento per stampa di tecnologia elettronica", 2016, P62449IT00.

leading to functional end-capped conducting PEDOT, with conductivity of 210 S/cm, 50 S/cm higher than the one of commercial PEDOT.

Thanks to the enhancement of solubility, leading to better processability, end-capped PEDOTs were formulated with a thermoplastic ink, Plastisol®, and electronic circuits were successfully screen printed on flexible substrates, in particular cotton, in order to obtain printed cross-linkable electronic circuits.

Poly(3,4-ethylenedioxythiophene): Background on polymerization route

**This chapter is based on the review of Roncali, J.* (66)

Introduction

The last few decades have been marked by the growing importance taken by two classes of materials, organic polymers and inorganic semiconductors. Thus the lightness of weight, processability, and resistance against corrosion of organic polymers have led in many applications to the replacement of metals or to the creation of new original materials. On the other hand, it is almost superfluous to mention the considerable impact of inorganic semiconductors on both everyday life and on the development of many fields of modern science and technology. In such a context, it is not very surprising that materials capable of simultaneously presenting the properties of organic polymers and of semiconductors have rapidly become a subject of considerable interest for both academic and industrial researchers.

Although their structure and physicochemical properties still pose a number of fundamental problems, conducting polymers (CPs) are at present intensively studied in view of their multiple potential technological applications extending from bulk utilizations such as antistatic coatings to sophisticated or selective modified electrodes and sensors.

The modern era of CPs began at the end of the 1970 when Heeger and MacDiarmid discovered that polyacetylene, synthesized via Shirakawa's method, could undergo a 12 order of magnitude increase of conductivity upon charge-transfer oxidative doping.

The essential structural characteristic of CPs is given by their conjugated π system extending over a large number of recurrent monomer units. This characteristic feature results in low-dimensional materials with a high anisotropy of conductivity which is higher along the chain direction. Polyacetylene is the simplest model of this class of materials and, despite its environmental instability which constitutes a major obstacle to practical applications, remains the archetype of CPs and is still subject to much theoretical and experimental work.

Poly(heterocyc1es) can be viewed as an sp2p, carbon chain in which the structure analogous to that of cis(CH), is stabilized by the heteroatom.

These CPs differ from polyacetylene, by (i) their nondegenerate ground state related to the non-energetic equivalence of their two limiting mesomeric forms, aromatic and quinoid, (ii) their higher environmental stability, and (iii) their structural versatility which allows the modulation of their electronic and electrochemical properties by manipulation of the monomer structure.

An important step in the development of conjugated poly(heterocyc1es) occurred in 1979 when it was shown that highly conducting and homogeneous free standing films of poly(pyrro1e) could be produced by oxidative electro-polymerization of pyrro1e. The electrochemical synthesis of poly(pyrro1e) from aqueous H_2SO_4 solutions had been initially reported ten years before but the poor mechanical and electrical properties of the obtained material did not give rise to further development.

The electrochemical polymerization has been rapidly extended to other aromatic compounds such as thiophene, furan, indole: carbazole, azulene, pyrene, benzene and fluorene. These pioneering works have also triggered a renewal of interest for electro-generated poly(aniline).

Among these numerous CPs, Poly(thiophene) (PT) has rapidly become the subject of considerable interest. From a theoretical viewpoint, PT has been often considered as a model for the study of charge transport in CPs with a nondegenerate ground state, while on the other hand, the high environmental stability of both its doped and un-doped states together with its structural versatility have led to multiple developments aimed at applications such as conductors, electrode materials, and organic semiconductors.

Synthesis of Poly(thiophenes)

Although the synthesis of polymeric materials from thiophene derivatives has been known for long, the origin of the intensive research efforts aiming the optimization of the preparation of PTs is in keeping with the emergence of the widespread general interest for CPs in the early 1980s.

PTs are essentially prepared by means of two main routes, i.e. the chemical and the electrochemical syntheses.

Chemical synthesis

Thiophene oligomers have been prepared by several methods and some of them have been proposed as generalizable to the preparation of polymers. Thus, mixtures of several thiophene oligomers have been obtained by reaction of 2-iodothiophene with copper bronze. Tri-thiophene has been prepared by cyclization of l,4-diketones containing one or more thiophene rings.

Quater- and sexithiophene have been synthesized by coupling of a-lithiated thiophenes in presence of cupric chloride or organ boranes. The synthesis of PT by oxidative coupling of bis-lithiated thiophene derivatives has been also reported. Grignard coupling of 2,5-dihalothiophenes in presence of transition metal complexes has been extensively employed for the synthesis of PTs.

A conductivity of 14 S/cm has been reported for PT prepared by nickel-catalyzed Grignard coupling of 2, 5-diiodothiophene. More recently thiophene and 3-methylthiophene oligomers have been synthesized by $NiC1_2$ (dppp) (dppp = Ph2PCH2CH2CH2PPh2c) coupling of Grignard compounds with the appropriate bromo thiophene.

PT has been also prepared by plasma polymerization, by oxidative polymerization of thiophene and bi-thiophene in the gas phase using AsF_5 under pressure.

Electrochemical synthesis

Although it is likely that chemical syntheses are the most adequate methods of preparation of oligomers of defined structure, until now the most extensively conjugated and most conductive PTs have been prepared by electrochemical polymerization.

Cathodic Route

Besides the oxidative anodic electro-polymerization of the monomer which is the most convenient and most widely used method, PT can be also prepared by a cathodic route involving the electro-reduction of the complex (2-bromo-5-thieny1) tri-phenylnickel bromide in acetonitrile. This method initially proposed for the synthesis of Poly (p-phenylene), has been extended to PT. The major drawback of this method is that the polymer is produced in its neutral insulating form which leads rapidly to a passivation of the electrode and limits attainable film thickness to ca. 100 nm. On the other hand, this technique presents the advantage to be applicable to electrode materials subject to anodic corrosion such as small band gap semiconductor.

Anodic Route

Compared to other chemical and electrochemical syntheses of conducting poly(heterocycles), the anodic electro-polymerization of the monomer presents several distinct advantages such as absence of catalyst, direct grafting of the doped conducting polymer onto the electrode surface (which is of particular interest for electrochemical applications), easy control of the film thickness by the deposition charge, and possibility to perform at first in situ characterization of the growing process or of the polymer by electrochemical and/or spectroscopic techniques.

The electro-polymerization of bithiophene was initially mentioned in 1980; following this initial work, a large number of studies have been devoted to the analysis of the electro-polymerization reaction and to the optimization of electro-synthesis conditions.

Mechanisms of electro-polymerization

The electrochemical formation of conducting polymers is a unique process. Although it presents some similarities with the electrodeposition of metals since it proceeds via a nucleation and phase-growth mechanism, the major difference lies in the fact that the charged species precursors of the deposited material must be initially produced by oxidation of the neutral monomer at the anode surface. The consequence of this is that various electrochemical and chemical follow-up reactions are possible, making the elucidation of the electro-polymerization mechanism a very complex problem.

Despite the large amount of work devoted to electro-generated PTs, the mechanism of the electro-polymerization of thiophene has been scarcely considered.

This situation probably arises from the fact that it is generally admitted that the electro-polymerization of aromatic compounds occurs via a unique mechanism which has been more extensively analyzed using pyrrole as a model compound. An important aspect of the electro-polymerization reaction is that it proceeds with electrochemical stoichiometry. The oxidation of the monomer requires 2 electrons/ molecule while the excess of charge corresponds to the reversible oxidation or doping of the polymer.

Figure 27 represents the mechanism proposed for the electro-polymerization of heterocycles, by analogy to the already known coupling reactions of aromatic compound.

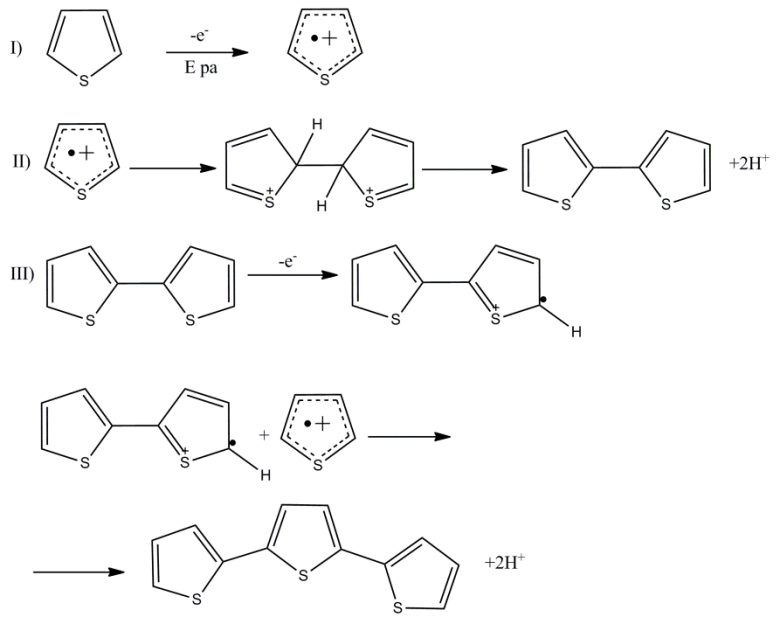

Figure 27. Mechanism of electro-polymerization of five membered heterocycles.

The first electrochemical step (I) consists in the oxidation of the monomer to its radical cation. Since the electron-transfer reaction is much faster than the diffusion of the monomer from the bulk solution, it follows that a high concentration of radicals is continuously maintained near the electrode surface. The second step (II) involves the coupling of two radicals to produce a di-hydro dimer dication which leads to a dimer after loss of two protons and re-aromatization. This re-aromatization constitutes the driving force of the chemical step (II). Due to the applied potential, the dimer, which is more easily oxidized than the monomer, occurs in its radical form and undergoes a further coupling with a monomeric radical. Electro-polymerization proceeds then through successive electrochemical and chemical steps, until the oligomer becomes insoluble in the electrolytic medium and precipitates onto the electrode surface (III).

This mechanism leaves however several questions in abeyance concerning the nature of the rate-limiting step, the exact role of oligomers in the initial deposition step, and the subsequent growth of the polymer chains, respectively. What is clearly established is the oxidation of the monomer to its radical cation and the fact that the electro-polymerization process is not diffusion-limited.

Thus a first characterization of the monomeric radicals by ultrafast cyclic voltammetry has been recently reported. On the other hand, chrono-absorptometric experiments have shown that during the electrodeposition of Poly(pyrrole), the absorbance increases linearly with time t and not with t1/2. This result implies that electro-polymerization is not diffusion-limited and that the rate-determining step is the radical-coupling process.

A similar behavior has been observed for the electrodeposition of Poly(methyl-3-thiophene) (PMeT) even in viscous electrolytic media or under high anodic potentials. The initial deposition step and the process of propagation of the electro-polymerization are less clearly understood and still a matter of controversy. Thus an alternative mechanism involving a radical attack on a neutral monomer has been proposed. The radical-coupling mechanism is supported by the lack of polymerization when the applied potential is adjusted to a value sufficient to oxidize the polymer but not the monomer. However, concerning the radical-monomer mechanism, it has been stressed that the potential required by the second oxidation step might be higher than the oxidation potential of the polymer itself.

In the case of the electro-polymerization of pyrrole in the presence of BF_4^-, it has been suggested that the polymerization process is initiated by the oxidation of the anion. However, this hypothesis appears unacceptable since the oxidation of BF_4^- occurs only at a potential ca. 2 V more positive than the potential where Poly(pyrro1e) is formed. On the basis of theoretical calculations, the deprotonation has been proposed as the rate-limiting step in the electro-polymerization of thiophenes. This hypothesis is however contradicted by the absence of isotopic effect on the electro-polymerization rate of [2,5-$^2H_2$] thiophene and [$^2H_4$]- thiophene.

The exact role of oligomers in both the initial steps and the propagation of the electro-polymerization has been also a point of debate. On the basis of the delay observed between the rise of the current and the onset of ellipsometric signals, it has been concluded that the formation of oligomers in solution precedes the polymer deposition. The growth of PT and Poly(bithiophene) has been analyzed by time-resolved UV-vis spectroscopy. The comparison of the solution spectra with

those of authentic neutral thiophene oligomers has led to the conclusion that oligomers involving ca. 7 and 12 monomer units were present in solution. However, taking into account for the applied potential and for the high stability of oligomeric radical cations, which increases strongly with their size, it seems likely that the observed spectra correspond to oxidized species (radical cation or dication) and hence to chain lengths considerably shorter than the assumed ones. The adsorption of thiophene on the electrode surface has been proposed as the first step by several groups and evidence for adsorption has been obtained by in situ IR spectroscopy. These observations appear difficult to reconcile with the hypothesis of the formation of oligomers in solution. As a matter of fact, it is not easy to imagine why, once adsorbed, the monomer leaves the electrode surface to form oligomers in solution which re-precipitate onto the electrode. On the other hand, monomer adsorption appears consistent with Near Edge X-ray Absorption Fine Structure (NEXAFS) spectroscopy experiments which indicate that the first polymer layer lies essentially flat on the electrode surface and that the polymeric chains are well ordered, in agreement with the electronic absorption spectra recorded at various stages of the electro-polymerization, which reveal a steady decrease of the mean conjugation length and of the resolution of the vibronic fine structure with the progress of the electro-polymerization.

Perhaps the major argument against oligomer formation as the main reaction pathway toward the polymer is provided by the considerable deterioration of the mechanical, electrical, electrochemical, and optical properties of the polymer observed when oligomers are used as the substrate for electro-polymerization instead of the monomer. As discussed below, if oligomers formation was actually a necessary step between the monomer and the polymer, the same polymer should be obtained with both types of precursor. Thus, although oligomers have been detected in the synthesis or extracted from as-grown PT films, these results do not constitute an unequivocal proof that the electro-polymerization proceeds via oligomers formation since the observed oligomers may well result from side reactions competitive to the growth of the polymer chains.

In short, although these various investigations have contributed to elucidate some aspects of the electro-polymerization mechanism, several steps of the process are not fully understood yet and are still subject to controversial interpretations.

Poly(3,4-disubstituted thiophenes)

It has been recognized that the introduction of a methyl group at the β position of the thiophene ring leads to a significant increase of the conjugation and conductivity.

This effect has been attributed to the statistical decrease of the number of α-β' couplings and to the decrease of the oxidation potential (ca. 0.2 V) caused by the inductive effect of the methyl group. As a further step, di-substitution at the β, β' positions has appeared as an interesting method to synthesize perfectly stereoregular polymers by suppressing any possibility of α-β' coupling. However, this approach is severely limited by the steric interactions between substituents grafted on consecutive monomers that distort the conjugated π system, producing a considerable loss of effective conjugation.

In Figure 28 the structures of the principal (3,4-disubstituted) thiophenes monomers are reported.

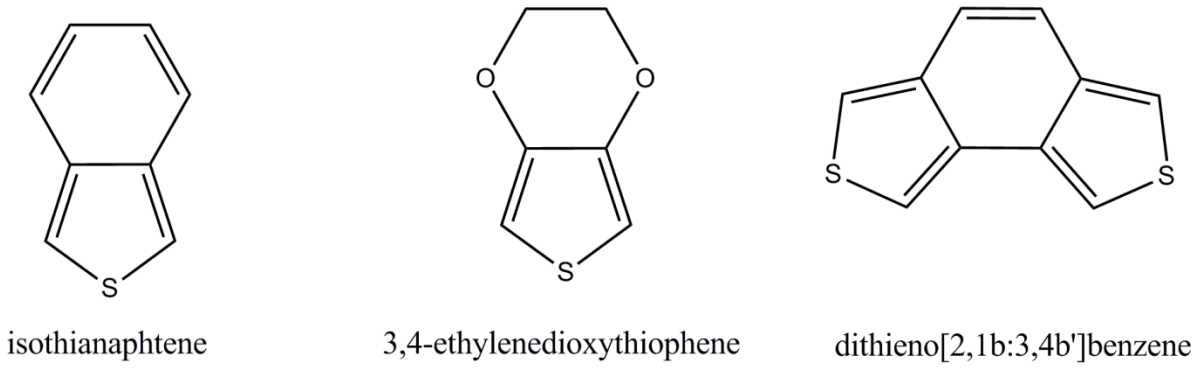

isothianaphtene 3,4-ethylenedioxythiophene dithieno[2,1b:3,4b']benzene

Figure 28. Structure of isothianaphtene, 3,4-ethylenedioxythiophene and dithieno[2,1b3,4b']benzene.

Introduction

In the last decade, fabrication of conductive electrodes on various organic substrates such as paper (66), fibres and tissues (67) and polymeric matrices (68) has been of significant academic and industrial research interest as a simple and fast method to achieve flexible and electrical conductive devices. Furthermore, the use of conductive patterns has been growing for many different applications in fields such as displays, photovoltaics, portable and flexible electronics; a few examples are smart devices, touchscreens displays, organic solar cells and transistors (69).

Over the last years, the integration of conductive electrodes in disposable products and applications has gained an increasing interest in the "printed electronics" field (70) -for example, printed electrochemical sensors represent an important class of conductive patterns that can provide several chemical information for various health-care and environmental applications (71)-. To date, the flexible and printed electronics market is estimated to exceed $300 billion over the next ten-twenty years (72).

Fabrication of electronic components or circuits by depositing conductive inks on organic substrates using very common printing technologies, such as inkjet and screen printing, is a preferred method for manufacturing flexible electronics due to their versatility and low cost of process.

Key to the success of such flexible, printed and electronic devices is thus the specialized engineering of the fabrication materials and device designs: one major challenge of printed electronics is to formulate suitable inks that can be deposited via printing technologies, while providing the required electrical and mechanical performances.

Currently, metal nanoparticles (73) and organic metal complexes or hybrids (74) are widely used materials to formulate conductive inks, but their industrial application is limited by several disadvantages, such as mechanical brittleness and expensiveness (75). Among them, silver-based inks are currently the most promising metal inks and are under rapid development for applications in flexible electronics. Even if different kinds of silver inks have been used for screen printing of conductive traces, the high cost and low content (due to silver poor processability) that influences

the final conductive performance of electrical circuits and electro migration behaviour of silver limit its widespread industrial applications (76).

Many research groups have created conductive inks by utilizing different fillers such as carbon nanotubes (CNT) (77), graphene (G) (78) and graphene oxide (GO) (79). Though all these materials offer excellent conductive properties, devices based on these technologies are commonly realized by lithography or spin-/spray coating: these techniques are either expensive or incompatible with large scale fabrication, thus leading to higher costs per device (80).

Thus, there is still a need to develop new types of conductive inks able to overcome the technical problems previously reported for metals and their complexes, CNTs, G and GO and, accordingly, there are pressing needs to develop large scale low cost fabrication routes of high performance conductive inks.

Several alternatives to CNTs, G, GO, metal nanoparticles and organic metal hybrids such as conducting polymers have been developed. PEDOT is considered the most promising candidate to be used to manufacture highly flexible and printable electrodes due to a number of advantages, such as ease of manufacture, stable formulation using environmentally friendly solvents -i.e. water and alcoholic solvents- good mechanical stability and high optical transmittance (81). On the other side, although PEDOT possesses good electrical conductivity (82), it is insoluble in organic and chlorinated solvents, making it difficult to be processed (83).

Poly(styrene sulfonate) (PSS) is in general introduced as a template to synthesize PEDOT:PSS water dispersion, which is currently the most successful commercial product based on conductive polymer (11): in fact, PEDOT:PSS water dispersions with different conductivities have been successfully used in many devices, including polymer light-emitting diodes, conductive inks and capacitors (84).

PSS works as a template and dopant in PEDOT:PSS dispersion, and provides water dispensability o PEDOT. However, insulating properties of PSS pose problems when it is used as the template.

This makes difficult to balance the conductivity and processing ability of PEDOT:PSS dispersion. A high PSS-to-PEDOT ratio results in good stability of the dispersion and film formation, but decreases conductivity of the film itself.

It is desirable to harness the useful properties of PEDOT and its derivatives in conductive patterns and thus there is a need to develop new types of PEDOT-based inks to solve the above-mentioned problems. The present study aims at filling this technological gap by demonstrating, for the first time, the use of screen printing technology to deposit conductive inks on flexible polymeric substrates: such inks are based on highly conductive and processable PEDOT particles.

A new synthesis of methacrylate end-capped PEDOT with controlled end-capper monomer amount and soluble in organic solvents, is illustrated; the new synthetic method is based on the direct oxidative polycondensation between 3,4-ethylenedioxythiophene (EDOT) monomer with a cross-linkable end-capper -methacrylate end-capped EDOT (mEDOT) prepared via Friedel Crafts acylation starting from methacryloyl chloride-, and with ferric sulfate, the latter used as oxidant species.

After discussing the synthetic and modification methods of PEDOT, the oxidative polycondensation between EDOT and mEDOT monomers in the presence of a new kind of doping agent, SPES -that was synthesized on purpose, with different DS- is illustrated. This polycondensation leads to functional end-capped PEDOTs, with conductivity of 210 S/cm, 50 S/cm higher than the one of commercial PEDOT.

End-capped PEDOTs were formulated with a thermoplastic ink, Plastisol®, and electronic circuits were successfully screen printed on cotton tissues, in order to obtain printed cross-linkable electronic circuits.

Experimental

Materials

3,4-Ethylenedioxythiophene (EDOT, >97%), aluminium chloride ($AlCl_3$, ≥99.99%), sodium hydroxide (NaOH, ≥98% anhydrous), sodium chloride (NaCl, ≥99), magnesium sulfate (>99.5% anhydrous) and ferric sulfate ($Fe_2(SO_4)_3.xH_2O$, >97%) were supplied by Sigma Aldrich and used without further purification. Methacryloyl chloride (≥97%) was purchased by Sigma Aldrich and purified by distillation at 60-70°C under vacuum (about 4 mbar). The purified methacryloyl chloride was stored under nitrogen atmosphere at 5°C.

4,4'-difluorodiphenylsulfone (BFPS, ≥99%) and 4,4'–dihydroxydiphenyl (BHP, ≥97%) were supplied by Sigma Aldrich; 2,5-dihydroxybenzene-1-sulfonate potassium salt (sulfonated hydroquinone, SHQ, ≥98%) was obtained from Alfa Aesar and potassium carbonate (K_2CO_3, ≥98% anhydrous) was purchased from Fluka; all the reagents were dried at 30°C in vacuum oven (about 4 mbar) for at least 24 hr before use and employed without further purification.

N-methyl-2-pyrrolidone (NMP, ≥99.5% anhydrous), toluene (99.8% anhydrous), dimethylacetamide (DMAc, ≥99.5%), distilled water Chromasolv® (≥99.9%), acetone (≥99.9%), methylene chloride (CH_2Cl_2, ≥99.5), acetonitrile (99.8% anhydrous) and dimethyl sulfoxide-d_6 (DMSO-d_6, 99.96 atom % D) were supplied by Sigma Aldrich and used without purification. Commercial Plastisol® was purchased by Excalibur®; commercial Polyarylethersulfone -Radel® A-A-300A- was supplied from Solvay SA S.p.A.

Synthesis of PEDOT

A 100 cm^3 two neck round-bottom flask equipped with magnetic stirring is charged with EDOT (2.50 g) and H_2O (3 cm^3). A solution of $Fe_2(SO_4)_3.xH_2O$ (5g) in H_2O (10 cm^3) is added drop wise via cannula to the solution of EDOT by stirring. The reaction mixture is stirred for 24 hr at room temperature and under air atmosphere. The obtained dark-blue deposition, i.e. the polymerization

product, is collected by centrifugation with Eppendorf centrifuge, 8000 rpm, washed by a 50% V/V solution of acetone and acetonitrile (two washing with 10 cm^3 of solution) and dried under vacuum at 30°C and 4mbar overnight. The reaction mechanism proposed is reported in Figure 29 (85).

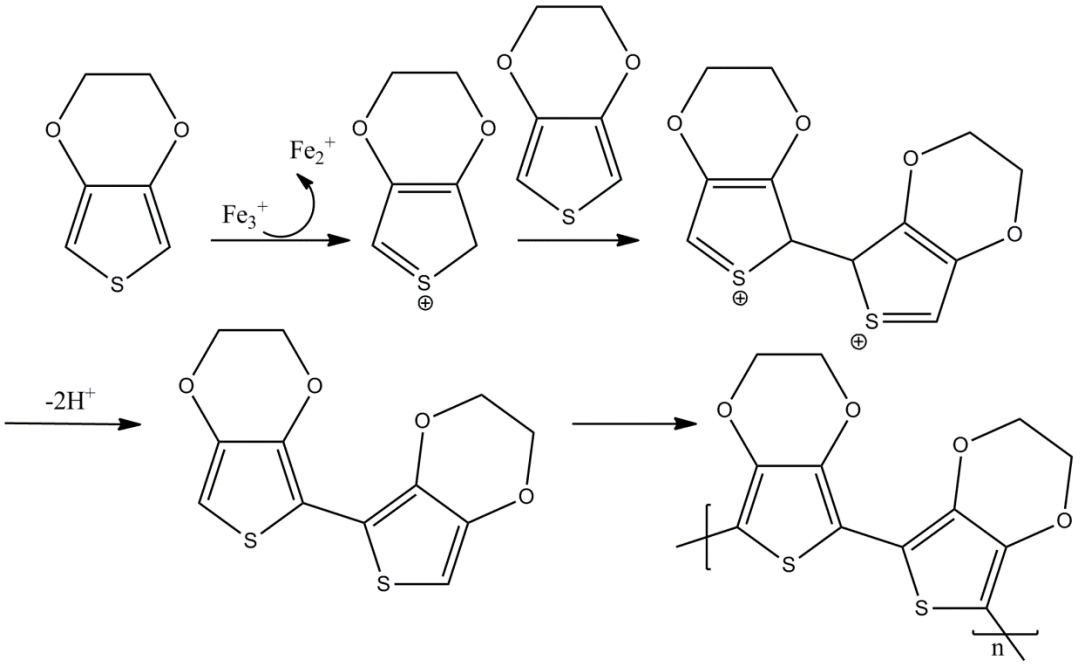

Figure 29. Proposed mechanism for the oxidative polycondensation reaction of PEDOT.

Synthesis of methacrylate end-capped EDOT monomer (mEDOT)

mEDOT is synthesized via Friedel Crafts acylation; $AlCl_3$ (1.03 g) and CH_2Cl_2 (10 cm^3) are introduced in a 50 cm^3 two-neck round bottom flask equipped with magnetic stirring; the flask, under nitrogen atmosphere, is charged drop wise via cannula with methacryloyl chloride (0.67 cm^3) under constant stirring.

The solution obtained is added drop wise via cannula in a 150 cm^3 three-neck round bottom flask charged with EDOT (0.75cm^3) and equipped with a nitrogen inlet adapter, a reflux condenser and an overhead mechanical stirrer. The solution is heated under reflux for 2 hr, cooled to room temperature and then precipitated in water. The separation between the organic layer and the chlorinated one is performed via a separatory funnel; the chlorinated layer is washed three times

with 10% w/w of NaOH solution (around 10 cm^3 for each washing) and three times with a solution of saturated NaCl (around 10 cm^3 for each washing), and then is dried with anhydrous magnesium sulfate. Magnesium salt is removed via filtration through a filter cannula. The residual solvent is removed from the resulting orange solution under reduced pressure (about 4 mbar) and the resulting yellow solid is dried under vacuum (about 4 mbar) at 30°C for 12 hr. The obtained mEDOT monomer is purified by flash column chromatography and its chemical structure is determined via ^1H NMR.

Synthesis of methacrylate end-capped poly (3,4-ethylenedioxythiophene) (mPEDOT)

Three mPEDOT polymers with increasing quantity of mEDOT monomer, -25/50/75% mol/mol respects to EDOT- were synthesized. The feeds are reported in Table 12.

Samples	Molar % of mEDOT	EDOT (g)	mEDOT (g)	DMAc (cm^3)
mPEDOT_0.25	25	2.19	0.81	2.50
mPEDOT_0.50	50	1.72	1.27	3.90
mPEDOT_0.75	75	0.42	1.51	6.50

Table 12. Feed of the reagents for mPEDOTs polymers with different molar percentages of mEDOT monomer.

In a representative polymerization procedure, a 100 cm^3 two neck round-bottom flask equipped with magnetic stirring is charged with EDOT and a solution of mEDOT in DMAc. A solution of $Fe_2(SO_4)_3.xH_2O$ (5g) in DMAc (10 cm^3), is added drop wise via cannula to the solution of EDOT and mEDOT by stirring. The reaction mixture is stirred for 24 hr at room temperature and under air atmosphere. The obtained dark-violet deposition, i.e. the polymerization product, is collected by

centrifugation with Eppendorf centrifuge, 8000 rpm, washed by a 50% V/V solution of acetone and acetonitrile (two washing with 10 cm^3 of solution) and dried under vacuum at 30°C and 4mbar overnight. The degree of polymerization and structure of mPEDOTs polymers are determined by ^1H NMR spectroscopy.

Synthesis of Sulfonated Polyethersulfones (SPESs)

SPESs syntheses were performed in according with the procedure reported on page 27.

Synthesis of methacrylate end-capped Poly(3,4-ethylenedioxythiophene) (mPEDOT) with SPESs as doping agent (mPEDOT_SPES)

The three syntheses of mPEDOTs were repeated introducing SPES as doping agent. For each molar percentage of mEDOT monomer, the polymerization reaction was performed changing SPES DS - 0.5/0.75/1 meq $SO_3^-*g^{-1}$ of polymer-.

The exact amount of the monomers used for the polymerization reactions are reported in Table 13. In a representative polymerization procedure, a solution of SPES in DMAc (2.5 cm^3) is mixed with EDOT and a solution of mEDOT in DMAc, in a 100 cm^3 two neck round-bottom flask equipped with magnetic stirring.

A solution of $Fe_2(SO_4)_3.xH_2O$ (5g) in DMAc (10 cm^3) is added drop wise via cannula to the suspension obtained by stirring. The reaction mixture is stirred for 24 hr at room temperature and under air atmosphere. The obtained dark-blue deposition, i.e. the polymerization product, is collected by centrifugation with Eppendorf centrifuge, 8000 rpm, washed by a 50% V/V solution of acetone and acetonitrile (twice for 10 cm^3) and dried under vacuum at 30°C and 4 mbar overnight.

Samples	Molar % of mEDOT	real SPES DS (meq SO_3^-*g^{-1} of polymer)	EDOT (g)	mEDOT (g)	DMAc (cm^3)	SPES (g)
mPEDOT_SPES_1	25	0.48	2.19	0.81	2.50	2.50
mPEDOT_SPES_2	25	0.70	2.19	0.81	2.50	2.50
mPEDOT_SPES_3	25	0.98	2.19	0.81	2.50	2.50
mPEDOT_SPES_4	50	0.48	1.72	1.27	3.90	2.50
mPEDOT_SPES_5	50	0.70	1.72	1.27	3.90	2.50
mPEDOT_SPES_6	50	0.98	1.72	1.27	3.90	2.50
mPEDOT_SPES_7	75	0.48	1.42	1.51	6.50	2.50
mPEDOT_SPES_8	75	0.70	1.42	1.51	6.50	2.50
mPEDOT_SPES_9	75	0.98	1.42	1.51	6.50	2.50

Table 13. Loading of the reagents for mPEDOT_SPESs polymers with both different amount of mEDOT monomer and SPES with increasing DS.

Ink formulation and screen printing procedure

mPEDOTs and mPEDOT_SPESs polymers are milled into powders of 600-800 nm in diameter on a hydraulic grinder Stanley Hydraulic®. Conductive inks based on mPEDOTs and mPEDOT_SPESs are prepared by mixing the polymer powder (0.1 g) with Plastisol® (0.5 g) on a mechanic stirring (150 rpm) at room temperature for 1 hr. Conductive inks are coated on 100% cotton textile substrates via screen printing using a mesh count of 32 lines/inch and to an estimated 20 µm wet-coating thickness. Coated films are obtained after the evaporation of water at 110°C in a drying oven for 20-30 seconds. Thickness of the films are measured with surface stylus profiling (Tencor P-6) and estimated to be approximately 100 nm for each sample.

Characterization of polymers

Nuclear magnetic resonance: ^{1}H NMR

^{1}H NMR spectra were collected at 25°C with a BRUKER 300 MHz spectrometer. Samples for the analyses were prepared dissolving 10-15 mg of mEDOT, mPEDOT and SPES samples in 1 cm^3 of DMSO-d_6.

Differential Scanning Calorimetry (DSC)

DSC analyses were conducted using a Mettler Toledo DSC 1, on samples of SPESs, mPEDOTs and mPEDOT_SPESs weighting from 5 to 10 mg each. Temperature program for SPESs is indicated on page 21.

Temperature program for mPEDOTs and mPEDOT_SPESs is the following: i) heating from 25°C to 250°C at 10°C/min; ii) 5 min of isotherm at 250°C; iii) cooling from 250°C to 25°C at 10°C/min; iv) 5 min isotherm at 25°C; v) heating from 25°C to 480°C at 10°C/min (as reported for SPES samples, T_g was measured here).

Thermogravimetric Analyses (TGA)

TGAs were performed using a TGA 4000 Perkin Elmer instrument; analyses were conducted under nitrogen atmosphere on samples weighting from 5 to 10 mg each, with a program that provides single heating cycle from 30°C to 800°C at 10°C/min.

Electrical conductivity

Conductivity data are carried out by a Powermeter GBC KDM-160T. Measurements are performed at room temperature measuring electrolytic conductivity by determining the resistance data between two electrodes separated by a fixed distance (15 cm).

Results and Discussion

Synthesis and characterization of mEDOT and mPEDOTs

mEDOT end-capper monomer was synthesized by Friedel Crafts acylation reaction between EDOT and methacryloyl chloride; mPEDOTs polymers were obtained via direct oxidative polycondensation reaction between EDOT and mEDOT monomers with increasing quantity of mEDOT monomer, -25/50/75% mol/mol respects to EDOT- and in the presence of an oxidant species, i.e. ferric sulfate (Figure 30).

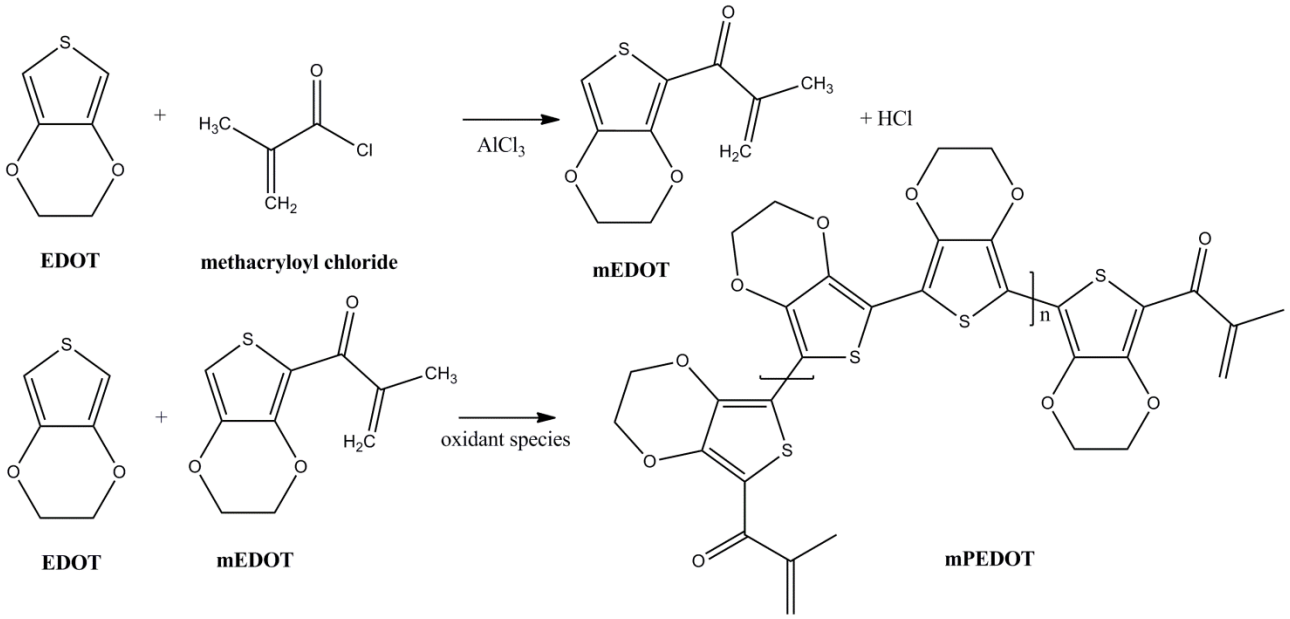

Figure 30. Synthetic route for mEDOT and mPEDOT.

Thanks to the use of methacrylate end-cap, mPEDOTs polymers showed an improved solubility in both apolar solvents, such as toluene, and polar ones, i.e. dimethylacetamide and dimethylformamide; furthermore, it was found that mPEDOTs solubility increases as the quantity of mEDOT monomer increases.

Figure 31 shows ^{1}H NMR spectrum of mPEDOT_0.25 with a mEDOT nominal molar percentage of 25% m/m respects to EDOT. The protons “1”at chemical shift δ (ppm) = 6.05-5.95 and “3” at

chemical shift δ (ppm) = 2.44 are respectively the protons from vinyl substituent and the protons by methyl group of methacryloyl chloride. The protons "2" at chemical shift δ (ppm) = 4.30 are the protons from EDOT.

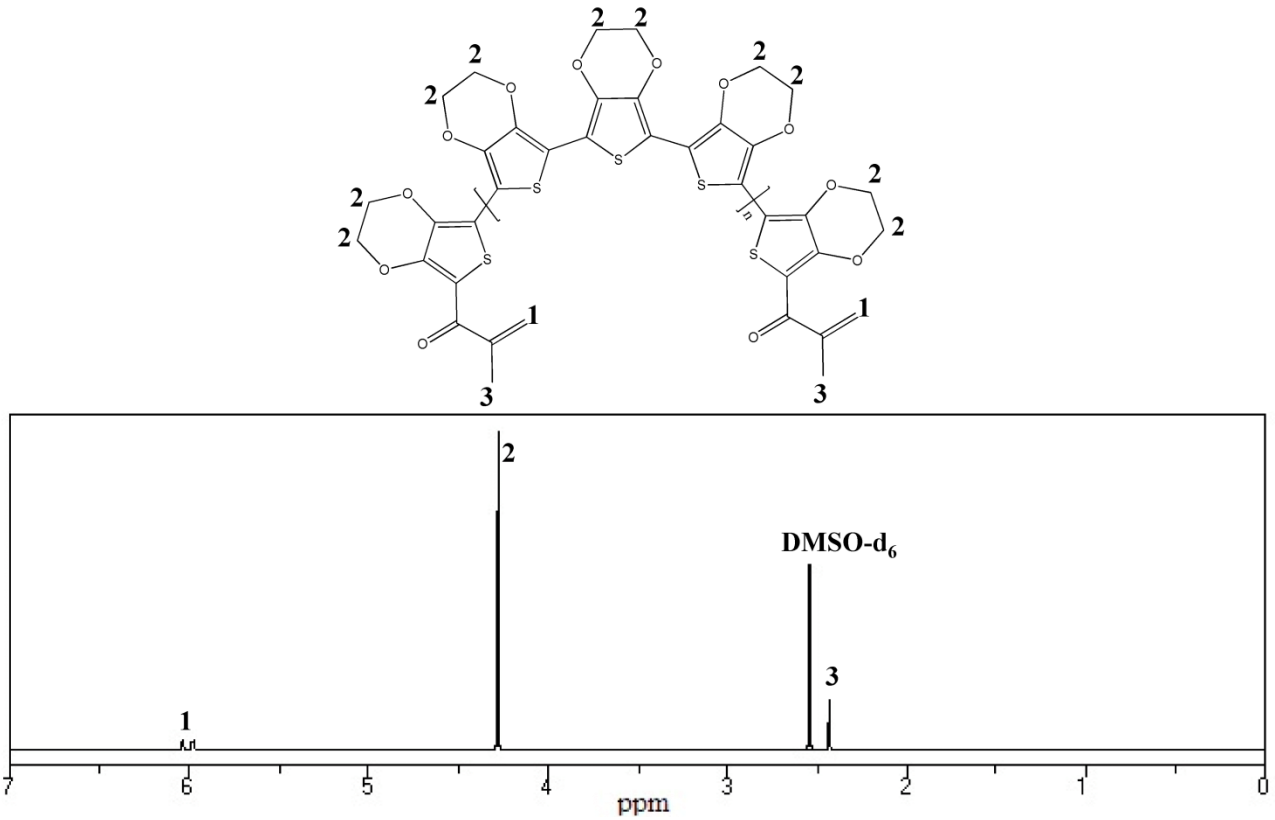

Figure 31. ^{1}H NMR spectrum of mPEDOT_0.25.

The ratios between mEDOT protons "3" and EDOT protons "2" were calculated via Equation 5, using the integral area shown in Figure 32:

$$\text{Integration ratio} = \frac{(area3 \div 3)}{\{[area2 - ((area3 \div 3) \times 4)] \div 4\}} \qquad (5)$$

Where "area3" is the area corresponding to methacryloyl chloride methyl group, "3" is equal to the numbers of methyl group protons, "area2" is the area corresponding to EDOT protons and "4" is

equal to the numbers of EDOT protons. The values obtained for mPEDOT_0.25, mPEDOT_0.50 and mPEDOT_0.75 are 0.21, 0.30 and 0.63 respectively.

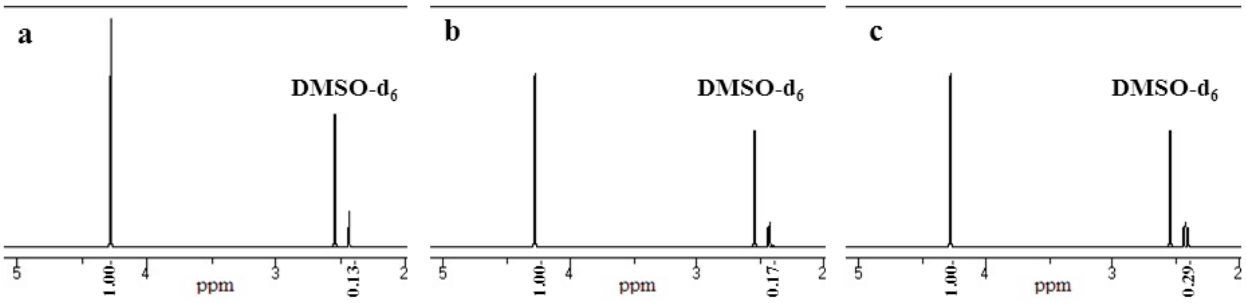

Figure 32. a) ^{1}H NMR spectrum of mPEDOT_0.25, b) ^{1}H NMR spectrum of mPEDOT_0.50 and c) ^{1}H NMR spectrum of mPEDOT_0.75.

Synthesis and characterization of mPEDOT_SPESs

PEDOT is generally synthesized via oxidative polymerization of EDOT in the presence of an agent carrying sulfonic moieties used both as a stabilizer and a dopant for PEDOT oligomers. Oxidative polymerization of EDOT generates the cationic charged PEDOT, which strongly interacts with the sulfonate ion of the doping agent to form a stable PEDOT/doping agent complex.

The dopants based on sulfonic groups commonly used with PEDOT are either organic molecules such as 2-naphtalene sulfonic acid and para-toluene sulfonic acid or sulfonated polymers, i.e. sulfonated polystyrene (PSS).

Although PEDOT:PSS is currently the most successful commercial product of PEDOT-based oligomers, PSS is so hygroscopic that the water-resistant property of PEDOT:PSS complex is very poor, and its conductivity easily changes depending on the temperature and humidity condition.

Besides the reported PEDOT dopants, also SPES can be used as PEDOT doping agent thanks to its stability with moisture (86), the possibility to appropriately modulate the moieties of sulfonic groups in the polymeric chains and to tailor SO_3^- groups distribution homogeneity along the

polymeric chains. To the best our knowledge, no use of SPES in the field of PEDOT dopants has been reported yet.

In view of the above considerations, SPES was here successfully used as doping agent for mPEDOTs, thanks to the charge separation due to the presence of the sulfonated comonomer, SHQ (Figure 33). mPEDOT_SPESs samples were synthesized with both different amounts of mEDOT monomer -25/50/75% mol/mol respects to EDOT- and SPESs with increasing DS -0.5/0.75/1 meq SO_3^-*g^{-1} of polymer-.

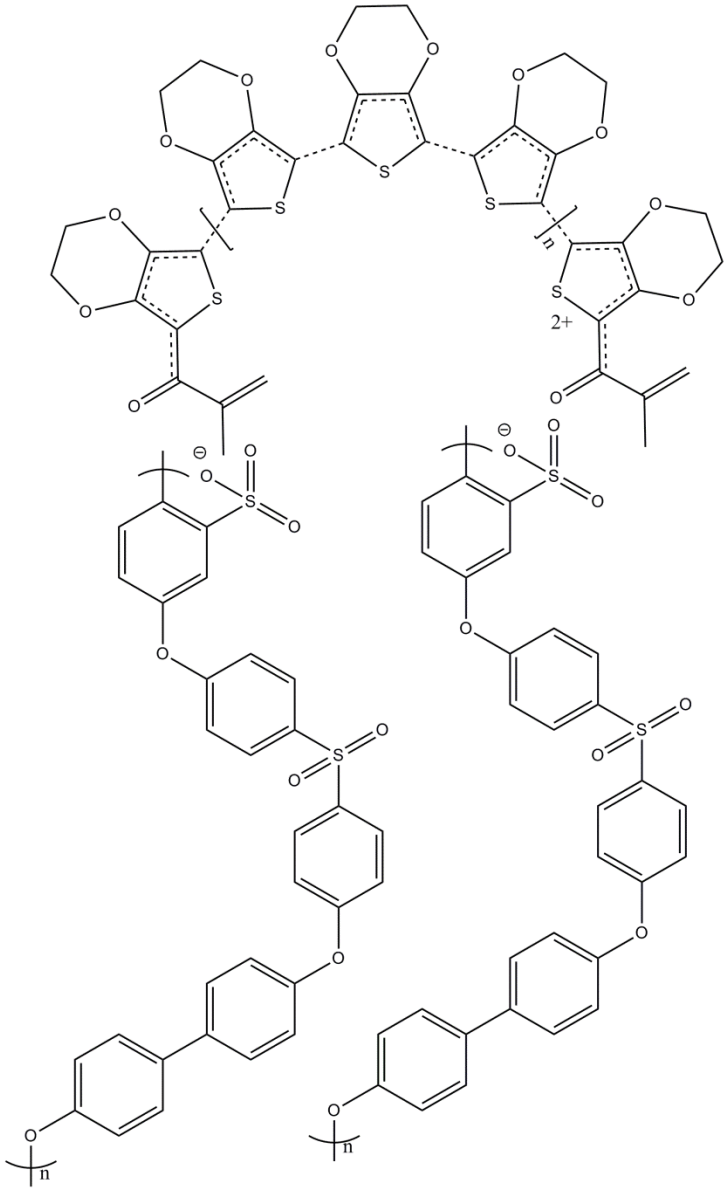

Figure 33. SPES as doping agent for mPEDOT.

The thermal stability of mPEDOT_SPESs samples was estimated via TGA analyses evaluating temperatures corresponding to 1%, 5%, 10% and 60% of weight loss ($T_{1\%}$, $T_{5\%}$, $T_{10\%}$ and $T_{60\%}$) and comparing results obtained with TGA data of PEDOT, mPEDOTs and SPESs samples (Table 14).

Samples	$T_{1\%}$ (°C)	$T_{5\%}$ (°C)	$T_{10\%}$ (°C)	T_g (°C)	Conductivity before screen printing tests (S/cm)
PEDOT	270.1	300.5	315.5	n.d.	160
SPES_0.5	328.4	338.4	378.5	259.7	n.d.
SPES_0.75	315.2	325.2	376.7	290.9	n.d.
SPES_1	312.2	322.2	372.1	303.6	n.d.
mPEDOT_25	269.8	300.3	315.4	293.6	101
mPEDOT_50	269.3	301.9	315.4	290.1	73
mPEDOT_75	269.0	300.1	314.9	287.8	55
mPEDOT_SPES_1	300.9	321.5	370.1	300.3	185
mPEDOT_SPES_2	300.3	323.9	371.5	301.9	196
mPEDOT_SPES_3	299.9	337.7	378.1	299.5	210
mPEDOT_SPES_4	299.5	320.5	370.8	292.6	181
mPEDOT_SPES_5	298.1	323.9	375.0	290.5	190
mPEDOT_SPES_6	296.3	337.5	378.1	290.2	198
mPEDOT_SPES_7	296.7	319.8	371.2	290.8	152
mPEDOT_SPES_8	295.9	323.5	374.9	288.1	169
mPEDOT_SPES_9	295.8	336.2	377.5	287.9	173

Table 14. Degradation temperatures, glass transition temperatures and conductivity values before screen printing tests of the samples synthesized.

PEDOT is rather stable up to the temperature of 270°C. From 270°C a continuous degradation occurs until major decomposition appears in the region between 300-350°C, owing to the thermal degradation of thiophene rings (87).

As previously described on page 31, two steps of weight loss characterize the typical TGA curve of SPES: thermal decomposition of SO_3^- groups at around 300-330°C and the thermal degradation of the polymer starting from around 450-500°C, related to the breaking of $-SO_2^-$ bonds and the degradation of the polymeric chains respectively.

Associating $T_{1\%}$ with the breaking of thiophene bonds, $T_{5\%}$ with the thermal decomposition of SO_3^- groups and $T_{10\%}$ with both the breaking of $-SO_2^-$ bonds and the degradation of thiophene rings, it can be clearly seen from Table 14 that $T_{1\%}$, $T_{5\%}$ and $T_{10\%}$ of mPEDOT_SPESs samples are much higher than the ones of PEDOT and mPEDOTs. Comparing the data trends of mPEDOT_SPESs, thermal stability significantly increases as the DS of SPES increases. As general statement, mPEDOT_SPESs seem to be more thermally stable up to 300°C ($T_{1\%}$) than unmodified PEDOT sample due to the bulky anionic structure of SPES which gives mPEDOT_SPESs better thermal stability. Starting from 300°C, a continuous degradation occurs with the thermal decomposition of SO_3^- groups ($T_{5\%}$) and the degradation of both SPES polymeric chains and thiophene rings ($T_{10\%}$).

No significant correlation between amounts of end-capper employed and mPEDOTs thermal stability was detected.

In addition, DSC was used to assess the thermal properties of PEDOT, mPEDOTs and mPEDOT_SPESs samples. As reported in Table 14, mPEDOTs synthesized have comparable T_g respect to SPESs ones and, furthermore, mPEDOTs T_g decreases as the end-capper amount increases, owing to the increasing quantity of methacrylic based alkyl chains introduced.

Besides, T_g of mPEDOT_SPESs samples tend to rise with the increased amount of SO_3^- groups introduced into the polymer chains, owing to the increasing quantity of the rigid and bulky SHQ comonomer present in the polymer chains.

After the thermal analyses, electrical conductivity measurements were performed to the samples of PEDOT, mPEDOTs and mPEDOT_SPESs. As reported in Table 14, electrical conductivity of PEDOT is as high as 160 S/cm, which is consistent with the results reported by other authors in previous work (88); data conductivity of mPEDOTs are lower than the one of PEDOT, with a significant decrease of conductivity as the loading of mEDOT end-cap increases.

The conductive properties of mPEDOT_SPESs were studied in function of different amounts of mEDOT end-capper monomer employed, Figure 34 (a), and in function of the increasing SPESs DS, Figure 34 (b).

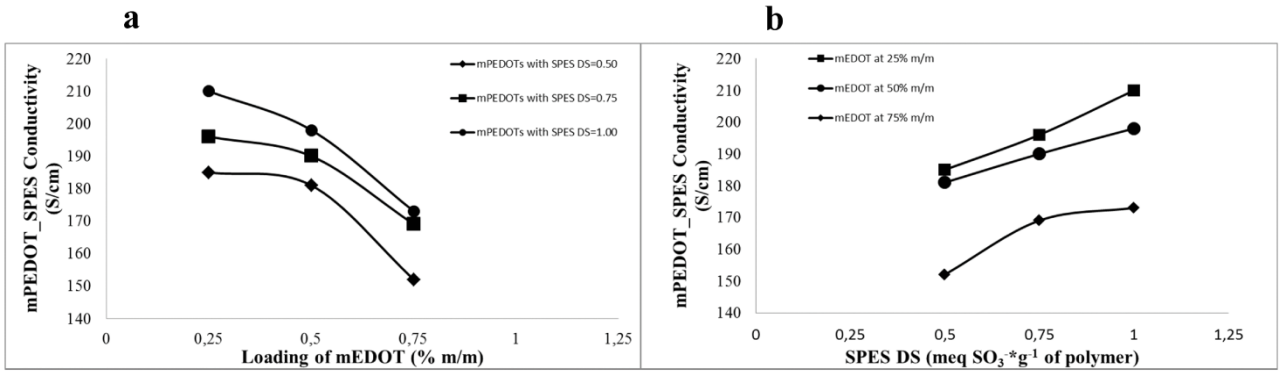

Figure 34. (a) mPEDOT_SPESs conductivity vs. mEDOT loading; (b) mPEDOT_SPESs conductivity vs. SPES DS.

Comparing mPEDOT_SPESs samples synthesized with both SPESs having the same DS and increasing amounts of mEDOT end-capper monomer, Figure 34 (a), it is possible to observe that the conductivity values decrease as the loading of the end-cap gets higher; however, the data obtained are always higher than the ones of unmodified PEDOT.

Figure 34 (b) shows that the conductivity of mPEDOT_SPESs samples characterized by the same amount of mEDOT increases as SPES DS increases: the conductivity data obtained for mPEDOT_SPES_3, synthesized using 25% m/m of mEDOT and SPES with DS of 1.00 meq SO_3^- *g^{-1} of polymer, is 50 S/cm higher than the one of PEDOT.

The results obtained suggest that mPEDOT_SPESs conductive properties are straightly dependent by the loading of mEDOT end-capper monomer and that the higher the DS of SPES used as doping agent, the higher the conductivity.

Screen printing tests

Although various kinds of PEDOT inks have been formulated and transferred onto different substrates and conductive circuits have been obtained, there are still some different shortcomings to be overcome for commercial applications. At present, the most serious limitation is that PEDOT loading is low in PEDOT-based inks, usually in the range of 0.05-1 wt%, and therefore poor electrical conduction of the resultant circuit pattern is obtained.

Thanks to the improved solubility, leading to better processability, in the present work mPEDOTs and mPEDOT_SPESs were formulated with Plastisol®, a thermoplastic serigraphic ink neutrally charged. The polymer powder was mixed with Plastisol® in the range of 20 wt%, and electronic circuits were successfully screen printed on cotton substrates (100% cotton fibers neutrally charged), in order to obtain printed cross-linkable electronic circuits.

Conductive inks were coated on 100% cotton textile substrates, Figure 35 (b), via screen printing technology using a mesh count of 32 lines/inch, previously printed with two electrodes separated by a fixed distance (15 cm), Figure 35 (a), and to an estimated 20 µm wet-coating thickness.

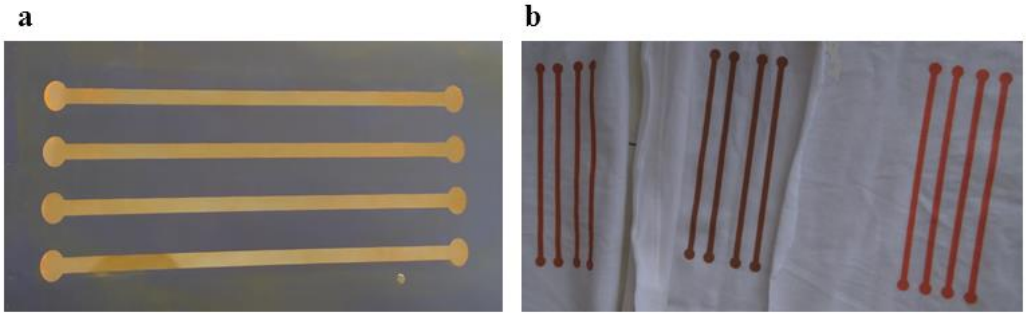

Figure 35. (a) Screen printing mesh printed with two electrodes; (b) Cotton substrates screen printed with mPEDOT_SPESs samples.

Cross-linked films were obtained after thermal exposure at 110°C in a drying oven for 20-30 seconds. Thickness of the final films was estimated to be approximately 100 nm for each sample.

The electrical conductivity of the printed circuits was measured by determining the resistance data between two electrodes separated by a fixed distance (15 cm); data obtained are reported in Table 15.

Samples	Conductivity after screen printing tests (S/cm)
PEDOT	32.4
SPES_0.5	n.d.
SPES_0.75	n.d.
SPES_1	n.d.
mPEDOT_25	53
mPEDOT_50	40
mPEDOT_75	21
mPEDOT_SPES_1	89
mPEDOT_SPES_2	95
mPEDOT_SPES_3	101
mPEDOT_SPES_4	88
mPEDOT_SPES_5	93
mPEDOT_SPES_6	95
mPEDOT_SPES_7	87
mPEDOT_SPES_8	88
mPEDOT_SPES_9	90

Table 15. Conductivity values obtained after screen printing tests of the samples synthesized.

As described previously, data conductivity of mPEDOTs are lower than the one of PEDOT, with a significant decrease of conductivity as the loading of mEDOT end-capper monomer increases. Comparing the data trends of mPEDOT_SPESs samples synthesized with both SPES based dopants having the same DS and increasing amounts of mEDOT end-capper monomer, Figure 36 (a), it is possible to observe that the conductivity values decrease as the loading of the end-cap gets higher; however, conductivity on these samples is always higher than in unmodified PEDOT. Figure 36 (b) shows that the conductivity of mPEDOT_SPESs samples characterized by the same amount of end-cap increases as SPES DS increases.

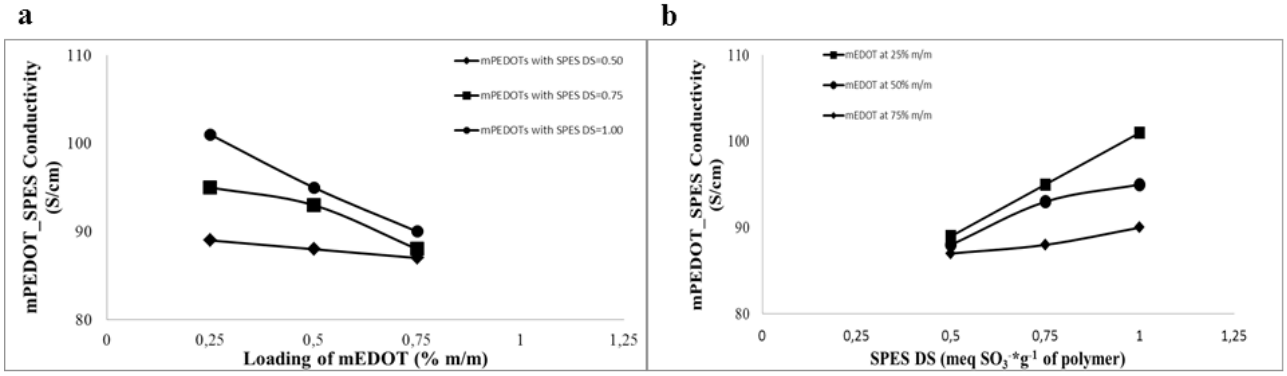

Figure 36. (a) mPEDOT_SPESs films conductivity vs. mEDOT loading; (b) mPEDOT_SPESs films conductivity vs. SPES DS.

As reported for mPEDOT_SPESs data conductivity measured before screen printing tests, the results obtained confirm that mPEDOT_SPESs conductive properties are straightly dependent by the loading of end-cap and, that the higher the DS of SPES used as dopant, the higher the conductivity.

Conclusion

This work studied and compared several PEDOT based oligomers for use in flexible and printed electronics as conductive fillers in formulation with a commercial serigraphic ink, i.e. Plastisol®.

A new synthesis of methacrylate end-capped PEDOT (mPEDOT) with controlled end-capper monomer amount and soluble in common organic solvents was successfully performed. This method includes: direct oxidative polycondensation reaction between 3,4-ethylenedioxythiophene (EDOT) and a cross-linkable methacrylate end-capper (mEDOT), obtained via Friedel Crafts acylation starting from EDOT and methacryloyl chloride, in different molar ratios and in the presence of an oxidant species, i.e. ferric sulfate.

The new material was synthesized in order to overcome the well-known technical problems of PEDOT during serigraphic printing processes, i.e. difficult processability and patterning, due to its insolubility in common organic and inorganic solvents.

Furthermore, the oxidative polycondensation between EDOT and mEDOT in the presence of a new kind of doping agent, SPES -characterized by different DS- was performed, leading to functional end-capped conducting PEDOTs (mPEDOT_SPESs), easy to process and pattern and with improved conductivity.

It was found that the use of cross-linkable end-caps makes PEDOTs soluble in different solvents and only after thermal exposure it is possible to obtain a stable crosslinked film. Furthermore, mPEDOT_SPESs showed excellent thermal stability and their conductive features increase as SPES DS increases.

Thanks to the improved processability, end-capped PEDOTs were formulated with Plastisol®, and electronic circuits were successfully screen printed on both polyesters and cotton substrates, in order to obtain printed cross-linkable electronic circuits.

5. Synthesis of Polyallyl carbonate – Polymethyl methacrylate block copolymers for use as transparent conductive films

Overview

An highly unsaturated molecule displaying a "cardo" structure, 9,9-bis(4-hydroxyphenyl) fluorene, was functionalized with methacryloyl chloride in order to obtain, after separation via flash chromatography, two different molecules: the bi-functional product carrying two vinyl functionalities, and the mono-functional one having at the same time a hydroxyl group and a vinyl functionality.

A new synthesis of Polyallyl carbonate - Polymethyl methacrylate block copolymer, functionalized with 9,9-bis(4-hydroxyphenyl) fluorene based molecules, was performed: the copolymers obtained, having two vinyl functionalities, can be cross-linked with methacrylate end-capped Poly(3,4-ethylenedioxythiophene) (mPEDOT) and with doped mPEDOT (mPEDOT_SPES), thus obtaining a cross-linked conductive Polyallyl carbonate-Polymethyl methacrylate block copolymer; furthermore, the copolymers carrying both an hydroxyl group and a vinyl functionality can be used also for subsequent derivatizations thanks to presence of –OH reactive groups.

The new synthetic method developed is based on a two steps free radical polymerization: the first step is characterized by the homo-polymerization of 4-vinyl-1,3-dioxolan-2-one in the presence of benzoyl peroxide (BPO) as radical initiator; the second step, thanks to the pseudo-living behavior of 4-vinyl-1,3-dioxolan-2-one based radicals, proceeds via block-copolymerization between 9,9-bis(4-hydroxyphenyl) fluorene based monomer functionalized with methacryloyl chloride and the propagating radicals deriving from 4-vinyl-1,3-dioxolan-2-one.

Thanks to the pseudo-living behavior of 4-vinyl-1,3-dioxolan-2-one based radicals it is possible to obtain a di-block copolymer between allyl carbonate based monomer (first block deriving from the first step of polymerization) and methacrylic one (second block deriving from the second step of

polymerization), carrying cardo functionalities. The new Polyallyl carbonate – Polymethyl methacrylate block copolymer was characterized by ^{1}H NMR, ^{1}H-^{1}H COSY, ^{1}H-^{13}C HSQC and ^{13}C spectroscopy.

Polycarbonates

**This chapter is based on the review of Baek, J. H.* (89)

Interest on polycarbonates, their invention and following developments and applications are immediately successive to the growth in aromatic polyesters chemistry.

First examples of aliphatic polyesters were reported in 1863 by Lourenco, who described reaction products from succinic acid and ethylene glycol. In the following years many other aliphatic polyester based materials were prepared and outlined. All these polymers, however, did not show interesting structural properties, and never found use as load-bearing materials.

In the early 1900 Einhorn reported the first synthesis of aromatic polycarbonates as reaction products between hydroquinone, resorcinol and cathecol with phosgene in pyridine solution. Reactions of hydroquinone and resorcinol yielded linear polymers, while reaction of cathecol gave a cyclic carbonate, all showing good thermal properties. The real turning point in the field, however, came almost 50 years later, when Fox discovered bisphenol A (BPA) polycarbonate, while looking for more hydrolytically stable aromatic polyester than polyethylene terephthalate.

The importance of this discovery appears clear when noticing that BPA-PC is still one of the most used polymeric material from an industrial point of view.

Nowadays two are the main methods that ensure high quality products while ensuring economical sustainability: these synthetic routes are known as “the two-phase interfacial” and “the melt transesterification processes”.

Interfacial technology

As shown in Scheme 6 the general procedure involves initial introduction of BPA into the reactor in methylene chloride with a monohydroxylic phenol as end capper in order to control the molecular weight of the final product. In the next step phosgene is added together with aqueous sodium hydroxide in order to quench the HCl produced.

The addition of the NaOH aqueous solution results in the formation of a two-phase liquid-liquid system. At high levels of pH (9-12), low organic phase volume and high BPA concentration, the system also contains a third solid phase, which is given by the mono/dianion of BPA. The reaction is brought to completion and then the mixture is washed with aqueous basic and acid solutions in order to remove residual base and salts. The polycarbonate product is collected via solvent exchange or precipitated in methanol.

The reaction is performed at low temperatures (40°C), therefore the product obtained is the result of kinetic control. This means that the addition of end-capping functionalities is absolutely necessary, in order to completely passivate the chains. In doing this, the lowering of molecular weights of the final product is avoided. Otherwise an unstabilized resin would tend to redistribute itself resulting in the formation of thermodynamic product.

Mechanistic studies had been performed. The hypothesis is that the reaction takes place at the liquid-liquid interface and involves the addition of BPA or its anion to an acyl ammonium species.

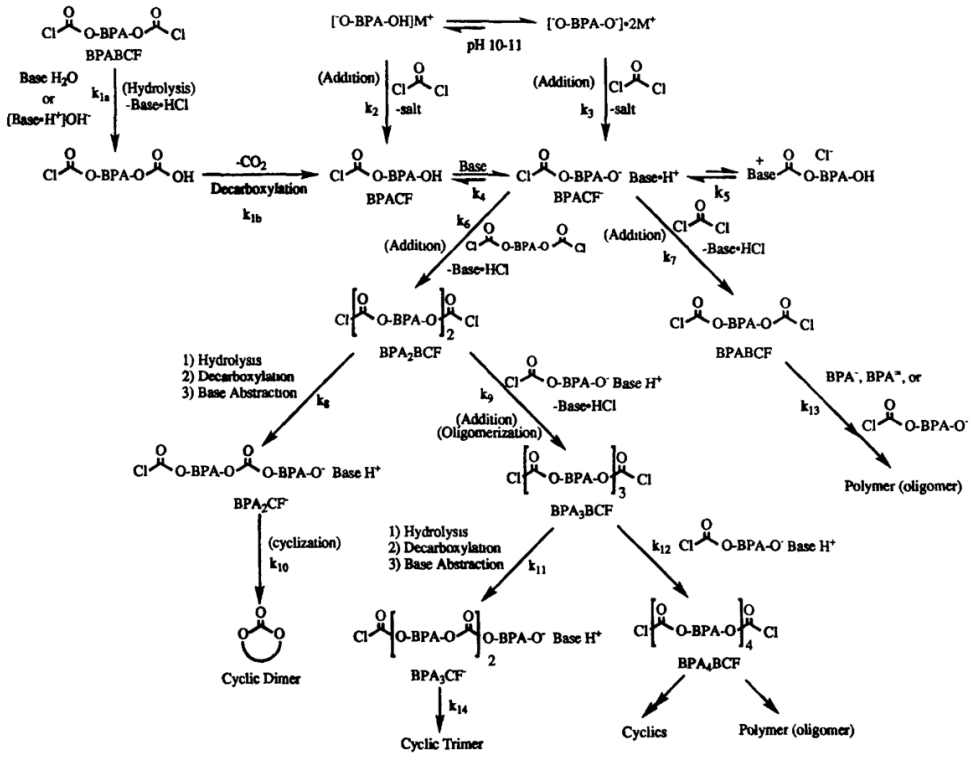

Scheme 6. General synthesis scheme of BPA-PC with interfacial technology.

Transesterification process

As shown in Scheme 7, this process involves a base catalyzed condensation reaction between diphenyl carbonate (DPC) and BPA.

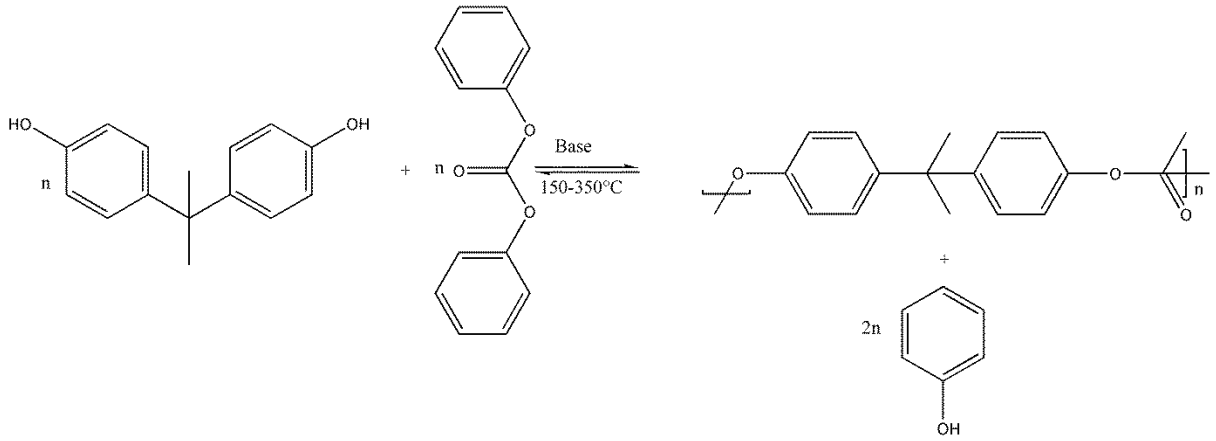

Scheme 7. General synthesis scheme of BPA-PC with transesterification process.

As indicated, the process is performed at high temperature, in order to maintain starting monomers, oligomers and final products molten throughout the course of the reaction. The pressure in the reactor is reduced in the later stages of conversion from 150-200 torr to 0.1-1 torr in order to effectively remove phenol which forms during the reaction.

The advantages of this methodology are not only the fact that it is performed without any solvents, drying steps and hazardous chemicals such as phosgene, but also that when this process is opportunely engineered, the purity of the products is directly related to the one of the reagents, thus giving the possibility to effectively control it.

From a mechanistic point of view the reaction proceeds with the initial formation of a phenoxy-based anion which attacks the diphenyl carbonate. The result is the production of a phenoxide anion that successively removes a proton from a molecule of BPA. At this point another phenoxy-based anion is formed (which can indeed continue the reaction) together with a phenol molecule.

Synthesis of Polycarbonate based copolymers

Lots of studies had been carried out for the synthesis of polycarbonate copolymers. In general the most used strategy for the synthesis of copolymers involves the use of condensation reactions with monomer showing similar intrinsic reactivity.

Examples of copolymers synthesized are the ones in which the expected result is an improved resistance to hydrolysis and solvent stability. In order to achieve these results hydroquinone, simple bisphenols and resorcinol can be used.

Given the fact that one of the most important features of polycarbonates is their transparency and optical behavior, one of the most important goals is to synthesize copolymers which show good UV resistance.

In all these examples, and among all others not cited here, one prerequisite for the synthesis of carbonate copolymers is, however, that the comonomer should have a similar intrinsic reactivity, as said before. Within this framework, results clear that such a prerequisite strongly limits possible variations of the starting monomers, thus making more difficult the research towards innovative features and applications.

Mechanical properties of Polycarbonates

Mechanical properties of Polycarbonates are strongly related to their structure, molecular weight and chain-end functionalities in addition to secondary finishing operations such as annealing and physical aging. These two processes differ by the fact that the first one relieves residual internal stresses, while the second one is a natural occurring process.

Early dynamic mechanical studies suggested the presence of three transitions, labelled as α, β and γ. α peak was assigned to the glass transition, β to the presence of residual stresses in the sample. Internal motions of the monomer were believed to be responsible for γ transition instead. Among all mechanical properties of BPA-PC, one of the most important is its unusual ductility. At first it was believed that this low-temperature γ transition was responsible for this outstanding ductility but,

however, other polymers with similar low-lying transitions do not show such pronounced ductility. Therefore this unique feature of BPA-PC had been attributed to the presence of excess of free volume together with residual stresses.

Dynamic mechanical analyses had been the most important instrument for the determination of the nature of the three transitions α, β and γ.

Studies on the stress relaxation, carried out at 60°C below T_g, allowed to determine that the morphology and topology of the amorphous chains are more critical in determining the amount of relaxation than the rate of relaxation. BPA-PC has a temperature-dependent strain-strain behavior. This material undergoes shear yielding similar to that observed for some metal, while at very low temperatures it undergoes a ductile-to-brittle transition. Impact behavior of polycarbonate had also been studied. Interestingly it was the first high-temperature amorphous thermoplastic material to show to be ductile in a notched Izod impact test. It is believed that the notched Izod impact value is not connected to the low-temperature γ transition. In fact, by repeating the test on thermally annealed products, in which the γ transition has a slight variation, a consistent loss in notched Izod impact strength is registered. It had been proposed that the toughness of polycarbonate is due to the presence of residual superficial stresses. The influence of thermal history on these properties had been studied as support to this hypothesis. To this regard, processes of thermal annealing below the T_g relieve the residual stresses on the surface. As a result the mechanical properties of the material are altered.

Optical features of Polycarbonates

What is interesting about Polycarbonates is that, alongside the before mentioned unusual mechanical properties, they show extremely good optical behavior too.

BPA-PC is an amorphous polymer. Studies had been performed in order to determine if any type of order is present in this system, but no evidence of ordering had resulted.

Refractive index of BPA-PC had been determined and reported in Table 16, compared with other materials ad also with a PDMS-BPA-PC copolymer with 1:1 composition.

By analyzing the data reported it appears that BPA-PC as such has a refractive index slightly higher than glass. In fact, in general, amorphous polymers containing aromatic groups in the chain show higher refractive indexes. For example, PS shows a refractive index which is quite close to the one of polycarbonate. Among the materials indicated, PMMA is the one with the best light-related behavior. However, its mechanical properties are worse than the ones of BPA-PC, making the latter preferable for the substitution of glass in many applications.

Material	Refractive Index (λ=586.7 nm)
Polyvinyl chloride (PVC)	1.528
Polyethylene (PE)	1.530
Polymethylmethacrylate (PMMA)	1.490
Polystyrene (PS)	1.591
GLASS	1.540
Bisphenol A-Polycarbonate BPA-PC	1.585

Table 16. Comparison of refractive index of BPA-PC with various materials.

Its optimal optical behavior together with its extremely good mechanical and thermal properties makes polycarbonate the material of choice for the substitution of glass in many applications, even for external applications in which good environmental resistance is required. However, on extended

exposure to light and γ-irradiation BPA-PC slowly degrades. As a result it turns yellowish and also mechanical properties could be affected. This phenomenon, together with erosion, is a surface phenomenon, which only slightly extends into the bulk.

Scheme 8 shows three different photochemical reactions which BPA-PC undergoes depending on the specific exposure conditions. It had been demonstrated that at $\lambda \leq 300$ nm the photo-Fries rearrangement and fragmentation/coupling reactions are favored. Photo oxidation reactions, such as side chain oxidation and ring oxidation, are instead more important at longer wavelength. In addition to these three processes a fourth one results quite important in the degradation mechanisms and is given by ring attack interactions which are thought to occur between phenolic end groups and methyl radicals. However, it is difficult to determine exactly not only how much each process contributes to degradation, but also the species responsible for the yellowing of the polymer. It is plausible to assume that the yellow color mainly comes from side chain photo oxidation products, which, in general, are highly colored phenol derivatives.

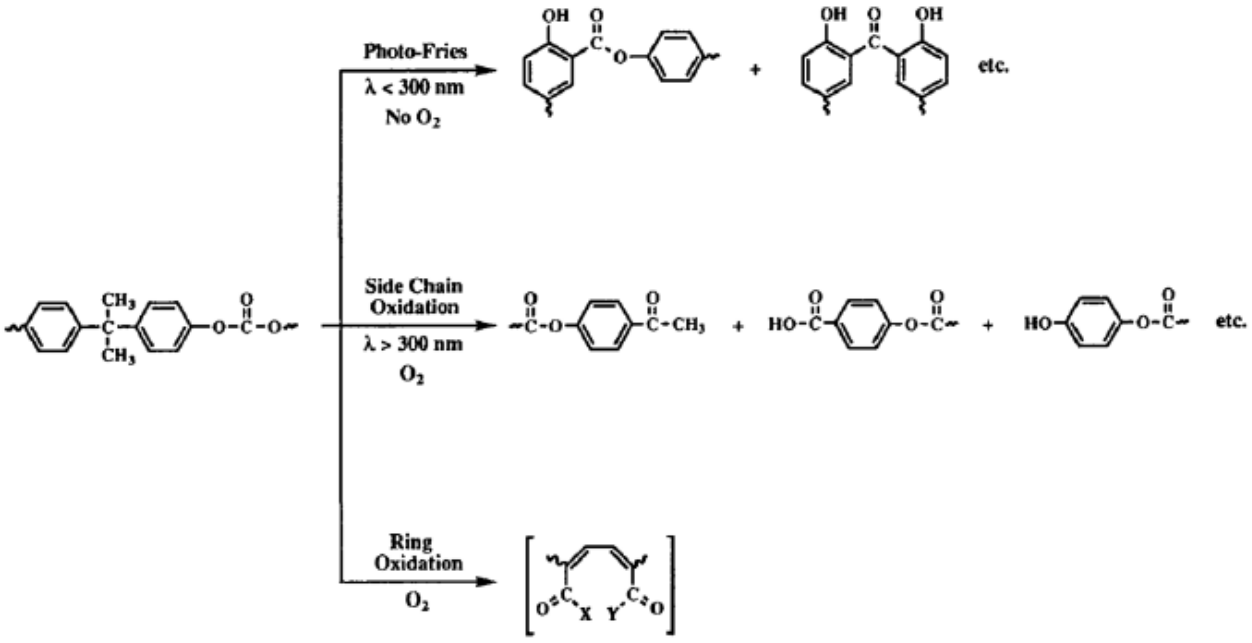

Scheme 8. Photochemical reactions for BPA-PC.

Free radical polymerization

**This chapter is based on the review of Matyjaszewski, K.* (90)

Free radical polymerization had been an important technological area for several years. Interestingly it was a process driven by technological and industrial development, even before scientific understanding. Polystyrene and Polyacrylate were synthesized for years without a full comprehension of the chain polymerization process.

A better understanding started in the period between 1940 and 1955, with the works of Mayo and Melville. However, the lack of control for such reactions was a critical issue. For this reason in 1980s industrial and academic attention was focused on polymerization reactions that offered the prospect of a better control such as cationic and anionic reactions. However, limitations of these ionic processes were too difficult to overcome, and free radical polymerization remained the industrial process of choice for several applications.

For this reason a lot of efforts were made in order to find a way to achieve full architectural control even through free radical polymerization, resulting in the development and study of controlled/living free radical polymerization in 1990s.

Free radical polymerizations proceed via a chain mechanism which can be divided into four steps involving free radicals:

1. Initiation: radical generation from non-radical species.

2. Propagation: radical addition to a substituted alkene.

3. Chain transfer and termination by disproportionation: atom transfer and atom abstraction reactions.

4. Termination by combination: radical-radical recombination reactions.

Initiation

The initiator free-radicals that are responsible for the start of the reaction are generated by thermal or photochemical homolytic cleavage of covalent bonds, or by a redox process. These primary radicals add to carbon-carbon double bond, generating primary propagating radicals that can propagate with other monomer molecules. The addition of the initiator radical on the first monomer molecule usually occurs as tail addition, but often this reaction is neither chemo-nor regioselective.

The fraction of primary radicals that actually initiate a polymer chain through formation of primary propagating radicals is indicated as initiator efficiency (f). It depends on a number of factors: first of all, as a molecule of initiator generates two germinal radicals these could either react with another initiator radical inside the "solvent cage" or diffuse outside the cage, to react with other species. This is called the "cage effect" and it is the main factor that lowers the value of f to less than unity. The extent of cage reactions for an initiator is related to the rate at which the initiator fragments can diffuse apart from one another and, thus, it depends on the viscosity of the reacting system. An example of this behavior is given by bulk polymerizations, in which, as conversion increases, the augmented viscosity lowers the value of f. It is important to underline that even if an initiator radical manages to escape the solvent cage it can undergo side reactions that diminish the initiator efficiency in the case they are competitive with the addition to monomer.

Different types of initiators exist, as well as different types of mechanisms for the generation of primary radicals. Here some will be briefly described.

Azo initiators

They generate carbon-centered and oxygen-centered radicals through homolysis of C-N (dialkyl diazenes) or O-N (dialkyl hyponitrites) bonds. The driving force for homolysis reaction for these molecules can be found in the generation of a nitrogen molecule. The most common azo initiators are aliphatic and symmetric and the radical generated is usually a resonance-stabilized tertiary radical.

Among all various azo initiators available some of the most used are 2,2'-azobisisobutyronitrile (AIBN), dimethyl 2,2'-azobisisobutyrate (MAIB), 1,1'-azobis(1-cyclohexanenitrile) and 2,2'-azobis(2,4,4-trimethylpentane).

The rate of decomposition as increases the delocalization of the unpaired electron of the generated radical increases. A significant increase of the decomposition rate is achieved also by introducing extensive branching and/or bulkiness on the γ-carbon.

Peroxide initiators

They generate oxygen-centered radicals through homolysis of O-O bonds. A wide range of peroxy compounds are being employed as initiators: acyl peroxides, dialkyl peroxydicarbonates, hydroperoxides, peresters and inorganic peroxides. Some of the most used peroxide initiators for each subclass are: BPO, di-tert-butyl peroxide, di-n-propyl peroxydicarbonate, cumene hydroperoxide, di-tert-butyl peroxalate and persulfate.

It is important to underline the fact that the oxygen-centered radicals generated though peroxides decomposition can undergo β-fragmentation.

The rate constant for the decomposition reaction of peroxide, namely k_d, increases as the nature of the substituents change as in the series aryl < primary alkyl < secondary alkyl < tertiary alkyl. The nature of the substituents on the carbon connected with the $(CO)O_2$ moiety affects both the rate and the mode of decomposition, with the rate increasing in the order: primary < secondary < tertiary carbon.

Both these two types of initiators generate the primary radical through homolysis. However other types of formation of radicals exist. For example it is possible to have thermal auto initiation for some monomers, such as styrene. Otherwise there is the possibility of induced decomposition, definition that refers to the reaction of a radical species with an initiator molecule, resulting in a new radical species that in turn is able to initiate a chain. The net effect is that a molecule of

initiator is consumed but the total number of radical does not change. Another possibility is the formation of a radical through a redox reaction. The last mode of initiation is the photo initiation, a mechanism in which a photon is absorbed to generate a radical that could initiate a radical chain reaction.

Once the primary radical formed through one of these mechanisms had escaped the solvent cage, it can undergo a great number of reactions, depending on the nature of the system monomer/initiator as well as reaction conditions. Tail/head addition to a monomer molecule, hydrogen abstraction, aromatic addition fragmentation or primary radical termination are all possible reactions.

It is important to underline that in the case of a binary copolymerization the situation is more complex.

The rate of addition of primary radicals to monomers is directly related to the nature of the monomer. Different rates for different monomers determine the distribution of end groups in the final product.

Propagation

The addition of primary radicals to monomer molecules generates primary propagating radicals. These species give a succession of propagation steps usually with high regio selectivity to generate radical centers bearing a substituent. The rate constants for the propagation steps were determined. It was found that the propagation rate constant (k_p) decreases for the first few addition steps, while remaining almost constant over several hundred degrees of polymerization.

At a general level the propagation reaction is highly regioselective, with head-tail linkages. In the case of monomers bearing non-conjugate substituents, however, it is possible to have head-head or tail-tail bonds, given the fact that the absence of conjugate substituents makes the difference in activation energies for the two sites smaller.

For what regards the stereospecifity of the propagation reaction, the addition of a pyramidal radical center on a planar double bond cannot be stereospecific. Thus a free radical polymerization occurs with no stereocontrol, only monomers with complex and bulky substituent could make an exception.

In order to obtain high molecular weight polymers, k_p must be higher than the rate constants for other elementary reactions, such as, for example, chain transfer. Ratio between rate constants for these processes is directly related to monomer nature. For example, α-(substituted methyl) vinyl compounds cannot be homopolymerized because a too stable radical is generated by hydrogen abstraction of the allylic hydrogen. This resonance stabilized radical cannot add to a monomer molecule.

At this point, it results clear that rates of addition of propagating radicals to monomers are affected by polarity, resonance, and steric factors, resulting from the substituents bound to both the propagating radical and the monomer double bond. For what regards the polar factors, the Hammett's polar substituent constant had been employed for the measurement of polar factors of substituted monomers and propagating radicals.

Dealing with resonance effects, it has to be said that in the case of homopolymerization both the monomer and the propagating radical have the same substituent, so the resonance effect may stabilize both species, affecting their reactivity in opposite directions.

Sterically hindered monomers appear to slightly influence the rate constant, while having a much higher effect on the stereochemistry of the product. Monomers with small substituents at the double bond result in random propagation with an atactic polymer as product or, at least, a little preference for syndiotactic propagation as in methyl methacrylate. The situation is different for hindered monomers such as triphenyl methyl methacrylate which yields an almost completely isotactic polymer. Effects are given also by the solvent used.

Chain transfer

Chain transfer in radical polymerization is the reaction of a propagating radical (Pi●) with a transfer agent (T) to yield a dead polymer (Pi) and a small new radical (T●) as indicated in Scheme 9. In this reaction the radical center is transferred to another molecule, but the total number of unpaired electrons remains unchanged. As a result for a chain transfer process, the degree of polymerization decreases and the number of chains increases. Transfer occurs for all species in solution and can be useful to reduce and therefore control the molecular weight of the products as well as to introduce precise end groups. The effectiveness of a transfer agent T to reduce the degree of polymerization is expressed in terms of chain transfer constant, C, which is given by the ratio between the overall rate constant for chain transfer, k_{tr}, and k_p.

The chain transfer constant can be determined for all species in solution, initiator (CI), and monomer (CM), polymer (CP) and transfer agent (CT).

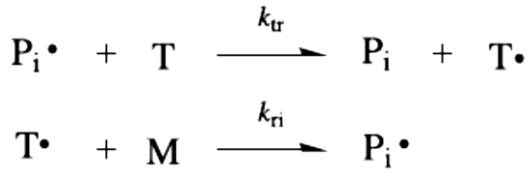

Scheme 9. Chain transfer reaction.

Termination

Termination is the fourth and the last among the elementary reactions in free radical polymerization. Termination is the process with which the propagating radicals give dead chains though combination or disproportionation reactions. It is the most complex among all other reactions because it involves consecutive steps: translational diffusion of polymeric radicals to come in proximity one with the other, segmental diffusion which brings chain ends in close contact and, finally chemical reaction. Because of the importance of these diffusive phenomena, the rate

constant for the termination reaction for polymeric radicals is significantly lower than the rate constant for reaction between two small radicals in solution. In the case of highly hindered monomers the rate constant could decrease even more. As the termination reaction rate is diffusion-dependent, it will exhibit chain-length dependence. In addition it is important to say that, since it is definitely unlikely for two terminating polymeric radicals to have the same length, the experimental values for termination rate will be average values. The mode of termination is extremely important, because it affects the molecular architecture of the product and therefore its properties. The molecular weight distribution as well as the polydispersity are directly connected to the mode of termination with the polydispersity ($\overline{Mw}/\overline{Mn}$) equal to 1.5 if polymer terminates only with combination, or to 2 if only with disproportionation. Interestingly, disproportionation reaction gives as a result one saturated and one unsaturated chain end, with the latter that could occasionally reacts further giving branched products.

The predominance of one of two modes of termination can be expressed as ratio between the rate constants for the two processes but, however, it is difficult to measure this rate constant. A strategy to determine if one of the two processes is prevalent is to analyze the end groups through NMR spectroscopy. Vinyl monomers usually terminate principally through combination, but also disproportionation becomes important for monomers which possess easily abstractable β-hydrogens or much hindered ones.

Another termination mechanism that can be important in free radical polymerization reactions is the primary radical termination. This definition refers to the bimolecular reaction between a primary radical and a propagating radical. This phenomenon is fairly common and important in situations of high initiator concentration. The occurrence of primary radical termination reactions lowers rates of initiation and propagation.

What results interesting is also the behavior of highly hindered monomers. Thanks to their bulkiness they tend to terminate exceptionally slowly. The ratio between propagation and termination rates is high enough to guarantee polymerization to high molecular weights products.

Controlled radical polymerization

**This chapter is based on the review of Matyjaszewski, K.* (90)

As already said, free radical polymerization is a synthetic methodology that is largely applied from an industrial point of view, thanks to its useful features which are, among others, the possibility of usage in a wide range of temperatures (from -80 to 250°C) and the variety of polymerizable molecules, which leads to an even greater number of homo- and copolymers that possess a great number of different properties dependent on their composition. However free radical polymerization has also many drawbacks. Its main limitation is the lack of control over some of the most important elements of macromolecular structure, in particular molecular weight, polydispersity, chain end functionality, chain architecture and composition. In fact, it has to be said that the typical lifetime of a propagating chain is very short, around 1s. During this small interval, around 1000 reaction acts take place. For this reason it results extremely difficult to control the macromolecular architecture as well as, for example introducing precise chain end functionalities. In order to obtain this level of control the one opportunity would be hypothetically to slow down the reaction rate significantly. However this would result in a predominance of chain transfer as mechanism controlling the molecular weight leading, again, to a poor control.

Well-defined macromolecular systems with greatly controlled structural parameters can be obtained through ionic living polymerization. However, this strategy has a limited applicability both for what regards the small number of monomers that can be used and the reaction conditions.

For these reasons it would be interesting to develop a free radical polymerization methodology that could allow a greater level of control over macromolecular structure of the products. This is why in recent years a lot of efforts are directed towards the so called living radical polymerization.

The definition of living polymerization was given for the first time by Szwarc as a polymerization reaction without chain breaking reactions (transfer and termination). Such a polymerization would provide chain end groups control as well as the possibility of block copolymers synthesis. However it does not mean control also over molecular weight and low polidispersity. To achieve these goals

a consumption of initiator at early stages is also required. If this additional prerequisite is met the definition of controlled polymerization can be used. However, the general definition of living radical polymerization will be here used, in order to simply compare it to the classical radical polymerization.

Living radical polymerization, should be carried out at very low concentration of growing radicals (to reduce termination reactions), but at sufficiently high concentration of growing chains (to reduce transfer reactions). In addition, an extremely fast initiation is required in order to have all chains to initiate simultaneously. These requirements are contradictory and against the general features of classical free radical polymerization. The best results in solving these problems were achieved with the introduction of equilibrium between active propagating species and dormant ones in solution. This is the main difference between living radical polymerization and radical polymerization, given the fact that both mechanisms can be divided into the same elementary reactions.

Initiation

The main difference between free radical polymerization and living radical polymerization in this step is how the radicals are generated. In the former, radicals are generated at low concentration, continuously and irreversibly. In living radical polymerization radicals are formed reversibly at both the initiation and propagation stages. At any moment in free radical polymerization the concentration of radicals is determined by the balance between continuous initiation and irreversible termination, while in living radical polymerization the concentration of radicals depends on the ratio between rates of activation and deactivation.

Propagation

Propagation is similar in both mechanisms, consisting in a radical addition to of the radical on the monomer double bond. No appreciable differences exist between free radical polymerization and

living radical polymerization in regio- and stereochemistry of the products as well as for what regards reactivity ratios. The greatest difference is found in the lifetimes of the propagating chains which increase from < 1 s in free radical polymerization to > 1 hr in living radical polymerization. This means that monomer molecules add every ≈ 1 ms in the former and every ≈ 1 minute in the latter.

Termination

Also termination step is very similar for living radical polymerization and free radical polymerization. Termination occurs in both systems with diffusion-controlled rates and it cannot be avoided. However, a substantial difference exists. As termination is chain length dependent, in the case of free radical polymerization it will be likely to occur between two short chains or one long chain and a short one. In living radical polymerization, the key element is that all propagating radical grow almost at the same rate. At a certain reaction time all chains are about the same length. This means that at higher conversions the termination rate constant drops, since only long chains are present. For this reason in living radical polymerization termination reaction may be more significant at lower conversion. However in this procedure, only less than 10% of chains are dead at any moment, values that reaches 99% in conventional radical polymerization.

Probably the most important feature of living radical polymerization is the exchange between growing radicals and dormant species with an equilibrium reaction. Mechanistically this equilibrium can occur in four different modes, shown in Scheme 10.

The basic concepts are the same for all four cases. The dormant species are reversibly activated with a rate constant of activation k_a to form the active species, Pn●, which react with a monomer molecule, M, with a rate constant k_p. The propagating radicals can also either be deactivated with a rate constant kda or terminate with other growing radicals with the rate constant k_t.

Examples of the four cases can be reported as follows:

-*Case 1:* the most important example is given by the nitroxide mediated living radical polymerization (NMP) that makes use of stable nitroxide radicals;

-*Case 2:* based on the catalyzed, reversible cleavage of the covalent bond in dormant species through a redox reaction. This process is called atom transfer radical polymerization (ATRP) and the catalysts used are Ru, Cu, Fe and other metal derivatives;

-*Case 3:* this mechanism is not as successful as the previous ones. It involves the formation of a radical species by reaction of the growing radicals with species with even number of electron. This molecule cannot react neither with each other nor with the monomer;

-*Case 4:* this process is based on a thermodynamically neutral equilibrium between the growing radical (which is at much lower concentrations) and the dormant species (present at higher concentration). Xanthates, dithioesters and other can be used in these processes that are addressed as ATRP reaction.

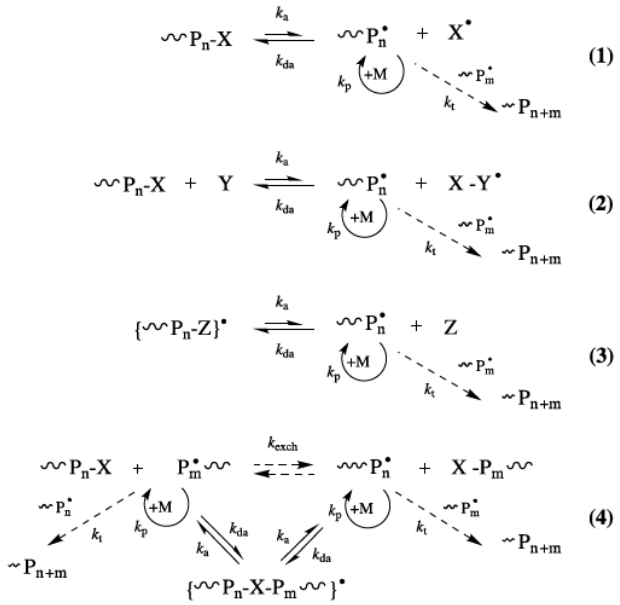

Scheme 10. Four cases of equilibrium between active and dormant species in living radical polymerization.

While cases 1-3 are very similar, with an equilibrium strongly shifted towards the dormant species, case 4 is very different. It has an equilibrium constant equal to K = 1 and the rates reduction are expected if the transition state in which the atom or group is transferred from one chain to another is strongly stabilized, being a long-lived intermediate product.

Even if lot of discoveries in this field had been made, a lot more can be still done, with the possibility of novel structures to be synthesized as well as the possibility of industrial application of these techniques.

9,9-Bis (4-hydroxyphenyl) fluorene properties and applications

9,9-Bis(4-hydroxyphenyl)fluorene (Figure 37) (Fluorene Bisphenol, FB)-based polymers exhibit remarkable features, for example high thermal stability, high solubility in most organic solvents, amorphous character of the products and conductivity properties. These excellent features are attributed to the so-called cardo structure of FB in which the aryl moieties at the quaternary carbon of the alicyclic group occupy different planes.

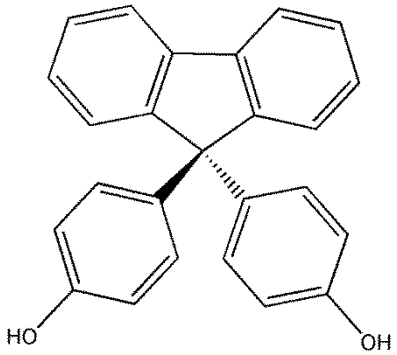

Figure 37. 9,9-Bis(4-hydroxyphenyl)fluorene

This molecule also has highly delocalized electronic structure and is extremely rigid. This is why electrons can travel freely alongside the whole backbone giving both conductivity and unique optical properties.

For these reasons FB had been used as backbone element in a lot of different polymers.

Okuda et al. (91) synthesized FB-PEEKs. This polymer has good solubility in common organic solvents, such as chloroform, DMAc and NMP, which is in contrast with solubility properties of typical PEEKs. Products were also characterized through DSC and TGA analyses, revealing a glass transition temperature over 220°C and a weight loss temperature of about 450°C. No melting points were determined indicating an amorphous nature of the polymer. Cardo structure of FB is largely responsible for these optimal thermal properties. The amorphous character of these PEEKs guarantees also great transparency in casted films which reached 80% at 400 nm. For what regards

other optical properties, polymers showed quite high refractive index (1.65 at 588 nm) probably due to the presence of numerous aromatic groups, but also low bi-rifrangence. Finally, FB-based PEEKs were found to possess outstanding mechanical properties.

FB derivatives had been used also as building blocks in polyamides synthesis by Ghaemy et al. (92) Authors in this work provided a synthetic methodology for the preparation of polymers bearing imidazole derivatives substituents. These functionalities show antimicrobial properties. The advantage of this approach comes from the fact that, by directly bounding imidazole derivatives to the polymeric chains, migration issues, which are a main concern in polymeric blends with antimicrobial agents, are solved. The use of fluorenebisphenol in these polymers could be interesting for the introduction of interesting features that would be beneficial for the final product. These polymers are expected to show high thermal stability and photoluminescence properties. Authors performed a polycondensation reaction with various commercially available dicarboxylic acids. Products were analyzed under many aspects. First of all they displayed good solubility in many polar organic solvents at room temperature. This is probably due to the presence of fluorene bisphenol, which also gives rise to strong absorption band in UV-vis region. Thermal properties were determined through DSC and TGA analyses: Polyamides appeared to be totally amorphous. This feature can be attributed to the presence of extremely bulky aromatic groups which make the packing of chain more difficult. T_g was determined over 220°C with values that reached also 330°C with some acids. TGA measurements showed the temperature of 10% weight loss in the range of 419-492°C. These polymers showed antimicrobial activity, given by imidazole moieties.

Conductivity properties given by FB units had been exploited by Zhou et al. (93) in the preparation of all polymer solar cells. In these devices semiconducting polymers are used as the electron acceptor and conductor (n-type). The use of polymers brings some advantages, for example an optimal tunability of conductivity properties through modifications of chemical structure. Authors synthesized an alternating copolymer of 1,4,5,8-naphtalene diimide (NDI) and FB derivative. The resulting polymer could have a high-lying LUMO energy level, due to the twisting of bonds

between two monomer units, resulting in the delocalization of LUMO density in NDI groups. As in previous examples, this polymer appeared to have good solubility in most organic solvents.

This polymer was used in blends with other organic polymers as electron donors, for example PT. These blend showed good semiconducting properties which appeared to be strongly connected to the solvent nature. It was demonstrated that different solvents cause differences in morphology that are presumably responsible for variations in conductivity properties.

Introduction

Organic electronics is a research area that is gaining more and more interest, both from an academic and industrial point of view. In fact organic conductive materials could open different possibilities in the production of new advanced electronic devices with improved properties: these materials conjugate useful features such as flexibility, transparency, durability and lightness typical of polymers, with conductive properties, conferred by highly conjugated organic systems. Even if they are not designed for the substitution of silicon-based technologies, new organic conductive materials will see as a natural consequence their use for the development of new advanced electronic devices that will couple outstanding mechanical features with good conductivity.

The aim of this work is the synthesis of an innovative organic polymer based conductive material. Polycarbonate (PC) and Polyacrylate (PA) were found to be suitable backbone components thanks to their useful properties. In fact both PC and PA are known for their extremely good optical behavior. In addition to this, PC is characterized by high durability and mechanical resistance coupled with good thermal properties. However their functionalization is quite difficult.

On the other side, the presence in PA structure of an ester moiety opens indeed multiple alternatives for functionalization, actually allowing the introduction of potentially conductive functionalities.

An highly unsaturated molecule displaying a “cardo” structure, 9,9-bis(4-hydroxyphenyl) fluorene, was functionalized with methacryloyl chloride in order to obtain, after separation via flash chromatography, two different molecules: the bi-functional product carrying two vinyl functionalities, and the mono-functional one having at the same time a hydroxyl group and a vinyl functionality.

A new synthesis of Polyallyl carbonate – Polymethyl methacrylate block copolymer, functionalized with 9,9-bis(4-hydroxyphenyl) fluorene based molecules, was performed: the copolymers obtained having two vinyl functionalities can be cross-linked with methacrylate end-capped Poly(3,4-ethylenedioxythiophene) (mPEDOT) and doped mPEDOT (mPEDOT_SPES), thus obtaining a cross-linked conductive Polyallyl carbonate-Polymethyl methacrylate block copolymers;

furthermore, the copolymers carrying both an hydroxyl group and a vinyl functionality can be used also for subsequent derivatizations thanks to presence of -OH reactive groups.

The new synthetic method developed is based on a two steps free radical polymerization: the first step is characterized by the homo-polymerization of 4-vinyl-1,3-dioxolan-2-one in the presence of benzoyl peroxide (BPO) as radical initiator; the second step, thanks to the pseudo-living behavior of 4-vinyl-1,3-dioxolan-2-one based radicals, proceeds via block-copolymerization between 9,9-bis(4-hydroxyphenyl) fluorene based monomer functionalized with methacryloyl chloride and the propagating radicals deriving from 4-vinyl-1,3-dioxolan-2-one.

Thanks to the pseudo-living behavior of 4-vinyl-1,3-dioxolan-2-one based radicals it is possible to obtain a bi-block copolymer between allyl carbonate based monomer (first block deriving from the first step of polymerization) and methacrylic one (second block deriving from the second step of polymerization), carrying cardo functionalities. The new Polyallyl carbonate-Polymethyl methacrylate block copolymer was characterized by ^{1}H NMR, ^{1}H-^{1}H COSY, ^{1}H-^{13}C HSQC and ^{13}C spectroscopy.

Experimental

Materials

4-vinyl-1,3-dioxolan-2-one (≥ 99%), styrene (≥ 99%), methacryloyl chloride (≥ 97%), thionyl chloride (≥ 97%), toluene, dichloromethane (≥ 99.9%), sodium sulphate (≥ 99%) and sodium hydrogen carbonate (≥ 95%) were purchased from Sigma Aldrich and used as received. Methacrylic acid (≥ 98%) triethylamine (≥ 99.5%) were purchased from Fluka and used without further purification. Benzoyl peroxide (BPO, ≥ 77%) was purchased from Merck and used without further purification. 9,9-Bis(4-hydroxyphenyl)fluorene (≥ 99.5%) was purchased by Ferrania Chemicals and used without further purification.

Methanol (≥ 99.8%), and acetone (≥ 99.5%) were purchased from Scharlau and used as received. Dimethyl sulfoxide-d6 (99.9 % atom D), dichlorometane-d2 (99.9 % atom D) and chloroform-d (99.8% atom D) deuterated solvents were purchased from Sigma Aldrich and used as received.

Synthesis of methacryloyl chloride based 9,9-Bis(4-hydroxyphenyl)fluorene

In a three-necked flask equipped with a magnetic stirrer, a thermometer and an addition funnel, a solution of 9,9-Bis(4-hydroxyphenyl)fluorene (3.00 g, 8.56 mmol) in dichloromethane (28.5 cm^3) is prepared under nitrogen atmosphere. Triethylamine (2.17 g, 21.4 mmol, 3 cm^3) is added as catalyst. A solution of methacryloyl chloride (1.88 g, 18.02 mmol, 1.76 cm^3) in dichloromethane (60 cm^3) is placed in the addition funnel and added dropwise at room temperature under stirring. Once the addition is complete, the reaction mixture is heated to reflux for 16 hr. The organic phase is washed several times at first with an aqueous solution of HCl (35 % solution) and then with an ice cold saturated solution of $NaHCO_3$. The organic phase is dried over Na_2SO_4 and then solvent evaporated to obtain a white solid (52% yield).

Synthesis of methacrylic acid based 9,9-Bis(4-hydroxyphenyl)fluorene

In a two-necked flask, equipped with a magnetic stirrer and an addition funnel, a solution of 9,9-Bis(4-hydroxyphenyl)fluorene (3 g, 8.56 mmol) and acrylic acid (1.30 g, 18.02 mmol, 1.24 cm^3) in dichloromethane (53 cm^3) is prepared under nitrogen atmosphere. Thionyl chloride (2.04 g, 17.12 mmol, 1.24 cm^3) was added dropwise to the reaction mixture under stirring. The reaction mixture was heated until the evolution of HCl stops (follow with pH indicator, approximately 24 hr), and then heated to reflux to bring the reaction to completion. Reaction mixture was quenched with ice-cold saturated solution of $NaHCO_3$. The organic phase was dried over Na_2SO_4 and solvent evaporated, to obtain a white solid (99% yield).

Synthesis of Poly-4-vinyl-1,3-dioxolan-2-one

Benzoyl peroxide (0.26 g, 0.876 mmol), toluene (20 cm^3) and 4-vinyl-1,3-dioxolan-2-one (5 g, 43.8 mmol, 4.21 cm^3) are placed in a two-necked flask equipped with a magnetic stirrer and a thermometer under reflux and nitrogen atmosphere.

The reaction mixture is heated to 70°C for 24 hr. The polymer is precipitated in acetone, to yield a white solid. The product is washed in reflux of acetone for 12 hr in order to remove residual solvent and unreacted monomer.

The same synthetic route is adopted for the kinetic polymerization study of 4-vinyl-1,3-dioxolan-2-one; the kinetic of polymerization is conducted for 167 hr and a controlled times, reported in Result and Discussion paragraph, aliquots of the polymerization reaction are taken via chromatographic syringe and freeze in liquid nitrogen, in order to stop radical activity. The samples are reported at room temperature and studied via GPC analyses.

Synthesis of methacryloyl chloride based 9,9-Bis(4-hydroxyphenyl)fluorene-4-vinyl-1,3-dioxolan-2-one copolymers and methacrylic acid based 9,9-Bis(4 hydroxyphenyl)fluorene-4-vinyl-1,3-dioxolan-2-one copolymers.

Benzoyl peroxide (0.50 g, 0.16 mmol), toluene (5 cm^3), 4-vinyl-1,3-dioxolan-2-one (0.64 mg, 5.59 mmol, 0.54 cm^3) are placed in a three-necked flask equipped with a magnetic stirrer, a thermometer and an addition funnel under reflux and nitrogen atmosphere. A solution of functionalized acrylate (2.4 mmol) in toluene (5 cm^3) is placed in the addition funnel. Acrylate monomer and dioxalone based monomer are used in molar ratio 30 to 70 respectively.

The reaction mixture is heated to 70°C for 24 h. Acrylate solution was added dropwise (approximately one drop per minute). The reaction mixture is left at 70°C under stirring for 24 hr. The polymer is precipitated in methanol to yield a white solid.

The product was washed in reflux of methanol for 12 hr in order to remove residual solvent and unreacted monomer.

Characterization of polymers

Nuclear magnetic resonance: ^{1}H NMR

^{1}H NMR spectra were collected at 25°C with a BRUKER 400 MHz spectrometer. Samples for the analyses were prepared dissolving 10-15 mg of samples in 1 cm^3 of DMSO-d_6 for ^{1}H NMR and ^{1}H,^{1}H COSY spectra and 50-60 mg of samples in 1 cm^3 of DMSO-d_6 for ^{13}C and HSQC spectra.

Size Exclusion Chromatography (SEC)

SEC data were obtained in according with the procedure described on page 30.

Results and Discussion

Omopolymerization of 4-vinyl-1,3-dioxolan-2-one

The first part of this work was focused on the study of reactivity of 4-vinyl-1,3-dioxolan-2-one, since no data are present in literature for what regards reactivity of this unsaturated species in conditions of free radical polymerization. As indicated above, the reaction was performed at 70°C in toluene with BPO as initiator. Product was analyzed through complete NMR characterization, spectra and attributions shown below in Figures 38 (^{1}H NMR), 39 (^{13}C NMR) and 40 (^{1}H,^{1}H COSY and HSQC NMR).

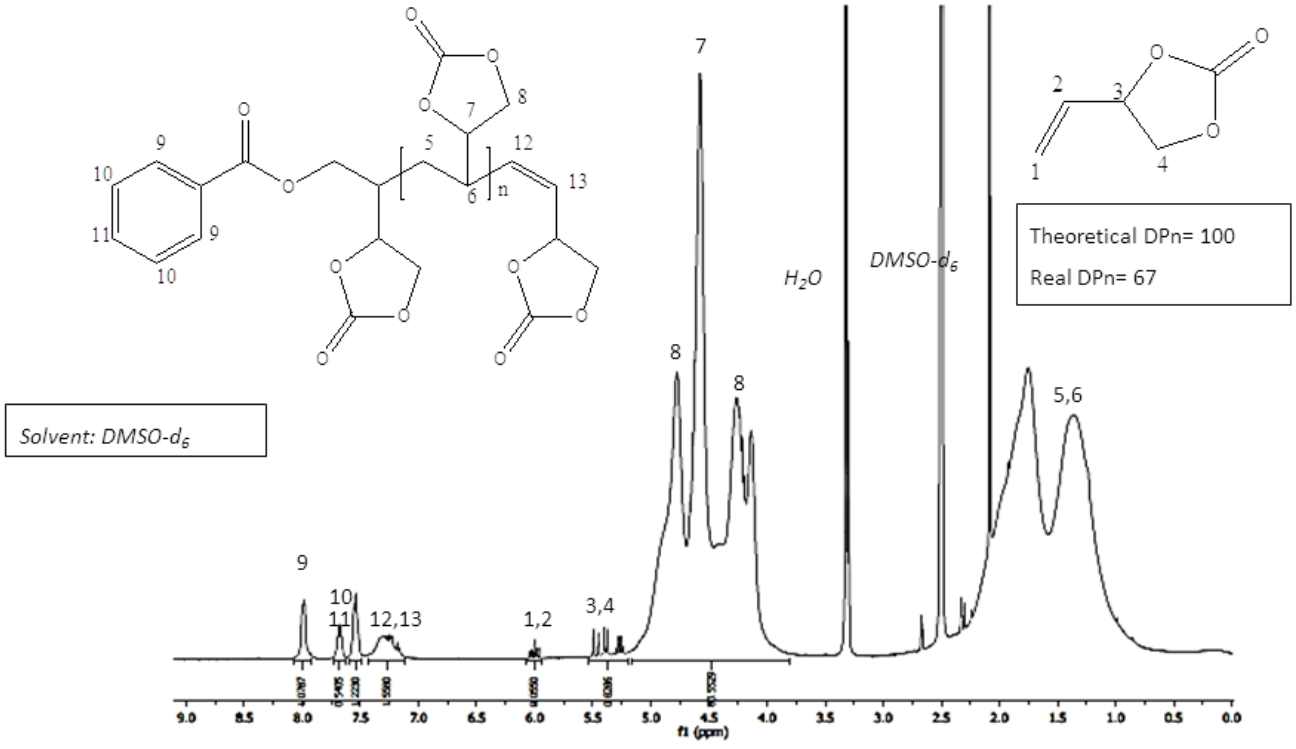

Figure 38. ^{1}H NMR spectrum of Poly 4-vinyl-1,3-dioxolan-2-one.

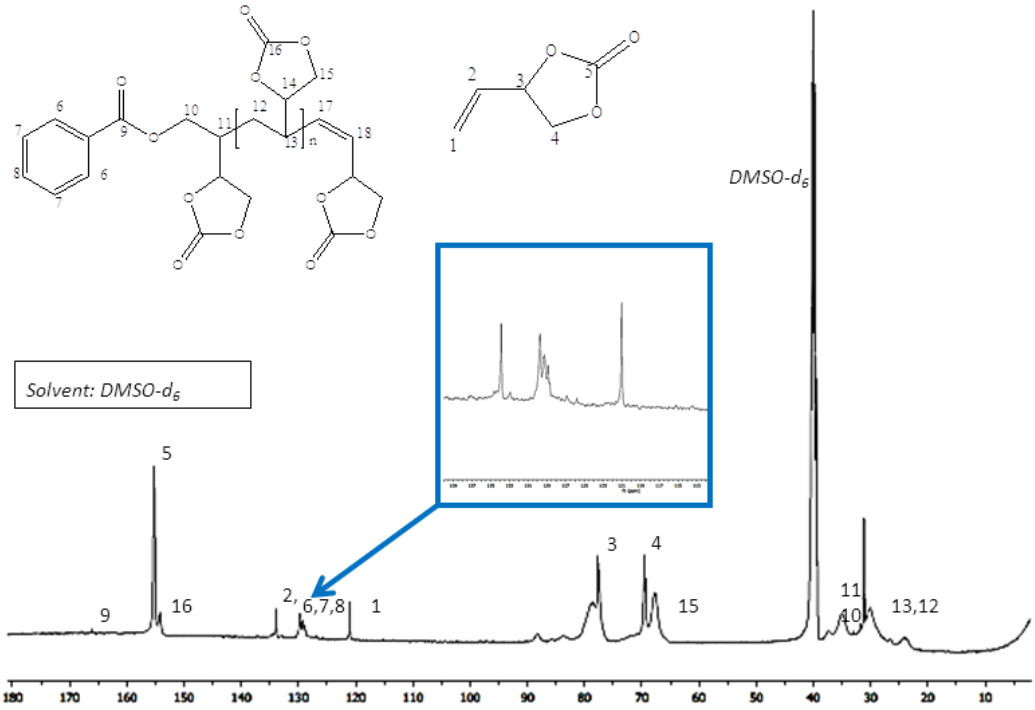

Figure 39. ^{13}C NMR spectrum of Poly 4-vinyl-1,3-dioxolan-2-one.

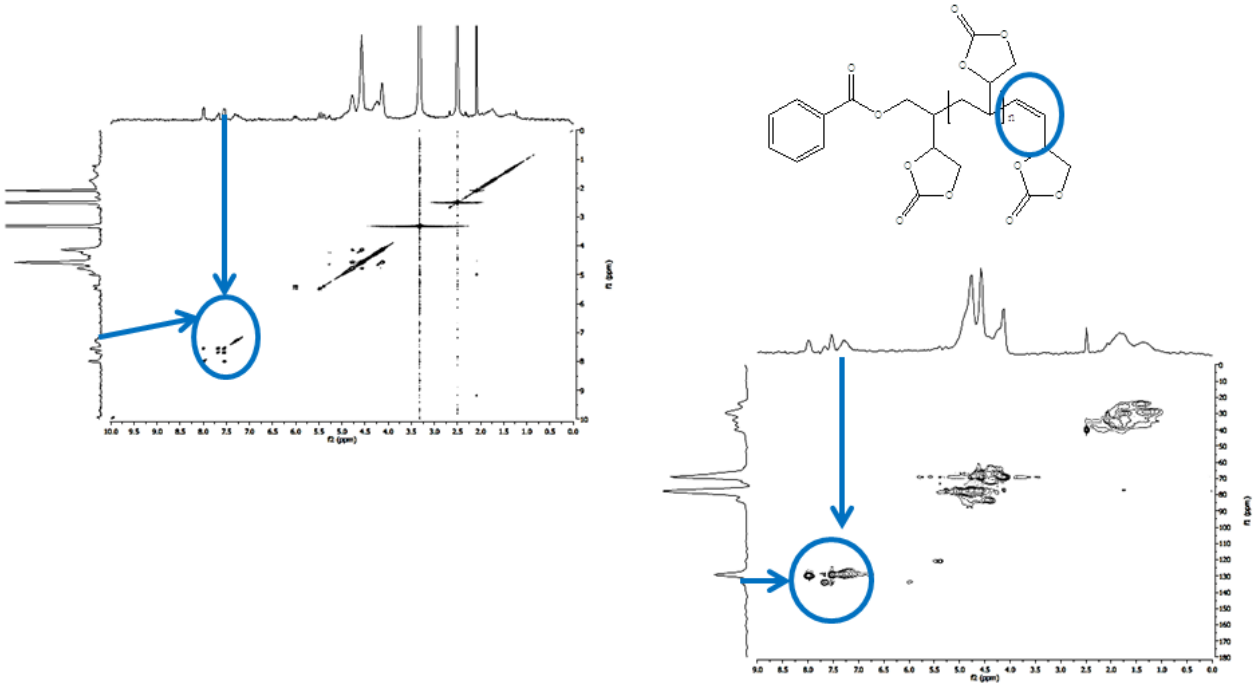

Figure 40. ^{1}H, ^{1}H NMR and HSQC NMR spectra of Poly 4-vinyl-1,3-dioxolan-2-one.

It is possible to hypothesize a mechanism for free radical polymerization of 4-vinyl-1,3- dioxolan-2-one, as indicated in Scheme 11.

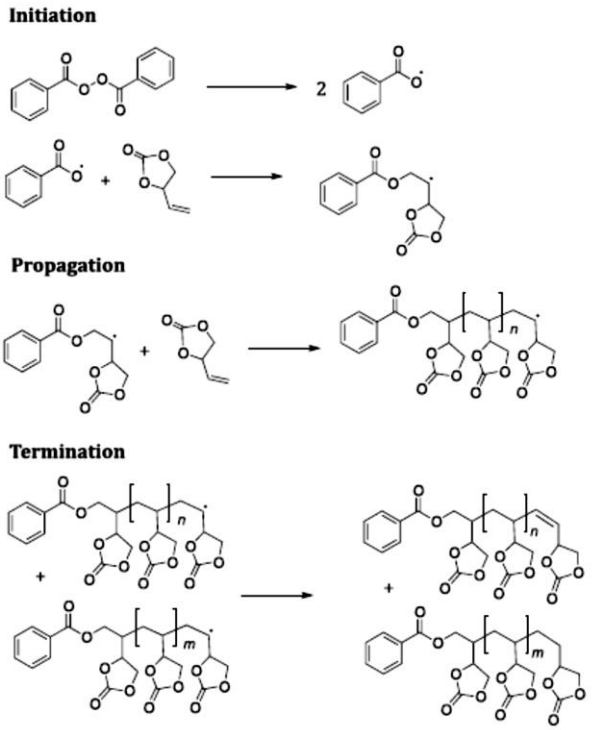

Scheme 11. Proposed mechanism of homopolymerization of Poly 4-vinyl-1,3-dioxolan-2-one.

As already said, since no data are present in literature for free radial polymerization reaction of this monomer, it is important to study the reactivity of the double bond. For this reason kinetic studies were performed. Samples were taken at predetermined times from the reaction mixture and investigated through GPC analysis, over a period of 167 hours.

Results of kinetic studies are reported in Table 17. What is extremely interesting about these data is that the polymer continues to grow even at very long reaction times. Alongside this growth in the molecular weights, also polidispersity values appear to be worth of interest. Since it is a free radical polymerization, polydispersity values should be comprised between 1.5 if termination occurs through combination reaction and 2 if termination occurs through disproportionation

In Figure 41 the increase of $\overline{Mn}$ in function of time reaction is reported. $\overline{Mn}$ increases, together with polydispersity values below 1.5, allows to hypothesize a pseudo-living character of the monomer radical. In other words, propagating radicals on growing chains appear to be extremely stable.

Samples	Time of reaction (hr)	$\overline{Mn}$ (Da)	D
0	0	0	0
1	0.02	21481	1.48
2	0.08	29768	1.45
3	0.25	34589	1.44
4	1.75	37798	1.44
5	2.00	37228	1.44
6	2.50	38048	1.44
7	4.00	39045	1.44
8	5.00	44879	1.44
9	5.50	49398	1.44
10	6.00	49648	1.44
11	7.00	52173	1.44
12	8.00	53327	1.44
13	9.00	53998	1.44
14	10.00	59998	1.44
15	23.00	62191	1.44
16	28.00	62426	1.44
17	58.00	65037	1.44
18	119.00	66802	1.43
19	167.00	68910	1.43

Table 17.Average numeral molecular weights and D data for samples taken at different times during 4-vinyl-1,3dioxolan-2-one free radical polymerization.

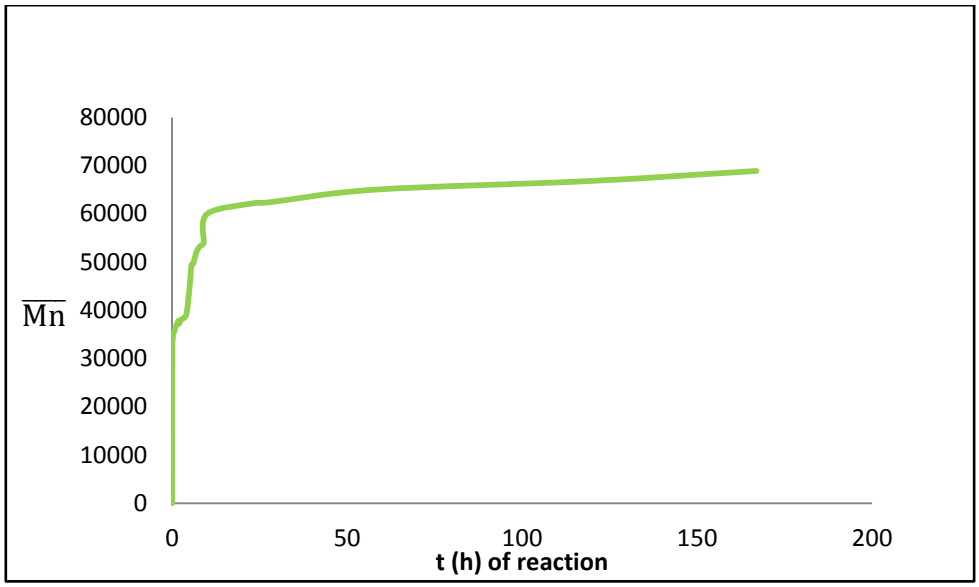

Figure 41.Average numeral molecular weights data for samples taken at different times during 4-vinyl-1,3dioxolan-2-one free radical polymerization over reaction time.

Synthesis of styrene-4-vinyl-1,3-dioxolan-2-one block copolymers

Even if Poly-4-vinyl-1,3-dioxolan-2-one possesses good properties, such as transparency and a pseudo-living character of the radical on the growing chain, it also suffers some drawbacks such as poor thermal and mechanical properties. For this reason copolymers were synthesized, using styrene as comonomer, in order to improve both characteristics.

The challenge was to determine if the stability of the radicals on Poly-4-vinyl-1,3-dioxolan-2-one growing chains could inhibits copolymerization reactions.

The simplest procedure involved the loading of both monomers from the beginning of the reaction. The first sample was named PSPC01 and the experimental procedure is indicated above. In this first attempt of copolymerization reaction a ratio of 70 to 30 between styrene and 4-vinyl-1,3-dioxolan-2-one had been used. The hypothesis was that, even if styrene is more reactive, the system could retain its reactivity due to the isolated entrance of one dioxalone molecule in the growing chain. This species could bear a stable radical which would reduce the probability of termination reactions. In order to determine if 4-vinyl-1,3-dioxolan-2-one monomer had entered the chain, the region between around 5.5 and 3.5 ppm in ^{1}H NMR spectra has been studied.

In addition, aliphatic protons of styrene and dioxalone monomers both fall in the same region from 1.0 to 2.0 ppm. For this reason they are not suitable to be studied if the presence of carbonate in chain has to be determined. In Figure 42 a comparison between PS1 a), PSPC01 b), PSPC02 c) and Poly 4-vinyl-1,3-dioxolan-2-one d) spectra in the area of interest has been made. Differences between various samples synthesized are reported in Table 18.

Sample	styrene:dioxalone molar ratio (mol/mol)	duration of the first step (hr)	duration of the second step (hr)
PS1	-	24.00	-
PSPC01	70:30	24.00	-
PSPC02	30:70	24.00	-
PSPC03	30:70	0.15	24.00
PSPC04	30:70	0.30	48.00
PSPC06	30:70	1.00	48.00
PSPC07	30:70	24.00	72.00
PSPC08	30:70	24.00	144.00

Table 18. Experimental data of styrene and styrene-4-vinyl-1,3-dioxolan-2-one copolymerization reactions.

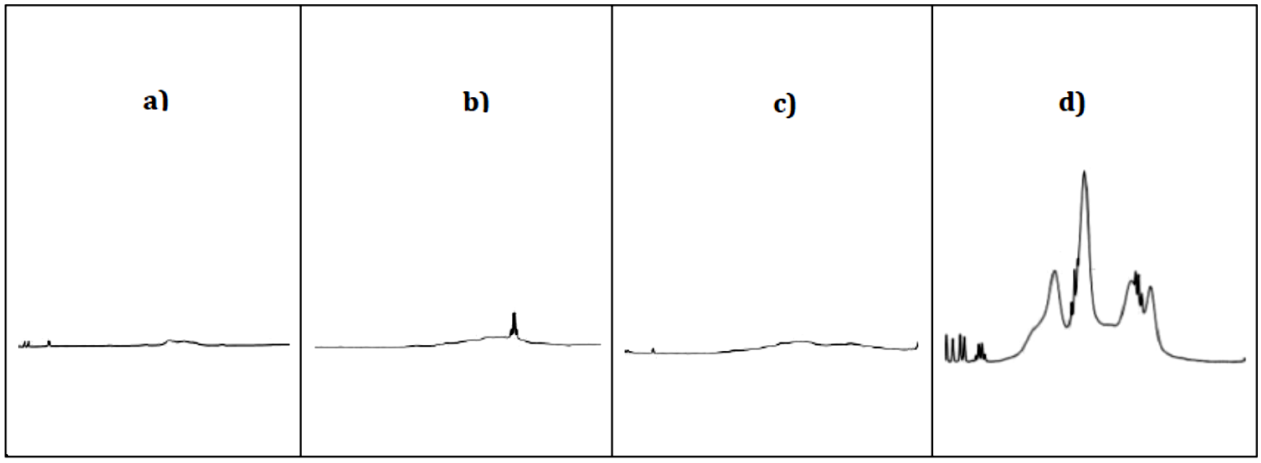

Figure 42. Comparison between 3.5-5.5 ppm regions in ^{1}H NMR spectra of PS1 a), PSPC01 b), PSPC02 c) and poly 4-vinyl-1,3-dioxolan-2-one d).

As can be seen, in PSPC01 sample only a slight presence of dioxalone moieties seems to be react, by comparison with PS1 spectrum.

In order to obtain a styrene-4-vinyl-1,3-dioxolan-2-one copolymer with a greater amount of dioxalone present, the first step was to reverse the relative quantities of comonomers. As already described, the synthesis of PSPC02 was performed in the same conditions of PSPC01, but using a styrene to dioxalone ratio of 30 to 70. The hypothesis was that, by strongly unbalancing the ratio between the two monomers, the less reactive 4-vinyl-1,3-dioxolan-2-one could enter the growing chain more easily.

By studying the ^{1}H NMR spectrum in the region of interest, it appears that signals are a bit more defined, with a slight doubling of the peak. However, the amount of dioxalone seems to be still very low, even if its loading at the start of the reaction is much higher than the one of styrene.

The idea was to take advantage of the pseudo-living character of the radical on the growing poly-4-vinyl-1,3-dioxolan-2-one, and let polystyrene grow on its stable radical. In order to accomplish this result the synthetic procedure was splitted into two steps, as indicated in Figure 43.

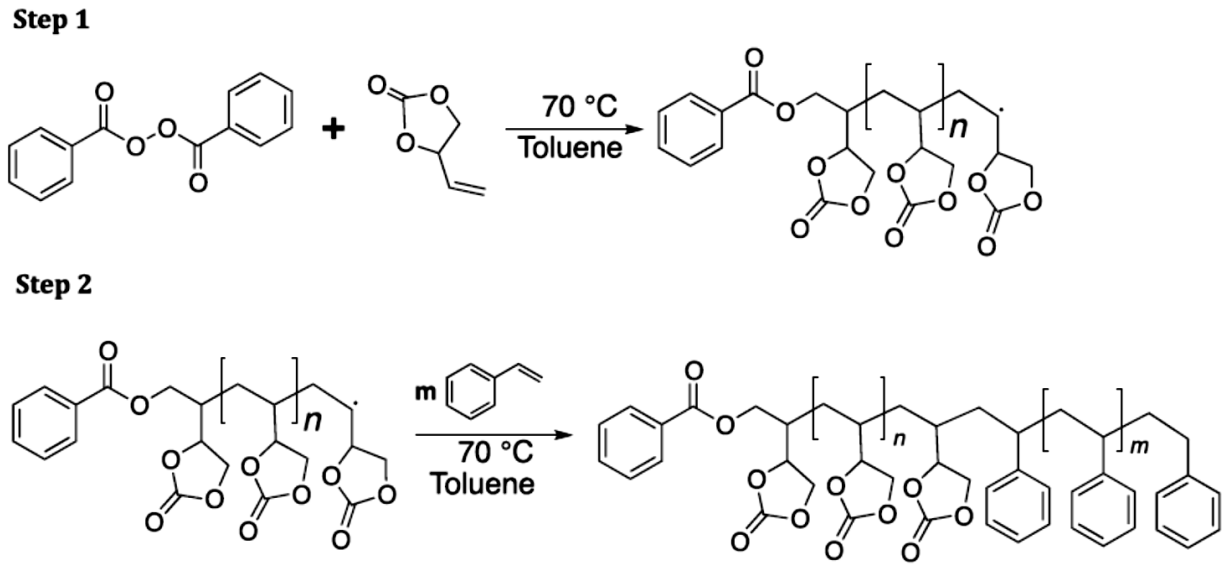

Figure 43. Synthetic route for the synthesis of styrene-4-vinyl-1,3-dioxolan-2-one block copolymers.

The first step involved the homopolymerization of 4-vinyl-1,3-dioxolan-2-one. At the end of this step, before the introduction of styrene, polyallyl carbonate based chains are formed bearing a stable radical on the chain end. The growth on polystyrene starting from this radical was indeed possible, resulting in the formation of a block copolymer.

The idea under this strategy is that, by increasing the delay time before the introduction of styrene, polyallyl carbonate chains would have more time to grow. As styrene is introduced, given its high reactivity ratio for the copolymerization with 4-vinyl-1,3-dioxolan-2-one, it will only homopolymerize. Again, in order to determine if copolymerization had actually occurred, ^{1}H NMR spectra were studied, in the region between 3.5 and 5.5 ppm. In Figure 44 spectral regions of interest for PS1 a), PSPC03 b), PSPC04 c), PSPC06 d), PSPC07 e), PSPC08 f) and poly 4-vinyl-1,3-dioxolan-2-one g) have been compared.

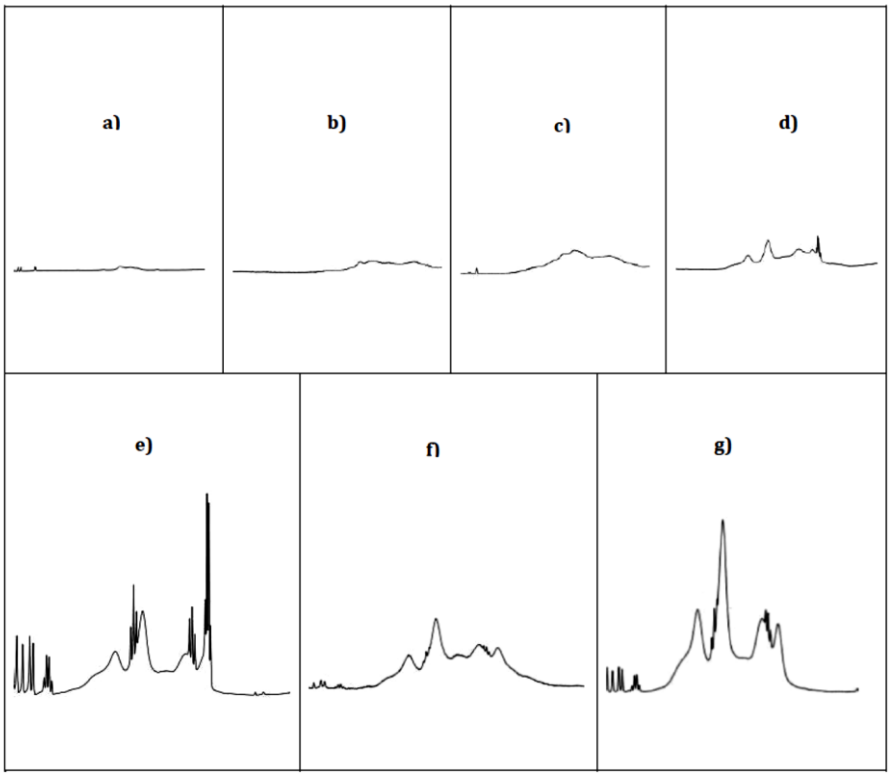

Figure 44. Comparison between 3.5-5.5 ppm regions in 1H NMR spectra of PS1 a), PSPC03 b), PSPC04 c), PSPC06 d), PSPC07 e), PSPC08 f) and Poly 4-vinyl-1,3-dioxolan-2-one g).

Signals patterns become more and more defined as well as more and more similar to allyl carbonate homopolymers ones as duration of the first step increases. For what regards PSPC03 and PSPC04 samples, peaks are still not well defined. In PSPC04, however, the doubling of signals, typical of poly 4-vinyl-1,3-dioxolan-2-one, is more pronounced with respect to PSPC03. The situation is markedly different for what regards PSPC06, PSPC07 and PSPC08. Starting from PSPC06, peaks are very similar to the ones of Polyallyl carbonate. However, the best results are obtained for PSPC07 and PSPC08, where a doublet, of doublets which closely resembles the signals for the homopolymer, appears clearly.

The key element in the synthetic procedure for the last two samples is the long lasting first step. As said above, styrene will tend to homopolymerize once is introduced in the reaction mixture. However, in PSPC07 and PSPC08 it is introduced only 24 hr after reaction has started. This means that as soon as styrene enters the system, only radicals available will be the ones on growing polyallyl carbonate chains, since BPO had fully reacted with allyl carbonate monomer.

In Figure 45 the ^{1}H NMR spectrum of PSPC08 is reported as an example.

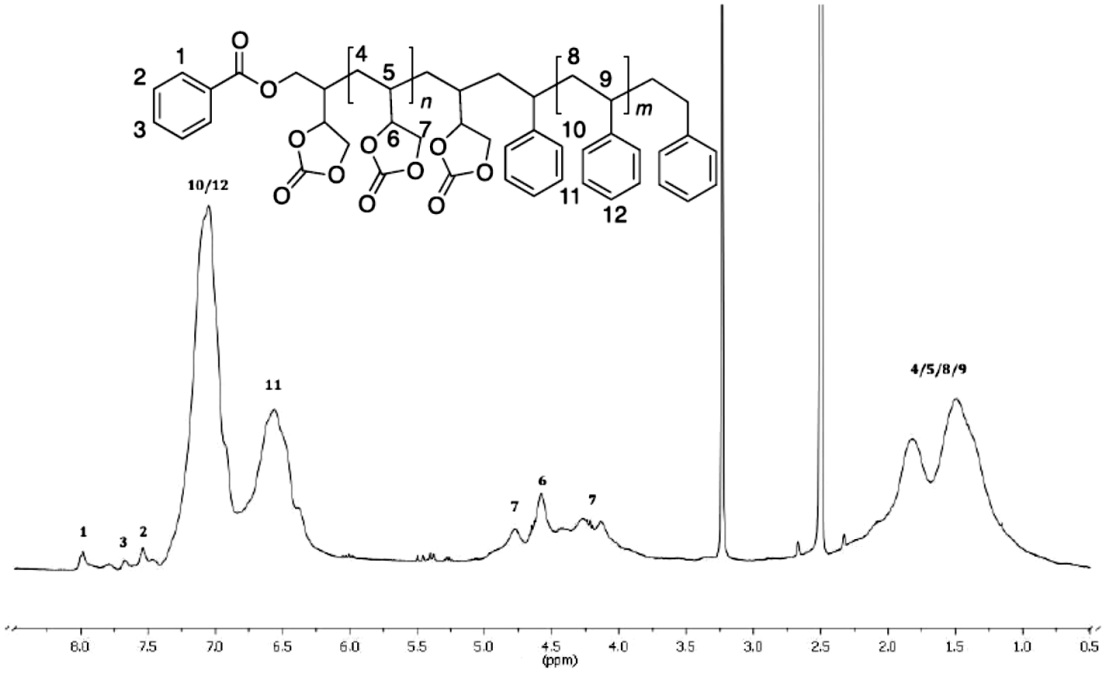

Figure 45. ^{1}H NMR spectrum of PSPC08.

As the ^{1}H NMR spectrum shows, even if signals of dioxalone moieties can be clearly distinguished by the others, it is impossible to determine only through NMR analysis the actual presence of a copolymer. In fact, alkyl protons for both the homopolymers fall in the same region, making therefore impossible to distinguish between the spectrum of a mixture of homopolymers and the spectrum of a block copolymer.

In order to determine if a copolymerization reaction had actually taken place, GPC analyses were performed. Different samples were taken at different reaction times, in particular before the introduction of styrene (first step) and at the end of the reaction (second step) in PSPC07 procedure. The idea under this approach was to determine if the polymer grew between the two steps or, alternatively, if two species were present at the end of the reaction. In the first hypothesis the occurrence of a copolymerization reaction would be demonstrated since it would mean the actual growth of polystyrene on the growing Polyallyl carbonate chains. Otherwise, the presence of two polymeric species at the end of the reaction would show the presence of two homopolymer species in the product.

In Figure 46 a comparison between GPC curves for the two samples is reported.

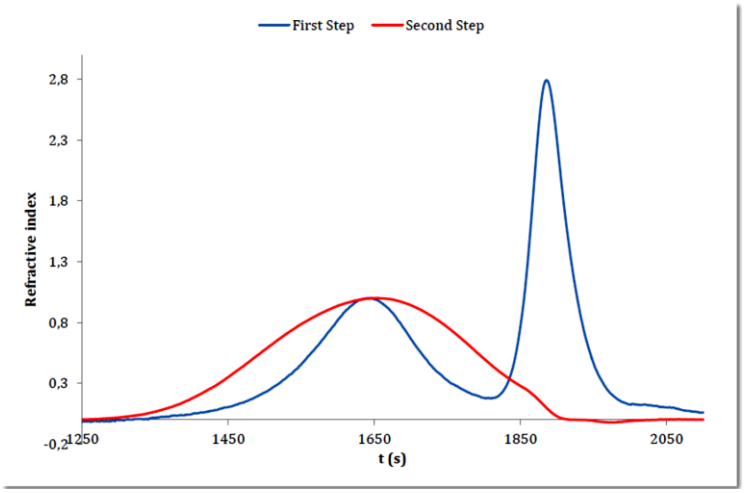

Figure 46. Comparison between SEC curves of samples taken at the end of the first and second step.

In Table 19 data relative to curves showed in Figure 46 are reported.

Sample	$\overline{Mn}$ (Da)	$\overline{Mw}$ (Da)	Mp (Da)	D
First step	12440	14880	12776	1.23
Second step	11589	15585	19313	1.34

Table 19. Molecular data of GPC curves reported in Figure 46.

As Figure 46 shows, only one species is present at the end of the reaction. In addition, a growth is registered, as indicated in Table 19. These observations therefore indicate that a copolymerization reaction has actually taken place.

Once the effectiveness of the two-step synthesis was demonstrated, PSPC03, PSPC04, PSPC06 and PSPC07 were studied through GPC analysis, curves reported in Figure 47 and related data in Table 20.

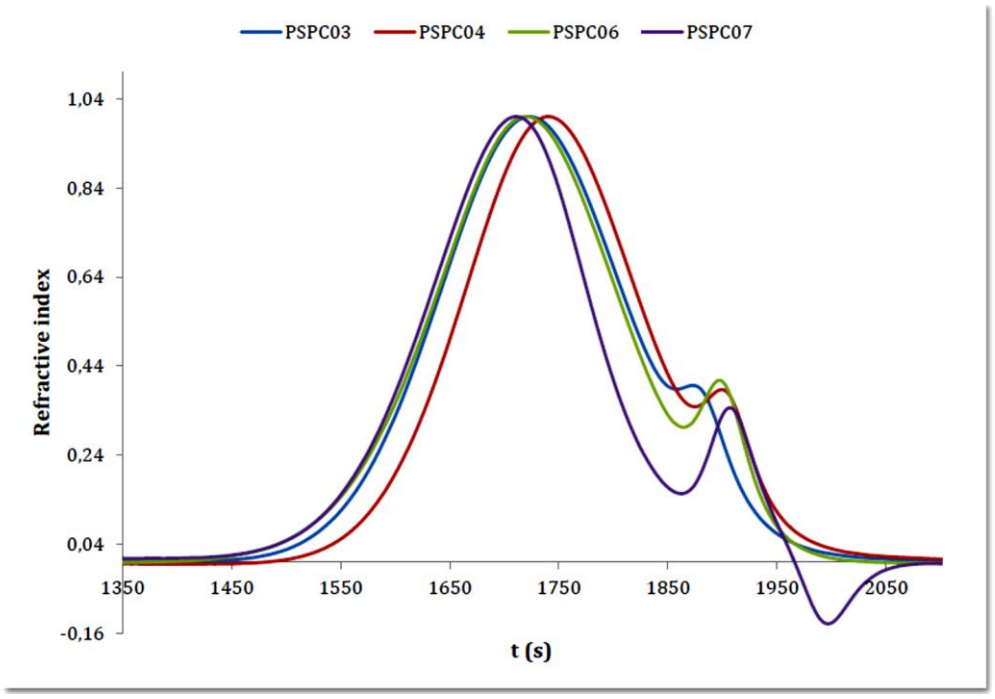

Figure 47. Comparison between GPC curves for PSPC03, PSPC04, PSPC06 and PSPC07.

Sample	$\overline{Mn}$ (Da)	$\overline{Mw}$ (Da)	Mp (Da)	D
PSPC03	6525	8625	8317	1.32
PSPC04	5721	7611	7585	1.33
PSPC06	6599	8886	8497	1.35
PSPC07	8802	10348	8901	1.18

Table 20. Molecular data of PSPC03, PSPC04, PSPC06 and PSPC07 samples.

Molecular weights for these samples appear to increase with the increase of the duration of the first step. Only PSPC04 does not seem to follow this trend, with the best results obtained with PSPC07 procedure.

Moreover, polidispersity values are low, and below the lower polydispersity limit for free radical polymerization reaction of 1.5, with the lowest value for PSPC07. Again, this is an indication of the pseudo-living character of the radical on 4-vinyl-1,3-dioxolan-2-one monomer. Since living or controlled radical polymerization reactions are based on equilibrium mechanisms between active and dormant species, temperature can have great effect on polymerization kinetics. Effects of temperature on the present system were studied in PSPC08 synthesis. The first part of the reaction was the same as PSPC07. The second part was modified by keeping the temperature at 70°C for 48 hr after the addition of styrene, and then by rising it up to 100°C for additional 96 hr. Effects of this variation were studied by taking samples at different times during the reaction. “Sample 1” was taken after the first step, “Sample 2” 24 hours after the addition of styrene, while “Sample 3” and “Sample 4” were taken 48 and 96 hours respectively after the increase of temperature. All of them were analyzed through GPC. Curves are reported in Figure 48.

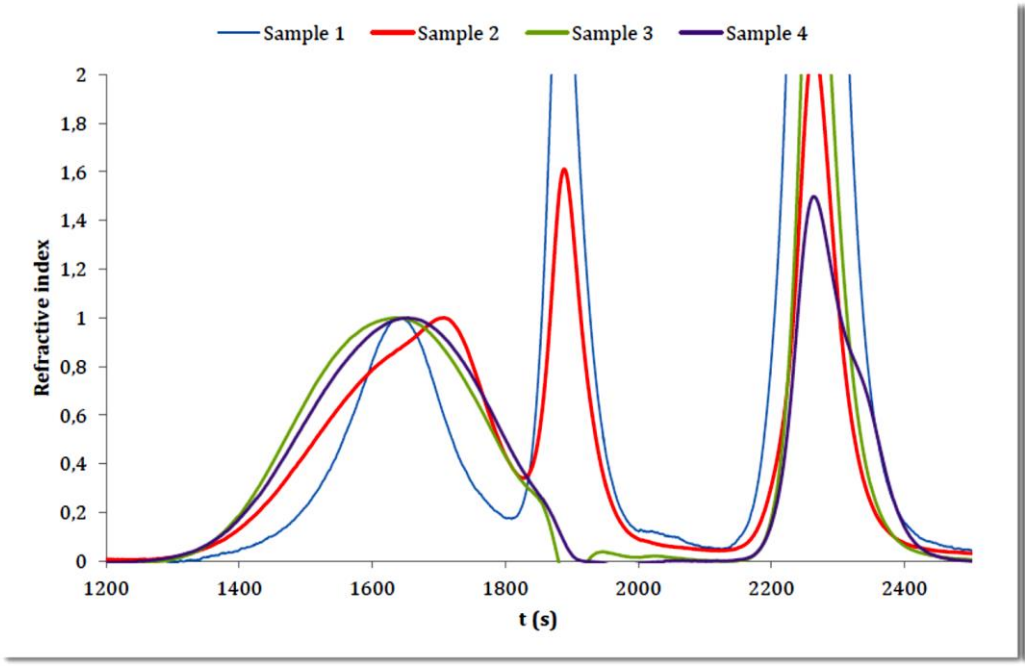

Figure 48. Comparison of GPC curves for all four samples of PSPC08 taken at different reaction times.

Data relative to GPC curves of Figure 48 are reported in Table 21. As Table 21 shows, an increase of the molecular weight of the polymer is registered, from Sample 1 to Sample 3. From Sample 3 to Sample 4 a decrease of molecular weight can be seen, which is probably due to degradation phenomena.

Sample	$\overline{Mn}$ (Da)	$\overline{Mw}$ (Da)	Mp (Da)	D
1	12440	14880	12776	1.19
2	11589	15585	19313	1.34
3	11509	16443	13232	1.39
4	10737	15681	11997	1.43

Table 21. Molecular data of samples reported in Figure 48.

Synthesis of fluorene bisphenol based acrylate 4-vinyl-1,3-dioxolan-2-one block copolymers

In the present study a novel functionalized acrylate was synthesized. As indicated in Scheme 12, two different methods were used for the preparation of this acrylate monomer.

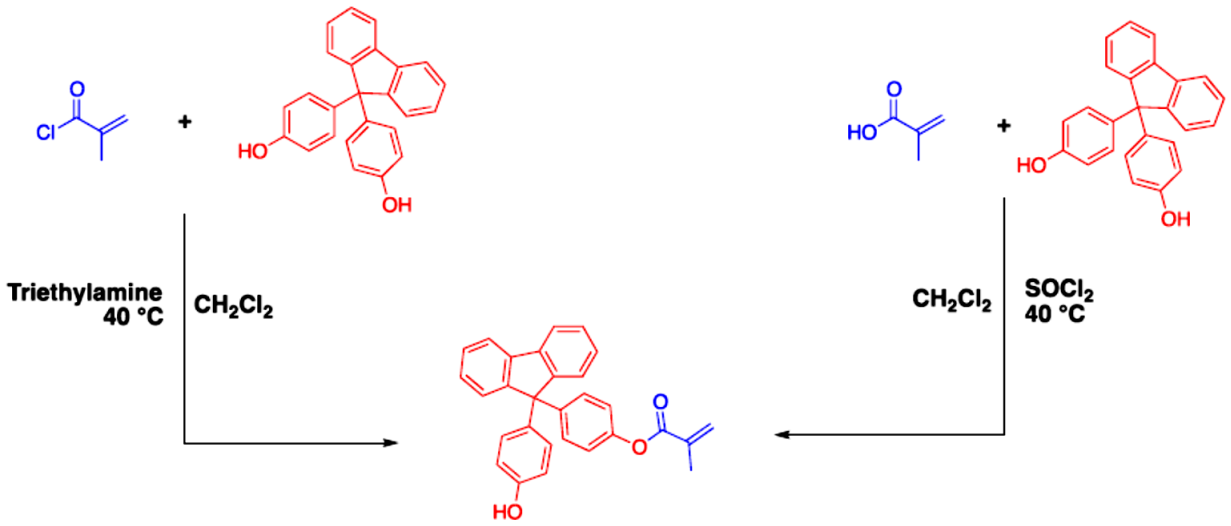

Scheme 12. Synthesis of functionalized acrylate monomers.

Scheme 12 shows two different synthetic strategies for the introduction of the unsaturated moiety either via acryloyl chloride or acrylic acid. In both cases the conductive functionality is introduced as phenol derivative. The molecule used has a highly aromatic structure, known as "cardo structure". This extremely high level of delocalization for π electrons guarantees useful properties, since such species possess great thermal resistance. In addition, the possibility that the electrons have to move within the structure is the key feature to confer conductivity properties to the final product, both from a thermal and electrical point of view. Again, the exploitation of this strategy allows to insert different functionalities in order to improve those properties which are missing in poly-4-vinyl-1,3-dioxolan-2-one, such as thermal and mechanical resistance.

Difficulties in these synthetic procedures arose from the bifunctional nature of the 9,9-Bis(4-hydroxyphenyl)fluorene. The aim of the synthesis was to prepare a mono-functionalized acrylate

derivative, in order to avoid crosslinking products after free radical polymerization. These products would have been indeed more difficult to characterize.

However, both reactions gave mainly the mono-functionalized derivative. Anyway, best results were obtained with the synthesis starting from acrylic acid. As one acrylic moiety bounds to the phenol, the extent of delocalization increases. This modification to the electronic distribution on the aromatic backbone is influenced also by the electron withdrawing character of the carbonyl. Apparently these effects make the other phenolic oxygen less nucleophilic, thus inhibiting a second esterification reaction, giving the mono functionalized species as main product.

Once the monomer was successfully synthesized, its reactivity towards free radical polymerization was tested, with the synthesis of an homopolymer in the same conditions previously used for the preparation of both PS1 and Poly-4-vinyl-1,3-dioxolan-2-one. In Scheme 13 the homopolymerization reaction of 9,9-Bis(4-hydroxyphenyl)fluorene based acrylate is described.

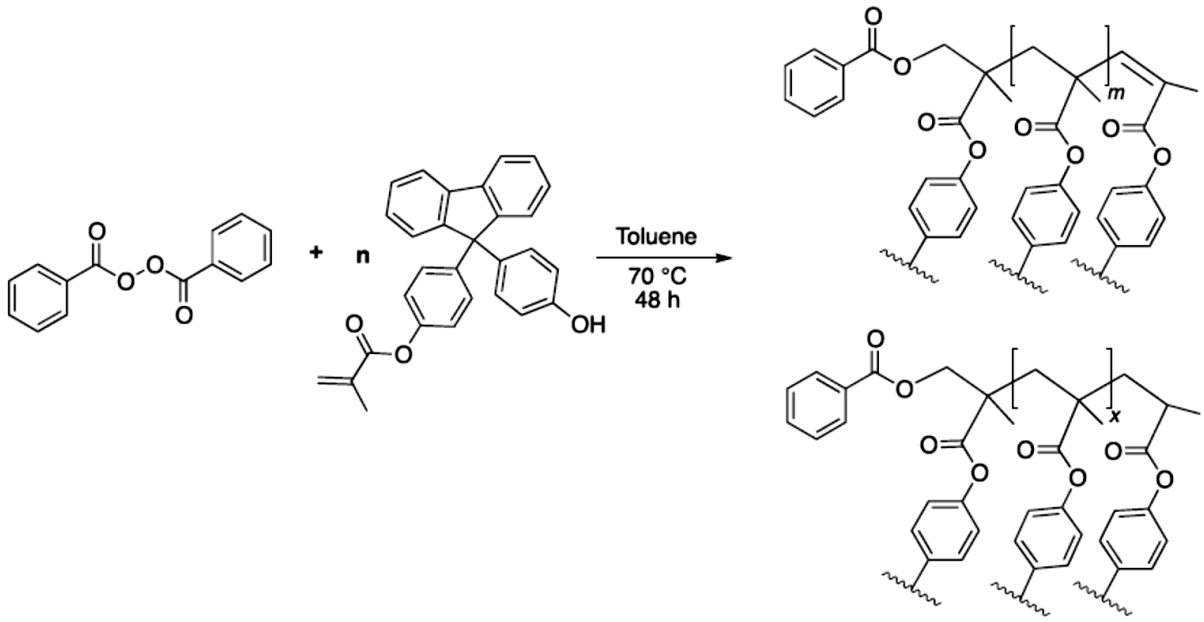

Scheme 13. Homopolymerization reaction of fluorene bisphenol based acrylate monomer.

This reaction proceeded easily, showing the high reactivity of this species. However, too much bi-functionalized monomer was present, giving as a result a crosslinked product which was difficult to characterize.

Since the acrylate monomer showed good reactivity, it was possible to use it as comonomer in a copolymerization reaction with 4-vinyl-1,3-dioxolan-2-one.

The same synthetic strategy described previously with PS was applied, as shown in Scheme 14.

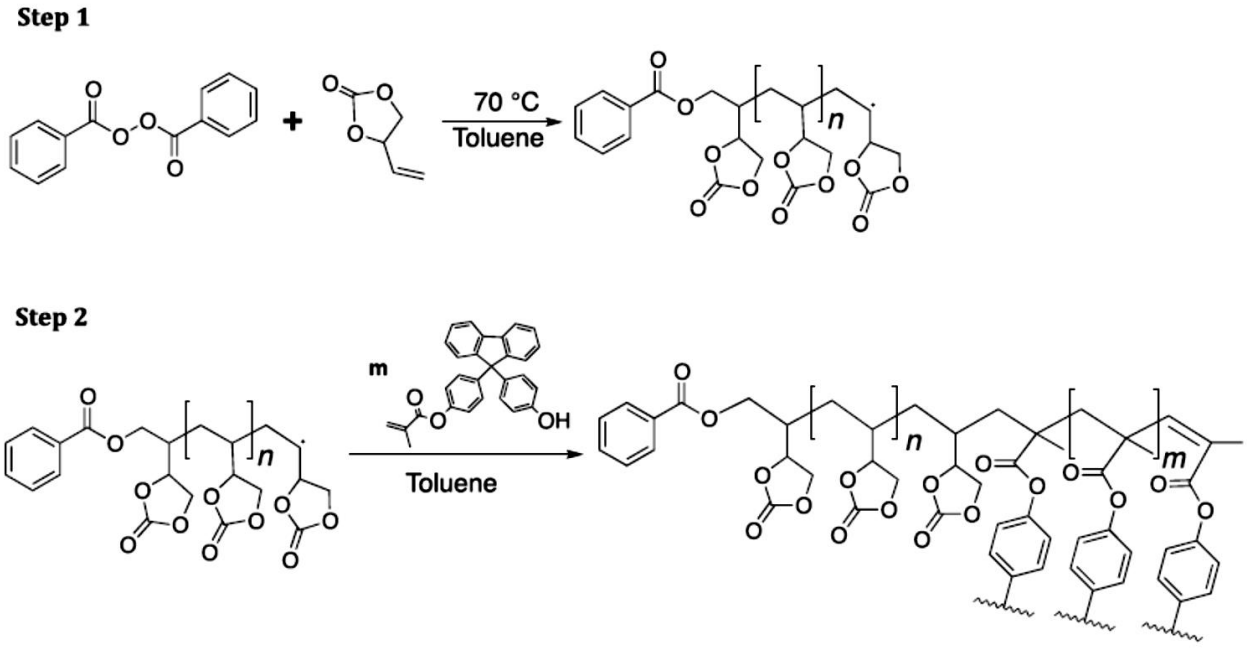

Scheme 14. Copolymerization reaction between 4-vinyl-1,3-dioxolan-2-one and fluorene bisphenol based acrylate.

The reaction is based on two steps. In the first one the homopolymerization of 4-vinyl-1,3-dioxolan-2-one was performed. After 24 hours the acrylate monomer was introduced. As demonstrated before, when the second monomer is introduced it reacts only with the stable radical on growing poly-4-vinyl-1,3-dioxolan-2-one chains. The result is a block copolymer, as shown in Scheme 14.

Obtaining a block copolymer is an important result from an application point of view. In fact this means that there's continuity for what regards conductive functionalities. This continuity is an extremely important prerequisite in order to have mobility of charge carriers along the chain.

Conclusion

Copolymers based on 4-vinyl-1,3-dioxolan-2-one comonomer were successfully synthesized. At first, studies on reactivity in free radical polymerization reactions of this allyl carbonate monomer were performed. The radical on this species appeared to possess a pseudo-living character, therefore resulting in a system that had not tendency to give termination reactions. Polyallyl carbonate homopolymer, however, showed poor thermal and mechanical properties. For this reason copolymerization reactions were performed, in order to introduce different functionalities to improve these features.

First studies of copolymerization were based on reactions between 4-vinyl-1,3-dioxolan-2-one and styrene. The stability of the radical on Polyallyl carbonate comonomer appeared to obstacle copolymerization reactions. In fact, first attempts demonstrated that, if both monomers were loaded at the beginning of the reaction, the only product obtained was polystyrene. In order to overcome the unfavorable reactivity ratios between these two species, a two-step synthetic methodology was developed. In the first step an homopolymerization of 4-vinyl-1,3-dioxolan-2-one took place. In the second step styrene was added. The result was a block copolymer since styrene could only grow on Polyallyl carbonate growing chains which brought a stable radical.

Once an efficient and reproducible synthetic procedure was developed for the synthesis of 4-vinyl-1,3-dioxolan-2-one based copolymers, a novel acrylate monomer was synthesized for use as comonomer. This species was synthesized starting from 9,9-Bis(4-hydroxyphenyl)fluorene, an highly unsaturated molecule displaying a so-called “cardo” structure. Structures of this type are known to confer high thermal stability as well as conductivity properties to the final material which are embedded in. These useful properties come from the extremely high π-electrons delocalization.

Once the monomer was successfully prepared, it was used as comonomer in a free radical polymerization reaction with 4-vinyl-1,3-dioxolan-2-one. Again a two-step synthesis was applied, resulting in the formation of a block copolymer. This was an important structural requirement in order to ensure continuity to conductive functionalities.

Abbreviations list

AFM: Atomic Force Microscopy

AIBN: 2,2’-azobisisobutyronitrile

ATRP: Atom Transfer Radical Polymerization

BBIM: 1,3-Dibutyl Imidazolinium bromide

BOIM: 1-Butyl, 3-Octyl Imidazolinium bromide

BPA: Bisphenol A

BPO: benzoyl peroxide

CI: initiator

CM: monomer

CNT: carbon nanotubes

CP: conducting polymer

CT: transfer agent

DPC: diphenyl carbonate

DPn: degree of polymerization

DPS: diphenyl sulfone

DS: degree of sulfonation

DSC: Differential Scanning Calorimetry

EDOT: 3,4-ethylene dioxy thiophene

FB: 9,9-bis(4-hydroxyphenyl)fluorene or fluorene bisphenol

FT-IR: Fourier Transform Infrared

G: graphene

GO: graphene oxide

GPC: Gel Permeation Chromatography

HLPES: heparin-like PES

IEC: Ion Exchange Capacity

I.L.: Ionic Liquid

MAIB: 2,2'-azobisisobutyrate

mEDOT: methacrylate 3,4-ethylenedioxythiophene

MEIM: 1-Ethyl, 3-Methyl Imidazolinium methyl sulfite

MOIM: 1-Methyl, 3-Octyl Imidazolinium bromide

NDI: 1,4,5,8-naphtalene diimide

NMP: nitroxide mediated living radical polymerization

OE: Organic Electronic

PA: Polyacrylate

PC: Polycarbonate

PEDOT: Poly(3,4-ethylene dioxy thiophene)

PEEK: Poly ether ketone

PES: Polyarylethersulfone

PMMA: Polymethyl methacrylate

PMeT: Poly(methyl-3-thiophene)

PSS: sulfonated polystyrene

PT: Poly(thiophene)

PV: photovoltaic

RMS: root-mean-square

SEM: Scanning Electron Microscopy

SPES: Sulfonated Polyarylethersulfone

SWCA: static water contact angle

TGA: thermogravimetric analyses

Bibliography

1. *Polym.* **Attwood, T.E.** 391-399, 1972, Vol. 4.

2. *J. Polym. Sci.* **Johnson, R. N.** 2375-2398, 1967, Vol. 5.

3. *Transaction of the Faraday Society* . **Carothers, W.** 32, 1936, Vols. 39-49.

4. *Polymer.* **Kricheldorf, H. R.** 1151-1156, 1984, Vol. 25.

5. *J. Am. Chem. Soc.* **Miller, J. A.Parker.** 117, 1961, Vol. 83.

6. *Canada Patent 847-963.* **Farnham, A. G.** 1970.

7. *Macromolecules.* **Colquhoun, H. M.** 107-111, Vol. 26.

8. *Biomater. Sci.* **Bai, P.** 12, 2010, Vol. 21.

9. *J. Membr. Sci.* **Koh, M.** 256, 2005, Vol. 1.

10. *Polymer.* **Higashibara, T.** 23, 2009, Vol. 50.

11. *J. Electrochem. Sci. Eng.* **Giordano, S.** 3, 2013, Vol. 3.

12. *Polymer.* **Al-Omran, A.** 9, 1996, Vol. 37.

13. *J. Membr. Sci.* **Nolte, R.** 1, 2010, Vol. 351.

14. *Polymer.* **Higashibara, T.** 23, 2009, Vol. 50.

15. *U.S. Patent 4,508,852.* **Bikson, B.** 1985.

16. *J. Membr. Sci.* **Lawrence, J.** 2, 2008, Vol. 325.

17. *U.S. Patent 5,013,765.* **Sluma, H.** 1991.

18. *Polymer.* **Yi, Z.** 2, 2012, Vol. 53.

19. *Acta Biomater.* **Wang, L. R.** 1, 2013, Vol. 9.

20. *Colloid Surf. A: Physicochem. Eng. Asp.* **Soliveri, G.** 1, 2015, Vol. 483.

21. *J. Membr. Sci.* **Zaidi, S. J.** 1, 2000, Vol. 173.

22. *J. Polym. Sci.* **Johnson, B. C.** 3, 1984, Vol. 22.

23. *J. Membr. Sci.* **Wang, M.** 1, 2006, Vol. 274.

24. *J. Catal.* **Liu, F.** 1, 2010, Vol. 271.

25. *Phys. Rev. Lett.* **Gronbech, N.** 12, 1997, Vol. 78.

26. *J. Phys. Chem.* **Zhao, M.** 20, 2015, Vol. 142.

27. *Polymer.* **Li, Y.** 11, 2006, Vol. 47.

28. *Thermodynamics and Rheology.* **Visakh, P.M.** 2014.

29. *Sep. Purif. Technol.* **Kumar, M.** 1, 2014, Vol. 127.

30. *Fuel Cells.* **Harrison, W. L.** 2, 2005, Vol. 5.

31. *Polym. Eng. Sci.* **Yeo, , J. K.** 11, 1981, Vol. 21.

32. *Eur. Polym. J.* **Zhao, W.** 3, 2013, Vol. 49.

33. *J. Membr. Sci.* **Klaysom, C.** 1, 2006, Vol. 368.

34. *Appl. Physics. A.* **Yuan, Z.** 2, 2016, Vol. 112.

35. *Chem. Eng. Res. Design.* **Vafaei, , S.** 414, 2016, Vol. 109.

36. *Sci. Tech. Advanced Mater.* **Dey, T.** 6, 2012, Vol. 13.

37. *J.Membr. Sci.* **Iwasaki, Y.** 6, 2012, Vol. 13.

38. *Tribol. Int.* **Wojciechowski, L.** 593, 2016, Vol. 93.

39. *Cleaner Prod.* **Qi, R.** 3555, 2016, Vol. 112.

40. *J. Appl. Catal. B.* **Rtimi, S.** 648, 2016, Vol. 180.

41. *J. Mat. Chem. .* **Smitha, V. S.** 1, 2013, Vol. 1.

42. *Soft Matter.* **Callies, M.** 71, 2008, Vol. 38.

43. *Annu. Rev. Mater. Res.* **Quéré, D.** 71, 2008, Vol. 38.

44. *Chem. Soc. Rev.* **Jordan, J. H.** 2, 2015, Vol. 44.

45. *Plasma Sci. technol. .* **Lu, X.** 1, 2015, Vol. 17.

46. *Plasma vapor deposition.* **Kato, K.** 1984, Vols. U.S. Patent No 4,446,168.

47. *Corros. Sci.* **He, T.** 8, 2009, Vol. 51.

48. *Langmuir.* **Marmur, A.** 20, s.l. : 2003, Vol. 19.

49. *Thin Solid Films.* **Nakajima, A.** 1, 2000, Vol. 376.

50. *Adv. Mat.* **Feng, L.** 24, 2002, Vol. 14.

51. *Langmuir.* **Chen, C.** 23, 2004, Vol. 20.

52. *Colloid Interface. Sci.* **Ghil, G. S.** 2, 2006, Vol. 298.

53. *J. Biomat. Sci.* **Bai, P.** 12, 2010, Vol. 21.

54. *J. Membr. Sci.* **Balster, J.** 1, Vol. 216.

55. *J. Membr. Sci.* **Kang, M. S.** 1, 2003, Vol. 216.

56. *U.S. Patent.* **Bikson, B.** 1985, Vols. No 4,508,852.

57. *Appl. Polym. Sci.* **Blanco, J. F.** 13, 2002, Vol. 84.

58. *J. Membr. Sci.* **Jutemar, E. P.** 1, 2010, Vol. 351.

59. *J. Polym. Sci. part A: Polym. Chem.* **Harrison, W. L.** 14, 2003, Vol. 41.

60. *Polym.* **Higashihara, T.** 23, 2009, Vol. 50.

61. *J. Colloid. Inter. Sci.* **Browne, C.** 449, 2015, Vol. 1.

62. *Polymer.* **Li, Y.** 11, 2006, Vol. 47.

63. *J. Membr. Sci.* **Wang, L. R.** 1, 2013, Vol. 9.

64. *Green and Suistanable Chem.* **Ghandi, Khashayar.** 53, 2014, Vol. 4.

65. *Chem. Rev.* **Roncali. J.** 711, 1992, Vol. 92.

66. *Appl. Physics. A.* **Yuan, Z.** 2, 2016, Vol. 122.

67. *Chem. Eng. res. Design.* **Vafaei, S.** 414, 2016, Vol. 109.

68. *Sol-Gel Sci. technol.* **Dey, T.** 1, 2016, Vol. 77.

69. *Sci. Tech. Advanced Mater.* **Iwasaki, Y.** 6, 2012, Vol. 13.

70. *Environ. Sci. Tech.* **Wang, Z.** 5, 2016, Vol. 50.

71. *J. Appl. Catal. B.* **Rtimi, S.** 648, 2016, Vol. 180.

72. *J. Mat. Chem.* **Smitha, V. S.** 12641, 2013, Vol. 1.

73. *Cleaner. Prod.* **Qi, R.** 3555, 2016, Vol. 112.

74. *Soft. Matter.* **Callies, M.** 55, 2005, Vol. 1.

75. *Rev. Mater. Res.* **Quéré, D.** 71, 2008, Vol. 38.

76. *Chem. Soc. Rev.* **Jordan, J. H.** 2, 2015, Vol. 44.

77. *Plasma Vapor Deposition.* **Liu, X.** 1984, Vols. U.S. Patent No4,446,168.

78. *Plasma Sci. Technol.* **Liu, X.** 1, 2015, Vol. 17.

79. *Corros. Sci.* **He, T.** 8, 2009, Vol. 51.

80. *Langmuir.* **Marmur, A.** 20, 2003, Vol. 19.

81. *Thin Solid Films.* **Nakajima, A.** 1, 2000, Vol. 376.

82. *Adv. Mat.* **Feng, L.** 24, 2002, Vol. 14.

83. *Langmuir.* **Chen, C.** 23, s.l. : 2004, Vol. 20.

84. *Colloid Interface Sci.* **Gohil, G. S.** 2, 2006, Vol. 298.

85. *Polym.* **Higashihara, T.** 23, 2009, Vol. 50.

86. *J. Colloid. Inter. Sci.* **Browne, C.** 449, 2015, Vol. 1.

87. *Polymer.* **Li, Y.** 11, 2006, Vol. 47.

88. *Acta Biomat.* **Wang, L. R.** 8851, 2013, Vol. 9.

89. *KEPCO Journal on Electric Power and Energy.* **Baek, J. H.** 2, 2016, Vol. 2.

90. *Chem. Rew.* **Matyjaszewski, K.** 9, 2001, Vol. 101.